DEPARTAMENTO DE CIÊNCIAS DA VIDA

FACULDADE DE CIÊNCIAS E TECNOLOGIA
UNIVERSIDADE DE COIMBRA

Altering protein degradation via the ubiquitin proteasomal system or autophagy, and its impact on tau degradation and aggregation

Dissertação apresentada à Universidade de Coimbra para cumprimento dos requisitos necessários à obtenção do grau de Mestre em Biologia Celular e Molecular, realizada sob a orientação científica do Professor Doutor Brian Hrupka (Jansen Pharmaceutica NV) e do Professor Doutor Carlos Duarte (Universidade de Coimbra)

Elvira Pequeno Leites

2014

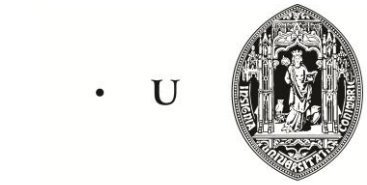

The work presented in this thesis resulted from a partnership between the University of Coimbra and Janssen. All experimental activities were performed at Janssen Beerse I, a Johnson & Johnson pharmaceutical research and development facility in Beerse, Belgium.

Beerse, 2014

Acknowledgements

I would like to thank all the people who in some way supported me, taught me, made me feel at home, this year. For everyone a big thank you.

I owe a great thanks to my supervisor Brian Hrupka for all the patience, help, confidence and support that had with me even when my English was not really comprehensible. Thanks for changing my way of looking at science.

I also want to thanks Dieder for the opportunity to belong to this group, for welcoming me in this group and for all the scientific support as well as for the demonstrated friendship.

To all Tau group meeting, thank you for all knowledge and help that you gave me during this year.

A really huge thank you to all *in vitro* lab members, for all the availability, practical and scientific support that you gave me. A special thank you to Guy Daneels for everything that you have done for me, I will never be able to properly thank you; to Marck Vandermeeren for all the conversations that we had and for all the support that you gave me; to Arjan Buist for everything that you taught me and for turn some days funnier with our "mini concerts"; to Arlette Kouwenhoven for your friendship, scientific support and funny conversations. This lab is an amazing place to work, thank you all.

Thanks also go to Ken Veys, my office mate for all the conversations (sometimes crazy), all the support and all the advices that you gave me.

Professor Emilia Duarte and Professor Carlos Duarte, thank you for trusting me and allowing me to have two fantastic years.

I would also like to thank Sara Calafate for all scientific advices and knowledge that you gave me as well as all the support, friendship and funny moments that we had inside and outside of the company.

To all Portuguese students, thank you for all this year, especially Johny and Nuno for letting me grow a little bit with you and for all the good and bad moments that we had together. Thank you to all my friends from the first year for the great year and still remain in my life and for making my life happier, especially Ana Bolhaqueiro, Ana Raquel, Ana Rita Pombo, Andreia Barbas, Cindy Pinhal and Iryna Voytyuk.

A special thank you to Gonçalo for all the support that you gave me since we met until now. Thank you for making my life easier and happier.

Como não poderia deixar de ser gostaria de agradecer a minha mãe, ao meu irmão e ao meu avô por todo o apoio que sempre me deram, por mesmo estando longe fazerem com que a distancia não se note e obrigado por significarem tanto para mim.

Abstract

Alzheimer's disease (AD) is a neurodegenerative disorder that places a substantial burden on patients, their families, and society. One of the several pathological hallmarks of this disease is intraneuronal phospho-tau accumulation in the form of neurofibrillary tangles. Tau is an intracellular protein that contributes to the stabilization and assembly of microtubules (MT) in neuronal axons, neurite outgrowth, axonal transport, cell signaling transduction, trophic signaling enhancement and heat shock cell protection. The interaction of tau with MTs is regulated through many mechanisms including alternative splicing and phosphorylation, the latter being fundamental in AD since the characteristic tangles seen in this disease are composed by filaments of abnormally phosphorylated tau. Paired helical filaments-tau (PHF-Tau) is ubiquitinated at its microtubule-binding domain at different residues, suggesting that ubiquitination of PHF-Tau may be an earlier pathological event and that ubiquitination could play a regulatory role in modulating the integrity of microtubules during the course of AD. Protein aggregate formation may be linked to misregulation of the ubiquitin proteasome system (UPS) and/or the autophagy pathway. UPS is usually responsible for degradation of many long-lived proteins and damaged organelles, while autophagy is usually related with degradation of short-lived proteins. Degradation targets must first be ubiquitin-tagged, a highly regulated process itself that requires a delicate balance between ubiquitinating and de-ubiquitinating enzymes (DUBs). USP5, USP7, OTUB1 and USP9x are the four DUBs studied in this project.

In these work we showed that mutations of the known ubiquitination sites Lys^{254}, Lys^{257}, Lys^{311}, Lys^{317} and Lys^{353} to prevent ubiquitination do not play a critical role in soluble or insoluble tau degradation or preventing its buildup in our cellular model; we show that overexpression of USP5 and OTUB1 attenuates the formation of tau aggregates or enhances its clearance.

Key-words: Alzheimer's disease, tau aggregates, Ubiquitin Proteasome System, autophagy, tau clearance

Resumo

A doença de Alzheimer (DA) é uma doença neurodegenerativa com elevado impacto para os pacientes, para os seus familiares e para a sociedade. Uma das características patológicas desta doença é a acumulação intraneuronal da proteína tau fosforilada, na forma de tranças neurofibrilares. A tau é uma proteína intracelular que contribui para a formação dos micrrotúbulos (MT) e a sua estabilização nos axónios, assim como para o crescimento das neurites, transporte axonal, sinalização intracelular, aumento de sinalização trófica e protecção celular heat shock. A interacção da tau com os MTs é regulada através de diversas formas, incluindo splicing alternativo e fosforilação, sendo este último processo fundamental na DA visto que as tranças características desta doença são compostas por filamentos de tau anormalmente fosforilada. Filamentos helicoidais de tau emparelhados (FHE-tau) são ubiquitinados em diferentes locais, no domínio de ligação da proteína aos microtúbulos, sugerindo que a ubiquitinação dos FHE-tau pode ser um acontecimento patológico primário e que este processo pode afectar a integridade dos microtúbulos durante o desenvolvimento da DA. A formação de agregados de proteínas pode estar relacionada com a falha de regulação do sistema de ubiquitina-proteossoma (SUP) e/ou a falha na autofagia. O SUP é geralmente responsável pela degradação de várias proteínas de elevada estabilidade assim como de organelos danificados, enquanto que a autofagia é geralmente responsável pela degradação de proteínas com uma meia-vida curta. As proteínas degradadas pelo SUP são primeiro marcadas com ubiquitina, um processo altamente regulado que requer um equilíbrio meticuloso entre a actividade das enzimas que promovem ubiquitinação e as que promovem a desubiquitinação (DUBs). USP5, USP7, OTUB1 e USP9x são as quatro DUBs estudadas neste projecto.

Neste trabalho foi mostrado que mutações na tau, nos locais de ubiquitinação conhecidos Lys254, Lys257, Lys311, Lys317 e Lys353, de modo a impedir a ubiquitinação da proteína, não alteram de forma significativa a degradação da proteína, quer esta esteja na forma solúvel ou insolúvel, e também não alteraram a sua agregação no modelo utilizado. Mostrámos também que o aumento da expressão da USP5 e da OTUB1 atenua a formação de agregados ou aumenta sua degradação.

Palavras-chave: Doença de Alzheimer, agregados de tau, Sistema de ubiquitina-proteosoma, autofagia, degradação da tau

Index

Abbreviations

ABCA7 - ATP-binding cassette transporter,

Ach - Cholinergic neurons and acetylcholine

AD - Alzheimer's disease

AMPK - AMP-activated protein kinase

APO E - Apolipoprotein E

APP - Amyloid precursor protein

Atg - Autophagy-related

Aβ - Amyloid-β protein

Bcl-2 - Phosphorylate B-cell lymphoma 2

BIN1 - Bridging integrator 1,

CaMKII - Ca2+/Cal-Modulin-dependent protein kinase II

CD2AP - CD2-associated protein,

CD33 - Sialic acid-binding immunoglobulin-like lectin

CDK5 - Cyclin-dependent kinase-5

CK1a/1d/1e/2 - Casein kinase 1a/1d/1e/2

CLU - clusterin,

CMA - Chaperonemediated autophagy

CR1 - Complement receptor 1,

CSF - Sulcal cerebrospinal fluid

DSBs - DNA double-strand breaks

DUBs - Deubiquitinating enzymes

DYRK1A - Dual-specificity tyrosine phosphorylation and regulated kinase 1A

EBNA1 - Epstein-Barr nuclear antigen

EOAD - Early-onset form of AD

EPHA1 - Ephrin receptor A1

ER - Endoplasmic reticulum

FOXO4 - Forkdhead box O4 transcription factor

GSK-3β - Glycogen synthase kinase-3 β

HAUSP - Herpesvirus-Associated Ubiquitin-Specific Protease

ICP0 - Herpes simplex virus type I regulatory protein

ISG15 - Interferon Stimulated Gene 15

IsoT - Isopeptidase T

JAMMs - JAB1/MPN/MOV34 metalloenzyme

JNK1 - c-Jun N-terminal kinase

LC3 - Microtubule-associated protein 1 light chain 3

LOAD - Late-onset form of AD

MA - Macroautophagy

MAPKs - Mitogen-activated protein kinases

MAPT - Microtubule Associated Protein tau

MARKs - Microtubule affinity-regulating kinases

MBD - Microtubule-binding domain

MCI - Mild Cognitive Impairment

MJDs - Machado-Joseph disease protein domain proteases

MS4A cluster - Membrane-spanning 4-domains subfamily A,

MT - Microtubules

NEDD8 - Neural Precursor Cell Expressed Developmentally Down Regulated Protein 8

NFTs – Neurofibrillary tangles

NL - Cognitively Normal

OTUB1 - OUT domain-containing ubiquitin aldehyde-binding protein 1

OTUBs - Ovarian tumor proteases

PDPKs - Proline-directed protein kinases

PFA - Paraformaldehyde

PHFs - Paired Helical filaments

PICALM - Phosphatidylinositol-binding clathrin assembly protein,

PKN - Protein kinase cAMP-dependent/B/C/N) and

polyUb - Polyubiquitin

PP1 - Phosphatases 1

PP2A - Phosphatases 2a

PP2B - Phosphatases 2b

PP5 - Phosphatases 5

PS-1 - Presenilin-1

PS-2 - Presenilin-2

p-tau - phospho-tau

REST - Repressor element 1-silencing transcription factor

RING - Really Interesting New Gene

RT- Room temperature

SUMO - Small Ubiquitin-Like Modifier

TC-NER - Transcription-Coupled Nucleotide Excision Repair

TTBK1/2 - Tau-tubulin kinase ½

Ub - Ubiquitin

UbL - Ubiquitin-like proteins

UCHs - Ubiquitin C-terminal hydrolyases

ULK1 - Unc-51-like kinase 1

UPS - Ubiquitin–proteasome system

USP5 - Ubiquitin-specific proteases 5

USP7 - Ubiquitin-specific peptidase 7

USPs - Ubiquitin-specific proteases

UVSSA - UV-stimulated scaffold protein A

Vps34 - Vacuolar protein sorting 34

Introduction and Project Objectives

1.1 Alzheimer's disease

Dementia has been generally defined as acquired persistent impairments in two or more cognitive domains, sufficient to cause decline in ability to carry out social or occupational functioning independently. The most prevalent types of dementia are classified by presumed etiology into vascular dementia caused by vascular lesions and Alzheimer's disease (AD) resulting from a neurodegenerative process, the most common cause (Wing 2003, Ding, Matthews et al. 2006, Honjo, Black et al. 2012).

AD is a chronic, progressive, neurodegenerative disorder that places a substantial burden on patients, their families, and society and is the most common cause of age-related cognitive decline (Singh, Kushwah et al. 2012). However this disease can be divided into two major groups based on age of onset: the early-onset (EOAD) forms that begin before the age of 65, and late-onset (LOAD) forms that begin after that age (Lambert and Amouyel 2011).

The progression of this disease, including widespread cortical atrophy, profound tissue loss in the hippocampus and medial temporal lobes, and expansions of the ventricular and sulcal cerebrospinal fluid (CSF) spaces (Ewers, Frisoni et al. 2011).

Several pathological hallmarks of AD have been identified, and they include decreased cholinergic neurons and acetylcholine (ACh) levels, amyloid-β protein (Aβ) deposition in extracellular senile plaques and vessels, intraneuronal tau deposition as neurofibrillary tangles associated with irregular phosphorylation of tau protein, inflammation and increased oxidative stress from reactive oxygen species (ROS), as well as dyshomeostasis and miscompartmentalization of metal ions such as Cu, Fe, and Zn (Honjo, Black et al. 2012, Eckroat, Mayhoub et al. 2013).

The proposed mechanism for Aβ to exert the neurotoxic effects was the assembly into Aβ plaques and oligomers (Pike, Burdick et al. 1993). This was further nurtured by the finding of a genetic component associated with the hypothesis of Aβ deposition. Mutations in the amyloid precursor protein (APP) that facilitate its cleavage to generate Aβ and/or mutations in presenilin-1 (PS-1) or presenilin-2 (PS-2), that promote Aβ formation and consequently its deposition have also been reported (Campion, Flaman et al. 1995, Borchelt, Ratovitski et al. 1997, Borchelt, Lee et al. 2002). Aβ was shown to activate apoptotic

pathways, leading to caspase activation, ultimately contributing to neurodegeneration, *in vitro* (Ding, Matthews et al. 2006, Mondragon-Rodriguez, Perry et al. 2012)

It is known that AD pathology begins years before clinical symptoms become evident (Bennett, Schneider et al. 2006). The evolution of disease can be divide in three stages such as AD patients preceded by Mild Cognitive Impaired patients (MCI) and Cognitively Normal (NL) populations (Randall, Mosconi et al. 2013).

1.1.1 Symptoms

Alzheimer's patients have different symptoms throughout the disease process. During milder stages, clinical signs usually include forgetfulness for latest events and other cognitive impairments, such as word-finding difficulties or augmented confusion in navigating unfamiliar environments (Bahar-Fuchs, Clare et al. 2013). During the pre-dementia phase, there is often no, or minimal, impairment in the ability of the individual to carry out most activities of daily living (Bahar-Fuchs, Clare et al. 2013). Throughout these MCI and NL, the patient's alertness is well preserved, and motor and sensory functions are essentially intact (Selkoe 2001, Bahar-Fuchs, Clare et al. 2013).

During dementia, most cognitive and functional abilities are profoundly impaired, memory impairment, behavioral changes such as apathy, depression, paranoia, delusions, aggression and agitation are frequently observed resulting in loss of social appropriateness

The findings of Alois Alzheimer, the father of AD demonstrated correlated neuropathologic changes with cognitive status of AD patients.

1.1.2 Risk factors

One of the risk factors involves Apolipoprotein E (ApoE), which is a plasma protein that transports lipids (e.g.cholesterol) and is associated with neuronal repair. The APOE gene, located on chromosome 19, has three allelic variations: ε2, ε3, and ε4. The APOE-ε4 allele is a genetic risk factor for both familial and sporadic late-onset AD (Slooter and van Duijn 1997, Reitz, Brayne et al. 2011, Honjo, Black et al. 2012).

Epidemiological evidence has shown that hypercholesterolemia is another important risk factor for AD. This is further supported by basic research suggesting that cholesterol may contribute to the development of AD pathology by altering APP processing (Honjo, Black et al. 2012). Hypertension is also associated with late-life cognitive impairment and increased amounts of senile plaques and neurotrophic factors (NTFs) (Sparks, Scheff et al. 1995, Honjo, Black et al. 2012). Furthemore, a large amount of studies have shown a positive relationship between diabetes mellitus and AD. The specific mechanisms remain unclear; however, diabetes mellitus related micro- and macrovascular changes could cause hypoperfusion, accelerating Aβ deposition, and perhaps clinical AD (Honjo, Black et al. 2012). Obesity and Metabolic syndrome are others important risk factors for AD development, as is hyperhomocysteinemia which is characterized by elevated plasma homocysteine (Honjo, Black et al. 2012).

In 2011 nine new loci were identified to be related with LOAD. These genes are CLU – clusterin, PICALM – phosphatidylinositol-binding clathrin assembly protein, CR1 – complement receptor 1, BIN1 – bridging integrator 1, ABCA7 – ATP-binding cassette transporter, MS4A cluster – membrane-spanning 4-domains subfamily A, CD2AP – CD2-associated protein, CD33 – sialic acid-binding immunoglobulin-like lectin and EPHA1 – ephrin receptor A1. These loci are involved in three pathways linked to immune system function, cholesterol metabolism and synaptic cell membrane processes (Morgan 2011).

However older adults who have no typical risk factors, such as genetic predisposition, vascular risk factors, or other, can still develop AD, so aging is a very important risk factor (Honjo, Black et al. 2012).

1.1.3 Diagnostic and Pathology

The diagnosis of AD is a problem because a definitive AD diagnosis can only be established postmortem and still relies on identification of the two pathogenic features defined by Alois Alzheimer in 1901. After cross-sectional analyses of post mortem human brain a characteristic progression of β-amyloid plaques and a highly stereotypical appearance of neurofibrillary tangles verify AD (Figure 1) (Jucker and Walker 2011). The development of Aβ plaques starts in the neocortex followed by the allocortex and then the

subcortex, and the progression of their appearance is often correlated with functionally and anatomically coupled brain regions. The first appearance of neurofibrillary tangles is on locus coeruleus and entorhinal/limbic brain areas, which later spread to interconnected neocortical regions (Jucker and Walker 2011). The pattern shown in these studies implicates a neuronal transport and synaptic exchange mechanisms in the spread of AD lesions within the brain.

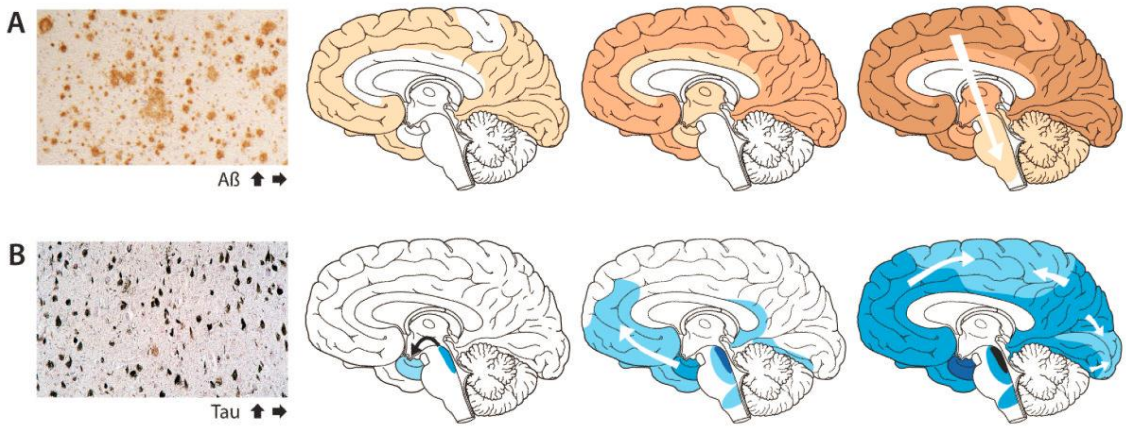

Figure 1 - Accumulation of misfolded proteins in AD (Jucker and Walker 2011)

Currently, confirmation of the disease can only be made by neuropathological confirmation of persons who have been studied in life and met criteria for dementia (Petersen 2004). In life the studies are made by cognitive evaluation, which is complicated because the cognitive dysfunction is similar in the beginning of the MCI stage and in the end of normal ageing, as well as in the early stages of AD compared with the late stage of MCI.

1.2 Tau protein

Tau is an intracellular protein that contributes to the stabilization and assembly of microtubules (MT) in neuronal axons (Figure 2) (Randall, Mosconi et al. 2013). MTs are dynamic polymers, able to grow and shrink, and these dynamics are regulated by a group of MT-associated proteins including tau (Duan and Goodson 2012). In neurons, MTs are linearly and densely packed along the length of the axon, inducing a global cellular polarity necessary for neuronal signaling (Witte, Neukirchen et al. 2008). In normal cells, tau is found distributed throughout axons and is localized to MTs. The interaction of tau with MTs is

regulated through many mechanisms like alternative splicing and phosphorylation (Alonso, Di Clerico et al. 2010, Fauquant, Redeker et al. 2011). Tau protein function is not just the stabilization of MTs, this protein is multifunctional and it has a variety of binding partners, including signaling molecules, cytoskeletal elements and lipids. Besides the direct interaction of tau with MTs including the binding, promotion of microtubule assembly and stabilization, tau interacts with them indirectly affecting others proteins that may or may not interact with microtubules by themselves (Figure 2) (Mietelska-Porowska, Wasik et al. 2014). In 2008, Dixit et al. suggested that binding of tau to MTs can also take part in axonal transport and can interfere with the binding of motor proteins (Figure 2). A gradient of tau along the axon, with the highest level around synapses, might promote detachment of motor proteins from their cargo at presynaptic terminals, consequently increasing axonal transport efficiency (Dixit, Ross et al. 2008).

Although tau is highly concentrated in axons, recent data suggest that this protein may also play a physiological role in dendrites (Mietelska-Porowska, Wasik et al. 2014).

Tau can also act as a postsynaptic scaffolding protein, modulating the activity of Src tyrosine kinases, s-Src and Fyn, and facilitating c-Src-mediated actin rearrangements (Figure 2) (Sharma, Litersky et al. 2007). It has been suggested that tau usually tethers Fyn (membrane-anchored non-receptor tyrosine kinase from the Src-family) to PSD-95/NMDA receptor signating complex. Although the amount of tau normally present in dendrites is low, it is essential, since in absence of tau Fyn can no longer traffic into postsynaptic sites. Moreover, tau can also act as a scaffolding protein in oligodendrocytes, where it is probably enabling extension of MTs through their interactions with Fyn (Mietelska-Porowska, Wasik et al. 2014).

Another function of tau is its involvement in growth factor signaling (Figure 2). Tau is distributed at ends of cellular extensions, under NGF stimulation, where it binds with actin in a microtubule-independent manner. MAPT (microtubule associated protein tau) enables signaling through NGF and EGF receptors, which may increase the activity of MAPK (mitogen-activated protein kinase) (Mietelska-Porowska, Wasik et al. 2014). Tau can also be involved in DNA repair and heat shock responses through its involvement with heat shock proteins (involved in most aspects of protein synthesis, folding, trafficking and assembly of

multiprotein complexes), in the nuclear organizing region of the cell (Figure 2) (Mietelska-Porowska, Wasik et al. 2014).

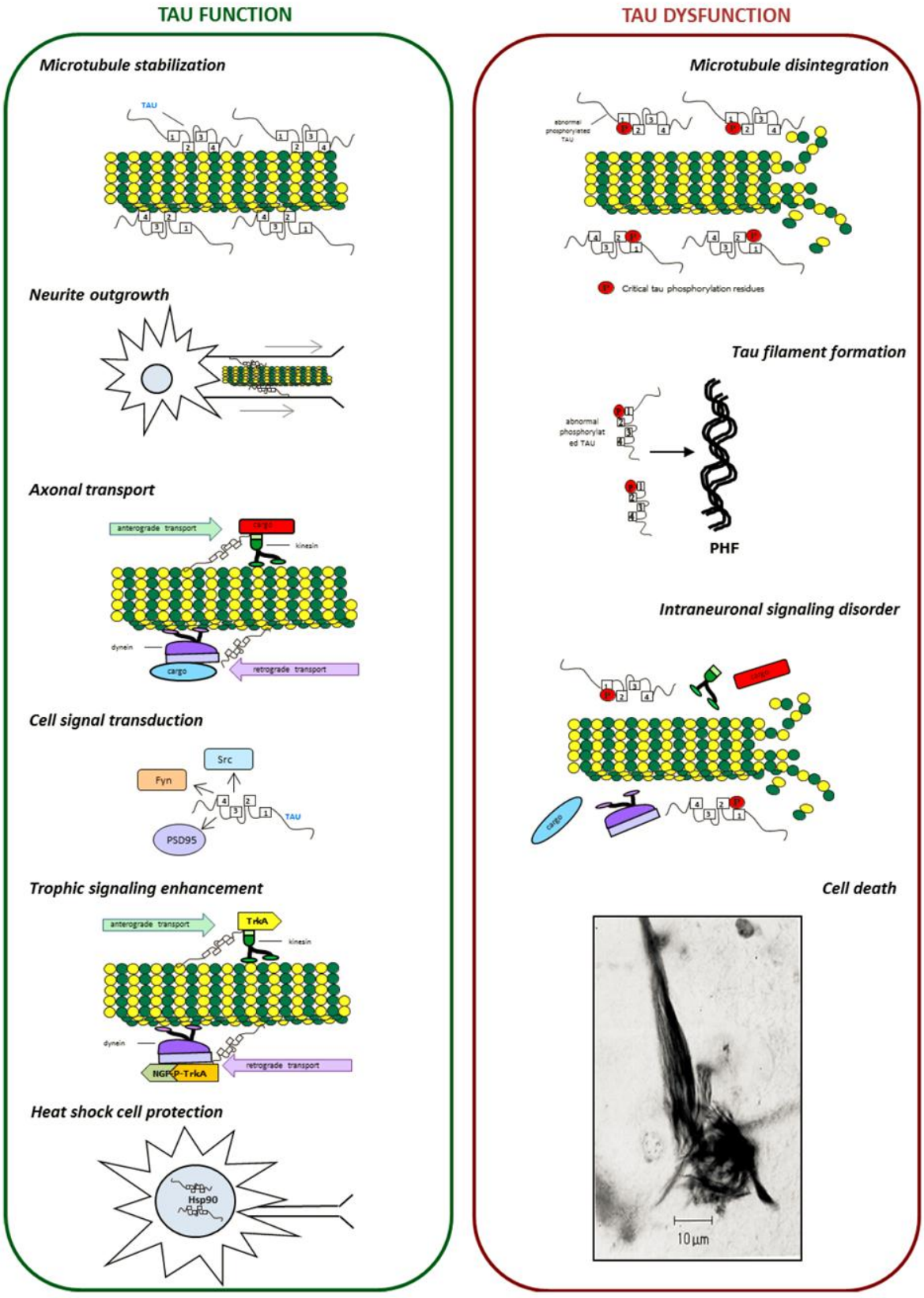

Figure 2 - Functions of tau in normal and pathologic conditions (Mietelska-Porowska, Wasik et al. 2014)

The MAPT gene, which encodes tau protein, is located on chromosome 21 and has six isoforms in adult humans (Billingsley and Kincaid 1997). These isoforms are derived from a single gene with 16 exons by alternative splicing (Ballatore, Lee et al. 2007). Until now, exons 6 and 8 have not been shown to be transcribed and the exon 4A is only transcribed in the peripheral nervous system. Exon 14 is transcribed but generates a premature stop codon preventing translation (Buee, Bussiere et al. 2000). In the central nervous system, molecular weight of tau ranges between 60 and 74 KDa depending on the alternative splicing of tau primary transcript that generates six isoforms of 352-441 amino acids (Figure 3) (Ballatore, Lee et al. 2007). Tau is composed of four domains: the N-terminal projection domain that is composed by an acidic region which is encoded by exons 1-5 whereas exon 2 and 3 encode for N-terminal inserts; the proline-rich region in the interior that is encoded by exon 7 and the first half of exon 9; the region responsible for tau binding with microtubules that is encoded by exons 9-12 that contain a microtubule-binding domain (MBD) with either three

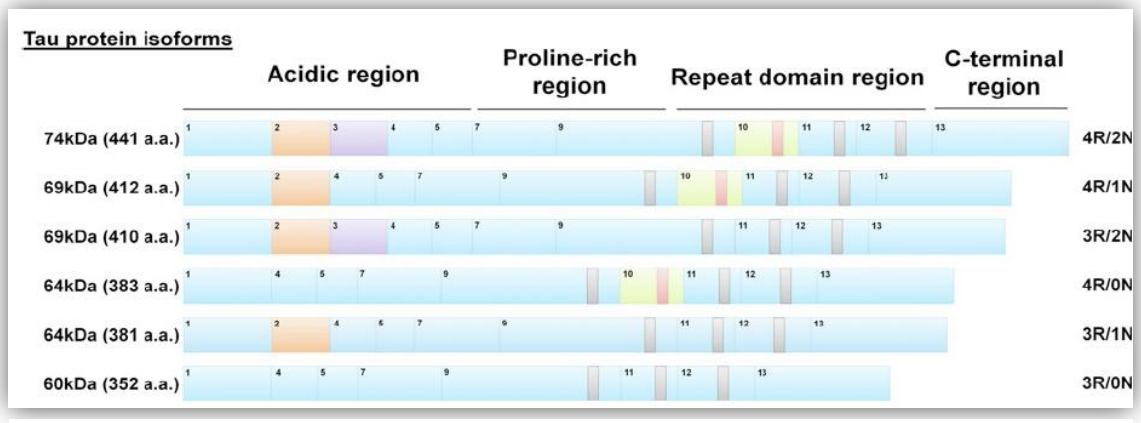

Figure 3 - Tau protein isoform constitution (Martin, Latypova et al. 2011)

or four microtubule-binding repeat domains (3R or 4R tau isoform, respectively), depending on the isoform; and the C-terminal region that is encoded by exon 13 (Figure 3) (Cripps, Thomas et al. 2006, Ballatore, Lee et al. 2007). The designation of 4R or 3R is dependent on presence or absence of exon 10, respectively (Martin, Latypova et al. 2011).

Diverse studies have suggested physiological roles of the N-terminal projection domain, as determining axonal microtubule spacing and interaction or interconnection with cytoskeletal components, mitochondria, and the plasma membrane (Cripps, Thomas et al. 2006). Loomis proved that specific forms of tau are associated with nuclear double-stranded DNA and might play a role in gene regulation (Loomis, Howard et al. 1990).

1.2.1 Tau protein in pathological conditions

The tangles characteristic of AD are made up of filaments formed from an abnormally phosphorylated form of tau called phospho-tau (p-tau) (Blennow 2004).

The conformational stages of tau protein change with physiological conditions. In order to form tau aggregates like PHFs (paired helical filaments) (Figure 4) or NFTs, tau affinity for microtubules must be decreased to release tau in a soluble form. This dissociation of tau from microtubules, most probably by phosphorylation, results in microtubule destabilization (Figure 4) (Martin, Latypova et al. 2011). For example, tau pseudophosphorylation (achieved by replacing a phosphorylation site with glutamic acid or aspartic acid) at specific sites was reported to induce tau conformational change that attenuate its binding to microtubules resulting in soluble tau that exerts neurotoxic effect (Fischer, Mukrasch et al. 2009, Martin, Latypova et al. 2011). Furthermore, tau is targeted by some post-translational modifications that directly or indirectly change its conformation, leading to tau dimerization in an anti-parallel way. Junctions of stable tau dimers results in oligomers that continue to aggregate into subunits

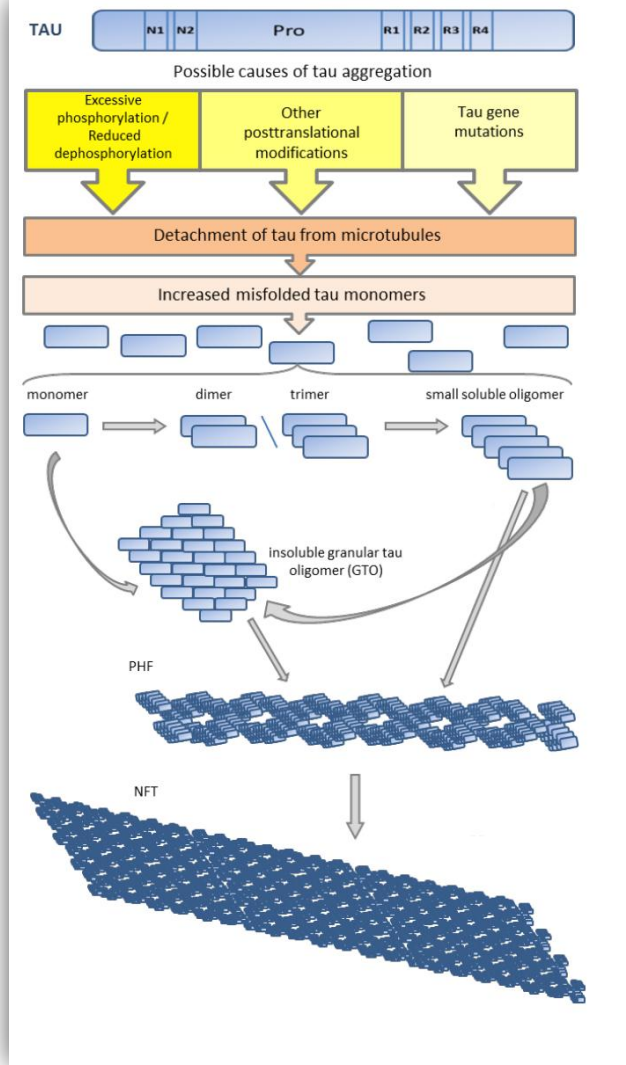

Figure 4 - Proposed sequence of stages leading to tau pathology (adapted from (Mietelska-Porowska, Wasik et al. 2014).)

of filaments called promoters. Two promoters around each other form PHFs, whose assembly eventually creates NFTs (Martin, Latypova et al. 2011).

One of the characteristics that induce aggregation is an increase in the degree of hydrophobicity. However other mechanisms such as oxidation of SH groups (Wille, Drewes et al. 1992) and interaction of tau with polyanions (e.g. herparin) polyglutamate (Friedhoff, Schneider et al. 1998), RNA and other molecules can have the same effect.

Tau protein contains more than 80 sites where kinases, like glycogen synthase kinase 3 (GSK-3β) cyclin-dependent kinase-5, p42/44 MAP kinase, p38 MAPK, stress-activated protein kinases and mitotic protein kinases, can attach phosphate groups (Singh, Kushwah et al. 2012). These are called phosphorylation sites (Martin, Latypova et al. 2011, Singh, Kushwah et al. 2012). When kinases add phosphate groups in different positions on the amino acid chain tau properties are altered. Contrary to GSK-3β, Lithium has been shown to reduce hyperphosphorylation of tau by inhibiting GSK3 in cell culture and in transgenic mice like protein phosphatases 1, 2a, 2b, and 5 (PP1, PP2A, PP2B and PP5) (Singh, Kushwah et al. 2012).

Besides compromising tau's capacity to stabilize microtubules, hyperphosphorylation of tau makes it more resistant to degradation, possibly contributing to the formation of fibrils and tangles as mentioned above (Johnson and Hartigan 1999).

Furthermore, the levels of t-tau and p-tau are strongly correlated both in NL and AD (Blennow, Wallin et al. 1995, Sjogren, Vanderstichele et al. 2001). According to Randall et al. p-tau181 levels are on average 166% higher in AD compared to NL which is a clear difference between the two cases.

Nonetheless a few reports indicate that t-tau as well as p-tau concentrations increase with age in NL individuals. Some authors think that phosporylation of tau and formation of neurofibrillary tangles is not toxic per se, but represents a protective cellular response to oxidative stress (Randall, Mosconi et al. 2013). According to this hypothesis, increased p-tau accumulation with age acts like an antioxidant and could reflect adaptive mechanisms (Castellani, Nunomura et al. 2008). Surpassing the cells' compensatory capacity could result in increased accumulation and cell death as seen in AD.

CSF t-tau concentration shows a marked increase in AD (Blennow, Hampel et al. 2010), reflecting the neuronal damage and cognitive dysfunction associated with the disease

(Lee, Lee et al. 2013, Randall, Mosconi et al. 2013). In this case tau becomes hyperphosphorylated and aggregated to form HPF and posteriorly NFTs, and is no longer associated to the MT network (Figure 3) (Mandelkow and Mandelkow 1998, Sun and Gamblin 2009). This increased t-tau concentration is not surprising given that tau reflects neuronal loss and correlates well with brain atrophy, both concomitant with brain aging (Randall, Mosconi et al. 2013). The tau in these tangles is quite different from that in normal cells, as it is hyperphosphorylated and has a different ratio of expressed isoforms. It is also structurally altered: normal tau is soluble with very little secondary structure, but tau in NFTs bind together to form straight, ribbon-like filaments or paired helical filaments containing β–sheet structure (Mizushima, Minoura et al. 2007, Jeganathan, von Bergen et al. 2008).

Lee and other authors think that tau acts as an important effector of Aβ-mediated neurotoxicity (Lee, Lee et al. 2013). Providing more evidence of tau's importance Roberson and Vossel demonstrated that reducing levels of endogenous tau can significantly decrease Aß- and excitotoxin-induced neuronal dysfunction and consequently functional loss (Roberson, Scearce-Levie et al. 2007, Vossel, Zhang et al. 2010). Furthermore some tau alteration or accumulation can lead to other neurodegenerative diseases named taupathies, including fronto-temporal dementia linked to chromosome 17 with Parkinsonism, progressive supranuclear palsy, corticobasal degeneration, and Pick's disease (Lee, Lee et al. 2013).

1.2.2 Tau Phosphorylation

Protein phosphorylation is the addition of a phosphate group by esterification at three types of amino acids: serine (S), threonine (T) and tyrosine (Y) (Martin, Latypova et al. 2011). This mechanism is the major tau posttranslational modifications that have been described unit now. Tau protein has 85 putative phosphorylation sites, where 45 are serines (53% of phosphorylation sites), 35 are threonines (41%) and only 5 are tyrosines (6%) (Figure 5) (Martin, Latypova et al. 2011).

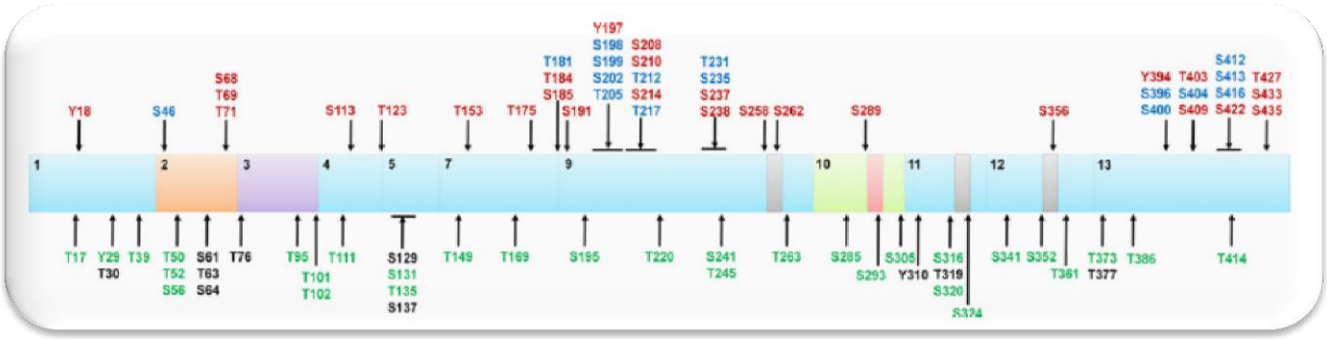

Figure 5 - Tau phosphorylation sites. In red are labeled the pathophysiological phosphorylation sites, in green the non-pathologic phosphorylation sites, in blue the phosphorylation sites found in both conditions and in black putative phosphorylation sites. (Martin, Latypova et al. 2011)

Tau phosphorylation at S262, S293, S324 and S356, respectively found in KXGS of R1, R2, R3 and R4 domains, have been shown to decrease tau binding to microtubules, so this binding can be necessary for the normal function of tau protein (Dickey, Kamal et al. 2007). On the contrary, tau phosphorylation at T231, S235 and S262 contributes to the dissociation of tau from microtubules (Sengupta, Kabat et al. 1998).

The formation of NFTs starts after abnormal phosphorylation of tau as mentioned above (2.1) and this phosphorylation is regulated through the action of various kinases and phosphatases (Martin, Latypova et al. 2011). Protein kinases act at specific phosphorylation sites of tau; these tau kinases are grouped into three classes: kinases PDPKs (proline-directed protein kinases), non-PDPKs and protein kinases specific for tyrosines. The proteins that belongs to the PDPKs family are GSK3β (glycogen synthase kinase-3b), CDK5 (cyclin-dependent kinase-5) and MAPKs. TTBK1/2 (tau-tubulin kinase 1/2), CK1a/1d/1e/2 (casein kinase a/1d/1e/2), DYRK1A (dual-specificity tyrosine phosphorylation and regulated kinase 1A), MARKs (microtubule affinity-regulating kinases), PKA, PKB/Akt, PKC, PKN (protein kinase cAMP-dependent/B/C/N) and CaMKII (Ca2+/Cal-Modulin-dependent protein kinase II) belong to the non-PDPK group (Sergeant, Bretteville et al. 2008). Altered expression and/or activity of kinases such as GSK3β, CDK5, DYRK1A, p38 and CK1 have been reported in the brains of AD patients, suggesting that one or several of them could be involved in tau hyperphosphorylation (Chung, Song et al. 2001). The function of GSK3β specific to the tau protein is phosphorylation at T231 that makes the C-terminus of tau an easier substrate for hyperphosphorylation (Martin, Latypova et al. 2011). However, other kinases, such as CDK5, p38 and PKA, also phosphorylate tau at the same site. In the other sites CDK5 regulates APP processing and tau hyperphosphorylation (Martin, Latypova et al. 2011). MAPKs also phosphorylate tau and are found in NFTs of AD brains (Martin, Latypova et al. 2011). CK1,

can be considered the major tau kinase and DYRK1A phosphorylates tau at least at S202, T212 and S404, while T212 phosphorylation is known to initiate tau hyperphosphorylation by GSK3b (Martin, Latypova et al. 2011). Tau protein can also be phosphorylated on 5 tyrosine residues by SFKs (Src family kinases) such as Src, Lck, Syk, Fyn and by c-Abl kinase (Martin, Latypova et al. 2011).

Tau hyperphosphorylation can be considered as the increase in the number of sites phosphorylated in the same tau molecule and/or as an increase in the number of tau molecules phosphorylated at a given site (Martin, Latypova et al. 2011). Phosphatases remove the phosphate molecules from tau, so tau hyperphosphorylation could result from inhibition of these enzymes. PP2A is one of the majors phosphatases as it accounts for more than 70% of cellular phosphatase activity (Liu, Grundke-Iqbal et al. 2005), is implicated in the regulation of tau phosphorylation level, and has been shown to be decreased by 50% in AD brains (Martin, Latypova et al. 2011). PP5 interacts in vivo with the regulatory subunit A of PP2A (Martin, Latypova et al. 2011). Tau phosphorylation level equilibrium is determined by a balance between the action of various protein kinases and phosphatases (Martin, Latypova et al. 2011). This balance is probably disrupted in AD, which contributes to the abnormal phosphorylation of tau (Martin, Latypova et al. 2011)

Excessive tau phosphorylation and aggregation could be determined by its interaction with several other proteins like Fyn kinase, β-amyloid, Pin1, heat shock cognate Hsc70 and heat shock protein Hsp90, immunophilins FKBP51 and FKBP52, α-synuklein or actin interacting protein PACSIN1. As a consequence tau accumulates in dendritic spines, where it suppresses synaptic responses. In neurons excessively phosphorylated tau is involved in microtubule destabilization, impaired axonal transport of substances, compromised cell signaling, post-synaptic dysfunction, and consequently cognitive impairments (Mietelska-Porowska, Wasik et al. 2014).

1.3 Tau clearance mechanisms in the cell

A given protein can be degraded by different systems depending on the cell type, cellular conditions, or functionality of each proteolytic pathway. The two principal protein degradation mechanisms are lysosomal and proteasomal (Park and Cuervo 2013). The first is

usually responsible for degradation of many long-lived proteins and damaged organelles, while the second is usually related with degradation of short-lived proteins (Wang and Mandelkow 2012). Some authors believe that both mechanisms are involved in clearance of tau and that dependent on the time point and form one or another can take place (Figure 6); others think that the proteasome pathway has the most important role in maintenance of normal levels of tau. Some studies suggest that the proteasome deficit may contribute to the

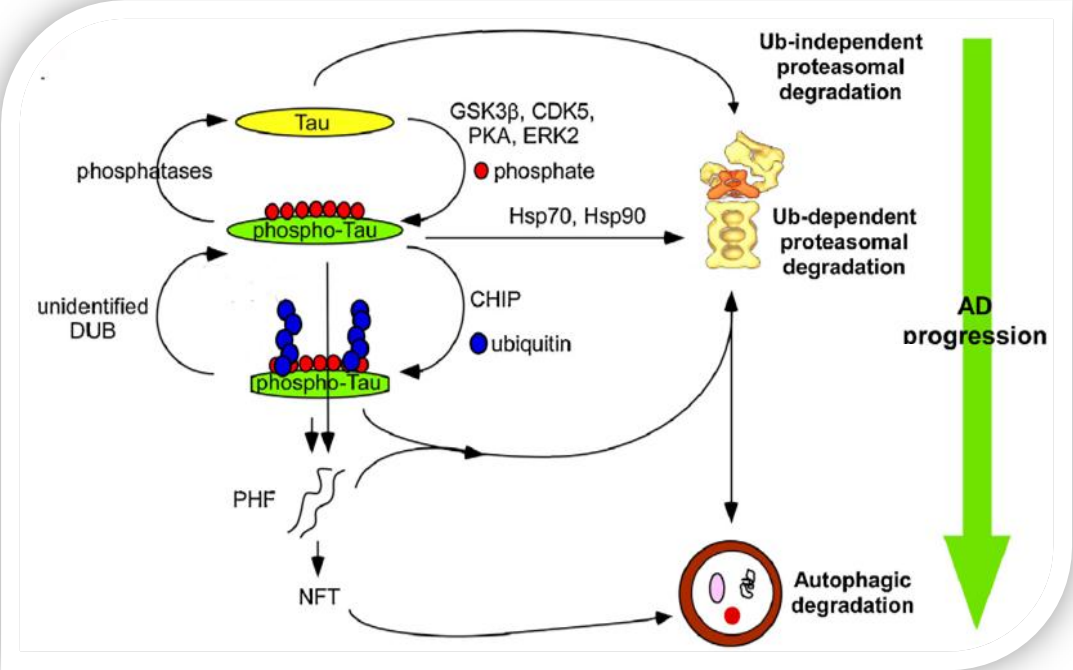

Figure 6 - Tau degradation mechanisms via the UPS and autophagy (adapted from (Lee, Lee et al. 2013))

accumulation of tau proteins in selective neurons in AD (Liu, Wei et al. 2009). However other authors as Lee et al. think that there is a reciprocal mechanism between abnormal UPS activity and PHF formation, where the proteasome function is a consequence of AD and not a cause. In sum, this mechanism is still not understood.

1.3.1 Autophagy

Autophagy is a conserved intracellular recycling process that arises in response to stress such as nutrient deprivation, hyperthermia, and hypoxia (Gelino and Hansen 2012).

This mechanism has emerged as a critical lysosomal pathway that maintains cell function and is essential for neuronal survival (Nixon and Yang 2011, Czaja, Ding et al. 2013).

It is responsible for the degradation of proteins, lipids, sugars, nucleic acids, and larger cellular components such as organelles (Czaja, Ding et al. 2013).

Increasing facts have implicated defective autophagy in the pathogenesis of several major neurodegenerative diseases, AD in particular (Nixon and Yang 2011). In this case a continuum of abnormalities of the lysosomal system has been identified in neurons of the brain, including pathological endocytic pathway responses at the very earliest disease stage and a progressive disruption of autophagy leading to the massive buildup of incompletely digested substrates within dystrophic axons and dendrites (Nixon and Yang 2011).

Autophagy is the ‘‘self-eating’’ of the cell through a process by which cellular components undergo degradation within lysosomes. These organelles are specialized molecules filled of luminal hydrolases that include proteases, lipases, nucleotidases, and glycases and are thus capable of degrading a wide range of substrates, ranging from macromolecular cellular components to entire organelles (Park and Cuervo 2013).

Different types of autophagy coexist in mammalian cells and diverge largely in their mode of cargo delivery to the lysosomes, which gives rise to macroautophagy (MA), microautophagy, and chaperone-mediated autophagy (CMA) (Park and Cuervo 2013).

Three different events can initiate MA: a) low insulin levels that will induce reduction in PI3K - Akt pathway, inactivation of mTOR (the mammalian target of rapamycin) and subsequent activation of the Unc-51-like kinase 1 (ULK1) and vacuolar protein sorting 34 (Vps34) complexes; b) low ATP levels, AMP-activated protein kinase (AMPK) may also activate the ULK1 and Vsp34 complexes in a mTOR-dependent and -independent, manner; and c) c-Jun N-terminal kinase (JNK1) can phosphorylate B-cell lymphoma 2 (Bcl-2) in response to starvation, allowing beclin-1 to dissemble from the beclin-1--Bcl-2 complex to join Vps34 and form the Vsp34 complex. This complex will finally stimulate the formation of the phagophore from the elongation of the endoplasmic reticulum (ER) membrane. After this formation, autophagy-related (Atg) 7 favors the construction of Atg12-Atg5-Atg16L1 complex and the lipidation of microtubule-associated protein 1 light chain 3 (LC3), which is the transformation of LC3-I into LC3-II. LC3-II will attach to the phagophore, permitting its elongation until membranes are completely closed and the autophagosome is formed, process named maturation. Following this, the autophagosome fuses with the lysosome (Figure 7). During this step the lysosomal membrane fuses with the peripheral membrane of the

autophagosome, allowing straight contact of the inner vesicle and its content with lysosomal hydrolytic enzymes. Finally, Atg4B may play a role in the delipidation of part of the LC3-II attached to the outer side of the autolysosome for its recycling (Gracia-Sancho, Guixe-Muntet et al. 2014).

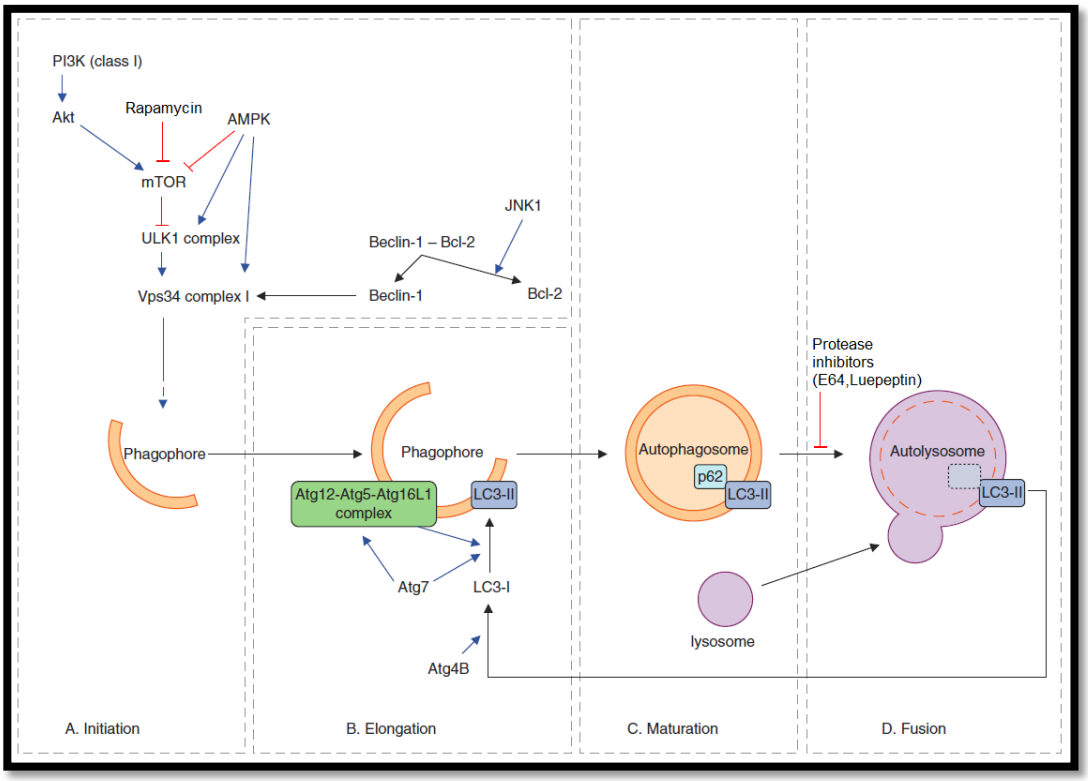

Figure 7 - The process of Macroautophagy (adapted from (Gracia-Sancho, Guixe-Muntet et al. 2014))

Evidence has implicated defective autophagy in the pathogenesis of several major neurodegenerative diseases, particularly AD as well as an increase in number of lysosomal complexes and an accumulation of autophagy vacuoles (Lim, Hernandez et al. 2001, Lin, Lewis et al. 2003, Nixon and Yang 2011).

1.3.2 Ubiquitin-proteasome system

The ubiquitin–proteasome system (UPS) is the principal pathway responsible for the recognition and degradation of misfolded, damaged, or strongly regulated proteins, in addition to performing essential roles in DNA repair, cell cycle regulation, cell migration, the immune response, transcription, apoptosis and synaptic plasticity (Jarome and Helmstetter 2013, Melvin, Woss et al. 2013). This is very important because degradation of regulatory,

damaged, and misfolded proteins is essential to appropriate cellular homeostasis (Schrader, Harstad et al. 2009).

The UPS comprises a 76-amino acid protein named ubiquitin (Ub) and a protein complex with multiple subunits, known as the 26S proteasome, consisting of two 19S regulatory subunits and one 20S catalytic subunit (Vlachostergios, Voutsadakis et al. 2013). The 20S proteasome is a multisubunit enzyme complex comprising seven different α-subunits and seven different β-subunits arranged as a barrel-shape stack of four heptameric rings (Chondrogianni and Gonos 2012).

Protein substrates are led inside the 20S core to undergo progressive degradation by the threonine residues in the β-rings that function as catalytic nucleophiles. The 19S regulatory complex, composed by two multi-subunit substructures (a base and a lid), is responsible for recognition of the target proteins, energy-dependent unfolding, recovery of Ub from its protein conjugates, opening of the gated channels in the α-ring and transfer of the unfolded protein into the inner catalytic core, inducing an allosteric activation of catalytic centers of the 20S proteasome (Chitra, Nalini et al. 2012).

Protein ubiquitination requires a cascade of three different enzymes: E1 ubiquitin activating enzyme, E2 ubiquitin conjugating enzyme, and an E3 ubiquitin ligase. First, the E1 ubiquitin activating enzyme forms an ATP-dependent high-energy thioester attachment with free ubiquitin (Figure 8). After that, the Ub-E1 complex interacts with E2 ubiquitin conjugating enzyme, transferring the ubiquitin from E1 to E2. Consequently, Ub-E2 complex proceeds to interact with the E3 ubiquitin ligases, which mediates either the direct or indirect transfer of ubiquitin to a proximal lysine on the targeted protein. This mechanism allows UPS to control the degradation of a specific class of proteins (Figure 8) with direct way using the Ring (Really Interesting New Gene) family E3 and the indirect one with HECT (homologous to the E6AP carboxyl terminus) family E3 ligases (Deshaies and Joazeiro 2009, Jarome and Helmstetter 2013, Melvin, Woss et al. 2013, Vlachostergios, Voutsadakis et al. 2013).

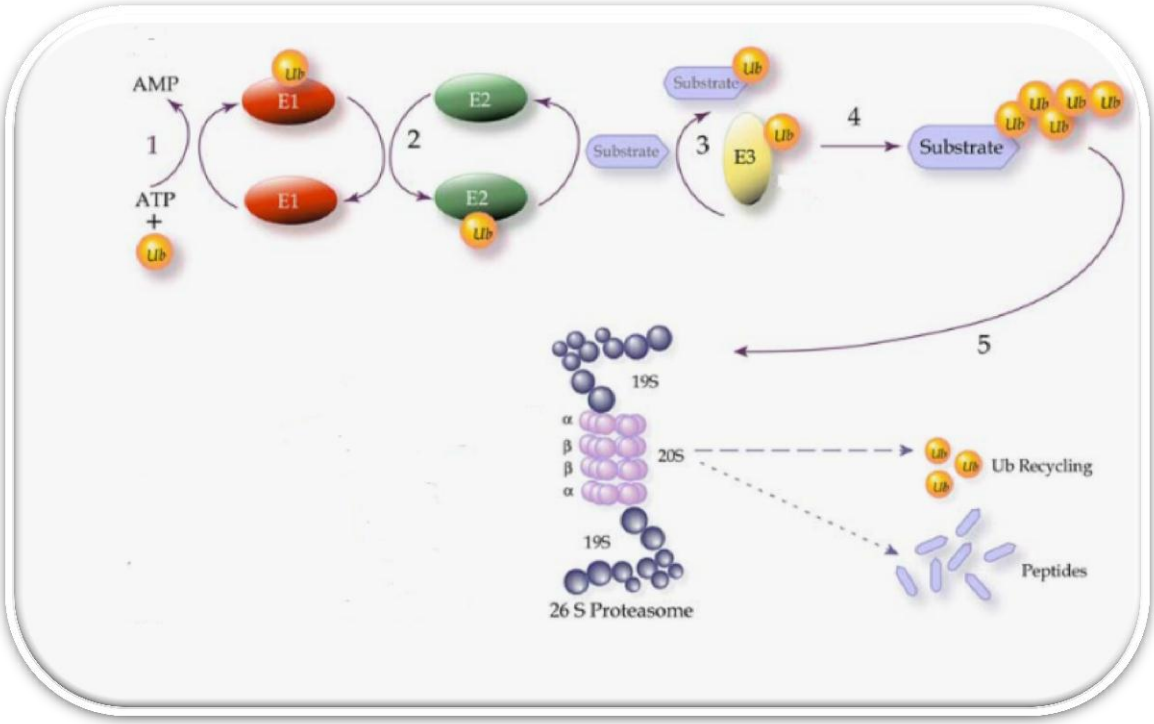

Figure 8 - Overview of the ubiquitin–proteasome pathway (Burger and Seth 2004)

The recognition of the target protein occurs through a unique degradation signal. However, following initial ubiquitin protein conjugation, additional ubiquitins are added to form a polyubiquitin (polyUb) chain, that can be linked via one of seven different lysine residues found on ubiquitin (e.g., K48, K63, or K11) or through the N-terminal methionine residue to form a linear ubiquitin chain (Behrends and Harper 2011, Melvin, Woss et al. 2013). Some authors suggest that polyubiquitiniation of K48, as well as K29 targets the protein to the proteasome, while polyubiquitiniation of K63 involves the lysosome (Vlachostergios, Voutsadakis et al. 2013). Depending on the manner in which the polyubiquitin chain is formed, proteins may be targeted towards the proteasome for degradation or play a role in cell signaling, DNA damage repair, and endocytic trafficking (Grabbe, Husnjak et al. 2011). The number of conjugated ubiquitins (mono vs. multiple monoubiquitination vs. polyubiquitination) can also define the eventual fate of the modified protein (Melvin, Woss et al. 2013). Generally, those that acquire four or more ubiquitin modifiers will provide the optimal signal for degradation. Mono-ubiquitination, on the other hand, regulates protein complex formation, or intracellular translocation of proteins, and multiple mono-ubiquitination is useful for endocytosis of receptor tyrosine kinases and subsequent lysosomal degradation (Vlachostergios, Voutsadakis et al. 2013).

Control of polyubiquitin chain formation is further refined by another class of proteins, deubiquitinating enzymes (DUBs) (Figure 8), which are comprised of two groups, the UCHs (ubiquitin C-terminal hydrolyases) and the USPs (ubiquitin-specific proteases). DUBs are able to cleave the isopeptide bond between ubiquitin and the target protein, initiating either the rescue of a polyubiquitinated protein or the recycling of ubiquitin from the proteasome (Holowaty, Sheng et al. 2003). The E1–E3 enzymatic cascade is paralleled by several ubiquitin-like proteins (UbL): SUMO (small ubiquitin-like modifier), ISG15 (interferon stimulated gene 15), and NEDD8 (neural precursor cell expressed developmentally down-regulated protein 8), all of which are activated and conjugated to proteins using similar machinery. Similarly to DUBs in the ubiquitin pathway, the isopeptide bond between an UbL and a protein is cleaved by UbL proteases allowing them to function as a reversible post-translational modification (Melvin, Woss et al. 2013).

The substrates of USP are covalently conjugated with Ub, which is a highly conserved 76-residue protein. This conjugation is based on isopeptide bonds between the ε-amine of internal lysine residues and the C-terminal carboxylic group of ubiquitin (Lee, Lee et al. 2013).

Ub proteins are encoded by four different genes; UBB, UBC, UBA52, and UBA80, in mammalian and are abundants in cells (Lee, Lee et al. 2013). Kudo show that the levels of Ub are significantly increased in AD brain (Kudo, Iqbal et al. 1994).

Recent evidence suggests that protein degradation may be a critical regulator of memory formation and stability in the mammalian brain. Therefore, the unique and vital functions carried out by the UPS in regulating protein levels have made it a very attractive target for novel therapeutics (Jarome and Helmstetter 2013, Melvin, Woss et al. 2013).

1.3.2.1 Tau Ubiquitination

The first evidence for the relation between tau and UPS appeared from the frequent co-localization and accumulation of ubiquitin in PHFs and NFTs (de Vrij, Fischer et al. 2004).

Supporting the theory that tau is degraded by UPS, some authors proved that *in vitro,* these proteins were degraded by the 26S and 20S, as well as the ATP/Mg2+-dependent proteasome protease system (Liu, Wei et al. 2009).

Tau ubiquitination was first proposed about three decades ago when it was found that anti-ubiquitin antibodies bound to NFTs. Ihara's group confirmed this by demonstrating that that insoluble PHF-tau isolated from an AD brain was ubiquitinated at tau residues Lys^{254}, Lys^{257}, Lys^{311} and Lys^{317} and that these ubiquitinations were done through Lys^{48}-liked ubiquitination (Morishima-Kawashima, Hasegawa et al. 1993). Some years latter Cripps provided evidence that soluble PHF-tau from AD brains was ubiquitinated at Lys^{254}, Lys^{311} and Lys^{353} and that these ubiquitinations were done not only through Lys^{48}-liked ubiquitination but also trough Lys^{11}-liked ubiquitination chains (Cripps, Thomas et al. 2006).

Under non-pathological conditions, in vitro, tau proteins have been shown to be ubiquitinated and proteolytically processed by UPS (Martin, Latypova et al. 2011). In these proteins the ubiquitination can occur in its C-terminus, at K254, K311 and K353 (Cripps, Thomas et al. 2006, Martin, Latypova et al. 2011).

One of the Ub, with a 19-residue C-terminal extension from the UBB gene (gene that encodes ubiquitin in humans), or UBB + 1 is often found to be accumulated in NFT in Alzheimer's disease and other tauopathies and these data suggest that tau ubiquitination is secondarily involved in tau pathology (Martin, Latypova et al. 2011, Lee, Lee et al. 2013). That is, these UB capped polyUb chains are resistant to deubiquitination and inhibit proteasomal activity, which may mediate neurodegeneration through mitochondrial stress and p53 activation in neurites (Tan, Sun et al. 2007)

Tau protein contained in PHFs has been reported to be ubiquitinated after its hyperphosphorylation and glycosylation, and increases as PHFs maturate, however studies indicate that PHFs inhibit the UPS so this relationship needs to be understood (Cripps, Thomas et al. 2006, Martin, Latypova et al. 2011). Moreover other things such the temporal relations between tau phosphorylation, tau ubiquitination need to be studied further to better understand what forms of tau, during this process, are responsible for disease pathology (Cripps, Thomas et al. 2006).

In sum, tau is reported to be degraded to be degraded by both autophagy and via the proteasome, but there is currently still significant debate about which pathway is degrading tau protein, and under which circumstances.

1.3.2.2 Ubiquitin-specific protease

Bonds between ubiquitin-ubiquitin complexes and ubiquitin-protein complexes can be cleaved by the action of DUBs (Dayal, Sparks et al. 2009). This cleavage is done because DUBs are cysteine proteases (excluding JAMM which are metalloproteases) that catalyse the removal of Ub from Ub-modified proteins (Stanisic, Malovannaya et al. 2009)

DUBs are divided into five subclasses based on their catalytic mechanism and their active site conformation, these subclasses include: UCHs (Ub C-terminal hydrolases), USPs (Ub-specific proteases), MJDs (Machado-Joseph disease protein domain proteases), OTUBs (ovarian tumor proteases), and JAMMs ((JAB1/MPN/MOV34 metalloenzyme) (Dayal, Sparks et al. 2009, Stanisic, Malovannaya et al. 2009, Wang, Yin et al. 2009). The largest of these is the USP family (Dayal, Sparks et al. 2009).

Some DUBs remove ubiquitin from substrates before proteasomal recognition, resulting in inhibition of substrate degradation, others regulate the pools of unanchored ubiquitin and polyubiquitin (Dayal, Sparks et al. 2009). The process of deubiquitination of Ub-protein substrates can be done by two different ways: by removal of the entire Ub chain from the protein or by removal of individual or multiple ubiquitins from the chain in a process termed “editing” (Stanisic, Malovannaya et al. 2009). One source of free unanchored polyubiquitin originates from the deubiquitination of proteins at the proteasome. After recognition of the ubiquitinated protein by the proteasome, the ubiquitin is released, allowing it to be recycled (Dayal, Sparks et al. 2009).

The largest subclass, the USP family, contains more family members than the UCHs, have higher molecular weights, and are thought to have specific protein targets (Dayal, Sparks et al. 2009) (Holowaty, Sheng et al. 2003). These proteases can be identified by conserved sequences contained in the active site, but not by the sequences outside of the catalytic domain because these are highly divergent, likely reflecting their role in mediating interactions with different protein targets (Holowaty, Sheng et al. 2003).

Studies have shown that USPs can play specific roles in various biological processes in higher eukaryotes, suggesting a more specialized role as cellular regulators in multicellular organisms (Holowaty, Sheng et al. 2003)

Sixty three putative human USP genes have been identified (Wing 2003). In our project we will focus on USP5, USP7, USP9x as well as the DUB OTUB1. These DUBs have been observed to co-immunoprecipiate with tau from mouse brain as quantified by iTRAQ MS quantification. Because of this observed interaction with tau, we evaluated whether overexpression of these DUBs could alter tau levels and tau aggregation.

1.3.2.2.1 USP5

The DUB called USP5 (more commonly known as isopeptidase T or IsoT) is involved in disassembly of free polyubiquitin chains. Conjugation of Ub to a target protein involves formation of a peptide bond between the c-terminal glycine of Ub and the ε-amino group of a lysine on the target protein. Subsequent ubiquitins are added by formation of a peptide bond between the c-terminal glycine of the next Ub, and an ε-amino group of a lysine on the first ubiquitin. In this manner, the proximal end of the ubiquitin chain is the c-terminal of the initial ubiquitin, and the distal ends are the n-terminals of ubiquitin branches. One role of USP5 is to sequentially remove ubiquitin from the proximal end of unanchored polyubiquitin chains.

A free ubiquitin carboxyl terminus is required at the proximal end of the polyubiquitin chains, to achieve efficient catalysis. This is because the free c-terminal occupies the S1' (leaving group) site of USP5 and activates the DUB (Dang, Melandri et al. 1998, Reyes-Turcu, Horton et al. 2006). (Reyes-Turcu, Ventii et al. 2009). When a polyubiquitin chain is still attached to a peptide or lacking the C-terminal glycine on the proximal ubiquitin it is not efficiently hydrolyzed. Thus, USP5 proofreads the C-terminus of polyubiquitin chains and will not cleave them if they are still attached to a protein or peptide. In this way USP5 can take away the polyubiquitin end products of proteasomal degradation but cannot prematurely deubiquitinate a polyubiquitinated protein (Reyes-Turcu, Ventii et al. 2009).

Fan et al. (2013) evaluated the impact of USP5 knockout in *Drosophila* model and concluded that: a) the loss of these DUB leads to severe defects in the specification and differentiation of photoreceptors and b) loss of USP5 activates apoptosis and the JNK

pathway (Fan, Huang et al. 2014). In addition Yoshioka et al. provide evidence that USP5 can be a key molecule for the production of TNF-α (Yoshioka, Ye et al. 2013)

Nakajima et al. (2014) demonstrated that USP5 is a novel factor functioning in the repair of DNA double-strand breaks via homologous recombination. They also suggest that disassembly of free polyubiquitin chains at DNA damage sites is necessary for efficient double-strand break repair and this disassembly is performed by USP5.

1.3.2.2.2 USP7

The human DUB called USP7 (DUB ubiquitin specific peptidase 7) or HAUSP (herpesvirus-associated ubiquitin-specific protease) is a cysteine protease that was originally identified by virtue of its interaction with the herpes simplex virus type I regulatory protein (ICP0). ICP0 is an E3 ubiquitin ligase and Epstein-Barr nuclear antigen 1 (EBNA1) during viral infection (Holowaty, Sheng et al. 2003, Huang, Zhou et al. 2011, Nicholson and Suresh Kumar 2011). ICP0 promiscuously activates gene expression and induces the degradation of some cellular proteins. This protease comprises four structural domains; an N-terminal domain, a catalytic domain, and a C-terminal domain that contains at least five ubiquitin-like domains (Holowaty, Sheng et al. 2003, Reverdy, Conrath et al. 2012).

Today, multiple proteins are identified as potential substrates/bindings partners of USP7. Some of these substrates play critical roles in tumor suppression, immune responses, DNA repair, viral replication, and epigenetic modulators (Nicholson and Suresh Kumar 2011). For that reason the deubiquitinating enzyme USP7 is an emerging oncology and antiviral target.

A proposed mechanism by which USP7 acts during DNA repair is presented by Schwertman et al., in this model Schwertman suggests that USP7 is critical for the protection of Cockayne syndrome group B protein by contracting their ubiquitin-dependent degradation (Schwertman, Vermeulen et al. 2013).

In a review discussing other functions of USP7, Huang et al (2011) describe how under oxidative stress conditions USP7 inhibits nuclear localization and transcriptional activity of FOXO4 (forkdhead box O transcription factor) through the interaction with and deubiquitylating FOXO protein.

This DUB can also deubiquitylates tumor suppressor PTEN, and thus regulates its nuclear exclusion; it can also regulates the stability of p53, other crucial tumor suppressor (Huang, Zhou et al. 2011).

In 2010 Kon et al. demonstrated that if USP7 was inactivated during early embryonic development the result would be early embryonic lethality (Kon, Kobayashi et al. 2010). Later on Huang showed that USP7 prevents degradation of the REST (repressor element 1-silencing transcription factor) by deubiquitylation and consequently promote maintenance of neuronal stem/progenitor cells (Huang, Wu et al. 2011).

USP7 can be involved in one mechanism of epigenetic regulation, the monoubiquitylation of histones H2B and H2A. Nicholson showed that this DUB can deubiquitylates monoubiquitylated H2B in vitro (Nicholson and Suresh Kumar 2011).

USP7 is also involved in the regulation of cell cycle or mitotic check points through Claspin and Chfr respectively (Nicholson and Suresh Kumar 2011).

1.3.2.2.3 OTUB1

OTU domain-containing ubiquitin aldehyde-binding protein 1 (OTUB1) is a deubiquitinating enzyme that has been shown via its *in vitro* deubiquitinating activity to preferentially deubiquitinate K48-linked polyubiquitin chains (Stanisic, Malovannaya et al. 2009). Despite the preference for K48-linked polyubiquitin, this Dub also regulates synthesis of K63Ub in a noncanonical manner.

Structurally this molecule has two distinct ubiquitin binding sites, a distal site and a proximal site that contains the ~45 N-terminal residues of OTUB1 (Wang, Yin et al. 2009).

A potential mechanism whereby OTUB1 regulates synthesis of K63Ub involves the N-terminal helix of OTUB1 positioning itself to interfere with UEV1a binding to the ubiquitin conjugating enzyme (E2) UBC13, as well as with attack on the thiolester by an acceptor ubiquitin, thereby inhibiting K63Ub synthesis (Stanisic, Malovannaya et al. 2009). The capacity of OTUB1 to bind preferentially to the UBC13~Ub conjugate and consequently inhibit ubiquitin transfer is suggested to be allosterically regulated by free ubiquitin binding to the distal site of OTUB1, which triggers capture of the conjugated ubiquitin in the OTUB1

proximal site (Stanisic, Malovannaya et al. 2009). Most studies performed with OTUB1 are done using UBC13 because is the only known E2 ubiquitin (Ub)-conjugating enzyme that produces Lys-63-linked Ub chains with its cofactor variant MMs2 or UEV1a (Sato, Yamagata et al. 2012).

In 2009, Edelmann et al. did ubiquitin-cleavage assays using a truncated from of OTUB, lacking the first 40 amino acids, and the result was no effect in proteolytic properties of OTUB1, indicating that the N-terminal region of these deubiquitinating enzyme does not influence cleavage preference *in vitro* (Edelmann, Iphofer et al. 2009).

The mechanism of non-canonical OTUB1-mediated inhibition of ubiquitination require more studies, however in 2013 Wiener et al. think have discovered a second role of OTUB1-E2 interactions (Sato, Yamagata et al. 2012, Wiener, DiBello et al. 2013). They think that this interaction is to stimulate OTUB1 cleavage of Lys48 polyubiquitin. In their hypothesis this stimulation is regulated by two factors: the ratio of charged to uncharged E2 and by the concentration of Lys48-linked polyubiquitin and free ubiquitin. They did studies of human and worm OTUB1 and UBCH5B they show that the E2 enzyme stimulates binding of the Lys48 polyubiquitin substrate through stabilization folding of the OTUB1 N-terminal ubiquitin-binding helix (Wiener, DiBello et al. 2013).

1.3.2.2.4 USP9x

Ubiquitin specific protease 9, also called FAM, is a substrate-specific DUB that is highly expressed in the CNS of developing humans and mice and is located on the X chromosome (Stegeman, Jolly et al. 2013).

The function of this DUB has been implicated in several aspects of CNS developing and was demonstrated that its expression is decreased when the CNS is already mature. However, its expression remains strong in the neurogenic regions (Stegeman, Jolly et al. 2013).

USP9x targets a large variety of substrates so is implicated in multiple physiological pathways including neurodevelopmental signaling pathways such as Notch, Wnt and TGF-ß. Some examples of its targets are ß-catenin, AF-6 (acute lymphoblastic leukemia-1 fusion partner from chromosome 6), Epsin, EFA6, MCL-1 and α-synuclein (Stegeman, Jolly et al. 2013, Xie, Avello et al. 2013). In the Notch pathway USP9 regulates the ubiquitin ligase Mind

Bomb1, as well as the trafficking accessory protein Epsin and stabilizes Itch, a Notch intracellular domain E3 ligase. As mentioned above USP9 binds ß-catenin, regulating cell-cell adhesion and Wnt signaling on mammalian cells and tissues, which is required for proper CNS development (Stegeman, Jolly et al. 2013). Signaling of Smad4 by members of the Tgf-ß family happens just after its deubiquitylation performed by USP9x. Through other substrates USP9x can regulate neuronal progenitor adhesion and proliferation (Xie, Avello et al. 2013). USP9X also stabilizes MCL1 and thereby promotes cell survival. MCL1 is essential for the survival of progenitor and progenitor cells of multiple lineages and increased USP9X expression correlates with increased MCL1 protein in some lymphomas (Schwickart, Huang et al. 2010).

The relation between USP9 and MCL-1 and α-synuclein suggests a possible role of the USP9 in tumor cell apoptosis and neurodegenerative disease (Schwickart, Huang et al. 2010, Xie, Avello et al. 2013) Beside these diseases it has been demonstrated that USP9x has been implicated in lissencephaly and epilepsy and is an X-linked Intellectual Disability candidate gene (Stegeman, Jolly et al. 2013).

1.4. Project goals

Taking into account that accumulation of pathogenic tau protein is one of the most important neuropathologic hallmarks of Alzheimer's disease and other Tauopathies and more importantly that aggregated tau is an important pathogenic player in AD pathogenesis, a decrease of tau aggregates seems to be a possible strategy to treat or at least attenuate diseases progression.

In this project, the major goals are:

- ✓ To evaluate the effect of ubiquitination on aggregation and degradation of tau protein;
- ✓ To evaluate the effect of overexpression of USP5, USP7, USP9x and OTUB1 on aggregation of tau protein;
- ✓ To evaluate the effect of proteasome and autophagy pathways on normal tau protein turnover and the effect of autophagy enhancement on tau aggregation and tau turnover.

Materials

2.1 Biological Materials

Material	Origin
Human kidney-derived QBI-HEK 293A Cells (QBI) WT	QBiogene
Human kidney-derived QBI-HEK 293A (QBI) inducible tau cells	Homemade
One Shot® TOP10 (C4040-10)	Invitrogen

2.2 Antibodies and dyes

Antibody	Target	Host specie	Source
Actin (C4) (MAB1501)	Actin	Mouse	Milipore
HT7	Human Tau	Mouse	Homemade and Thermo Scientific
AT8	Phosphorylated residues Ser202/Thr205	Mouse	Produced in house
hT10 biotinylated	aa. 29-36	-	
pTX biotinylated	confidential	-	
LC3B	LC3B	Rabbit	Sigma
HAUSP	USP7/HAUSP	Rabbit	Cell Signaling
OTUB1	OTUB1	Rabbit	Cell Signaling
USP5	USP5	Rabbit	Atlas Antibodies
USP9x	USP9x	Rabbit	Cell Signaling
TAP	C-terminus of TAP	Rabbit	Thermo Fisher

	(tag)		Scientific
HA	HA-tagged fusion proteins	Rabbit	Invitrogen
FLAG	FLAG-tagged fusion proteins	Rat	BioLegend
Ubiquitin	Ubiquitin, polyubiquitin and ubiquitinated proteins	Rabbit	Cell Signaling
Alexa Fluor® 555 Goat Anti-Mouse IgG (H+L) (A-21424)	IgG	Mouse	Life Technologies
DAPI (62247)	Nucleus	-	Thermo Science
HT7 biotinylated	-	-	Thermo Science Promega
HaloTag® TMR Ligand (G825A)	TMR Ligand-tagged fusion proteins	-	
HaloTag® Coumarin Ligand	Coumarin Ligand-tagged fusion proteins	-	Promega

2.3 Lab material and Reagents

Product	Company
Falcon 15 mL (352196)	**Corning**
Falcon 50 mL (352070)	
Pipettes P2, P10, P20, P100, P200 and P1000	**Gilson PIPETMAN Classic**
Pipette tips	**Eppendorf**

Tubes of 0.5, 1.5 and 2mL	
Blotto non-fat dry milk (sc-2325)	**Santa Cruz**
Smart leader (MW-1700-10)	**Eurogentec**
Conical Tubes Screw Caps of 50mL(358206) and 15 mL(352097)	**BD Falcon**
Tissue culture flasks (353028)	
DMEM-Dulbecco's Modified Eagle Medium (1965)	**Life technologies**
Dulbecco's phosphate-buffered saline (D-PBS) (1x) (-) calcium (-) magnesium chloride (D8537)	
Dulbecco's phosphate-buffered saline (D-PBS) (1x) (+) calcium (+) magnesium chloride (D8662)	
E-Gel® single comb (G5018-08)	
L-Glutamine (25030)	
MagicMark™ XP Western Protein Standard (LC5602)	
NuPage® MES SDS Running Buffer (NP0002)	
NuPage® MOPS SDS Running Buffer (NP0001)	
NuPage® Sample Reducing agent (10x)	
NuPage® LDS Sample Buffer (NP0007)	
OPTIMEM medium (11058)	
Penicilin-Streptomycin antibiotic solution (15140)	
S.O.C medium (15544034)	
SeeBlue® Plus2 Pre-Stained Standard (LC5625)	

Sodium Pyruvate (11360)	
Trypsin-EDTA 0.05% (25300-054)	
cOmplete mini ETDA-free Mini Protease Inhibitor Cocktail Tablets (04693159001)	**Roche**
PhosphoSTOP Phosphatase Inhibitor Cocktail Tablets (04906837001)	
E64 protease inhibitor (E3132)	**Sigma-Aldrich**
Leupeptin hemisulfate salt (L5793)	
Luria Broth – Liquid Medium (L2542)	
Methanol (32213)	
RIPA buffer (R0278)	
Sodium acetate (S2889)	
Triton™ X-100	
Tween 20 (P1379)	
FuGene 6 (E2691)	**Promega**
Pierce™ BCA Protein Assay Kit (23225)	**ThermoScientific**
SuperSignal West Dura Chemiluminescent Substrate (34076)	
SuperSignal West Femto Chemiluminescent Substrate (34096)	
10x FastDigest Green Buffer (B72)	
BioPORTER Reagent QuikEase Single-Use Tubes (BP509696)	**Genlantis**
CriterionTM Precast Gel 4-12% Bis-Tris	**Bio-Rad**
Trans-Blot® Turbo™ Transfer System Transfer Pack	
iBlot® Gel (IB3010-01)	**Invitrogen**
PureLink™ HiPure Plasmid Filter Maxiprep Kit (K210017)	
Rapamycin (1292)	**Tocris bioscience**

Multiwell plates of 96 (655946) and 24 (354414)	**Falcon**
AlphaLISA buffer	**PerkinElmer**

2.4 Lab equipment

Equipment	Company
Vi-Cell Counter XR	Beckman Coulter
Trans-Blot® Turbo™ Transfer System	Bio-Rad
Leica DMI4000 B	Leica Microsystems
Thyphoon	Molecular Dynamics
Myc Microscoop	Olympus
Envision® 2102 Multilabel Reader	PerkinElmer
Envision® Multiplate Reader	
G:BOX	Syngene
iBlot® Gel Transfer Device	Invitrogen

Methods

3.1 Cell Culture

Human kidney-derived QBI-HEK 293A Cells (QBI) are an immortalized line of primary human embryonic kidney cells. They are very easy to grow and transfect and have been widely used in cell biology research for many years. In this project these were the cells that were used, stably expressing hTauP301L and not expressing tau. QBI cells were cultured in DMEM medium containing 10% heat inactivated Fetal Bovine Serum, 10 mM pyruvate, 20 mM L-Glutamine and Penicilin-Streptomycin.

Tau expression in stably expressing hTauP301L cell line was under control of the tet repressor protein, and was induced by addition of 0.1µg/mL doxycycline to the cell culture medium.

To detach cells, cells were washed twice with magnesium/calcium-free PBS, trypsin 0.05% was added, and the flask was placed in the incubator for 3min. Following detachment, to inhibit trypsin activity, DMEM medium was add to the cells at a DMEM:trypsin ratio of 4:1. Quantities of trypsin and DMEM medium added varied based on flask/well size.

3.2 Plasmid transfection

Cells were seed in a 24 well plate at a density of 25000 per well in 1mL of medium or in a 96-well plate at a density of 8000 cells per well in 100µl of medium and were left to grow overnight.

FuGene6 was added directly to optimem medium in a ratio of 3:1 or 1.5:1 (FuGene:µg of plasmid) and incubated for 5 minutes at room temperature (RT) after gently mixed. Then the plasmid was added to the mix and incubated for 15 minutes at RT after gentle mixed. At the end of the incubation the mix was added to the cells and they were incubated overnight at 37°C, 5% CO2. For transfection of a 24 well plate, optimem / Fugene (3:1) - DNA/Pen-Strep-free medium volumes per well were added at quantities of: 20µl/ 0.25 or 0.5 – 1µg / 200µl respectively per well. For 96 well plates, the optimum/ Fugene (3:1) - DNA/Pen-Strep-free medium quantities used were 3µl/ 0.08 – 0.15µg / 33µl respectively per well.

3.3 *In vitro* fibrilization of recombinant tau

K18tau-P301L is corresponding to amino acids 244-372 of 2N4R MAPT with the proline at 301 mutated to a leucine (Figure 9) (von Bergen, Barghorn et al. 2005). MT-binding repeats of tau are essential and sufficient for in vitro fibrilization, and repeat domain alone assembles into fibrils more readily than full-length tau (von Bergen, Barghorn et al. 2005, Guo and Lee 2011). K18tau-P301L was expressed in bacteria and then the protein was purified by TeboBio.

Tau was induced to fibrilize through a mix of 40 µM (0.6 mg/ml) K18tau-P301L with 40 µM low-molecular-weight heparin and 2 mM DTT in 100 mM sodium acetate (pH 7.0) and incubated for 3 days at 37°C. Then the fibrillization mixture was centrifuged at 100,000g for 30 min at 4°C. The pellet was washed once with 100 mM sodium acetate (pH7.0) and resuspended in an equal volume of 100 mM sodium acetate (pH 7.0). The final result was frozen as single-use aliquots at -80°C (Guo and Lee 2011).

The interaction of repeat domain with polyanions leads to a conformational switch from mostly random coil to a beta sheet structure, through the formation of nucleus of aggregation, and the nucleus previously formed can be elongated to build PHFs (von Bergen, Barghorn et al. 2005).

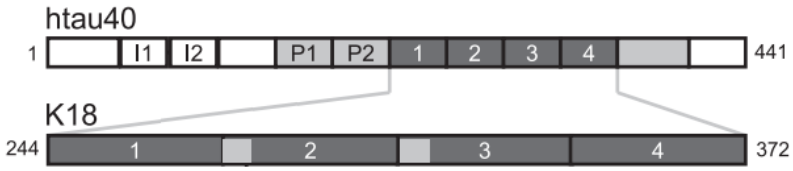

Figure 9 - The isoform htau40 is the longest isoform in the human CNS. Construct K18 comprises the sequence of four repeats and in this case contains the point mutation P301L (adapted from (von Bergen, Barghorn et al. 2005))

3.4 Fibril transduction with BioPorter

Introduction of minimum quantities of misfolded performed tau fibrils into tau-expressing cells will rapidly recruit large amounts of soluble tau into filamentous inclusions resembling NFTs (Guo and Lee 2011).

Before adding the fibrilized K18P301L tau to cells to induce aggregation, the fibrils need to be broken into smaller pieces. To do this, the K18P301L fibrils were diluted to 10µM with 100 mM sodium acetate (pH 7.0) and sonicated with 25 pulses of 2 seconds with 30 seconds of pause between each pulse, while maintained continuously on ice. Fibril seeding was performed 24 hours after plasmid transfection in QBI cells. Eighty µl of the sonicated fibrils were added to one tube of BioPORTER reagent, vortexed gently for 5 seconds and allowed to stand at RT for 5-10 minutes. The cells were washed with OptiMEM and 100 µl OptiMEM were added to each well (24 well plate). The pre-mix fibril-BioPorter was diluted with 1420µl OptiMEM. After a gentle mix 100µl of this was added to the cells. The cells were replaced in the incubator at 37°C. After 4 hours 0.2 ml of cell culture medium was added and cells were incubate for 2 days at 37°C to allow for aggregate formation. Protocol adapted from (Guo and Lee 2011).

3.5 Protein Extraction

Cells were washed on ice with cold magnesium and calcium-containing Dulbecco's Phosphate-Buffered Saline followed by 100µL of RIPA lysis buffer containing protease and phosphatase inhibitor (Roche) was added to each well (for 24 well plate). The wells were scraped with pipette tips and the plate was frozen at -80°C for 5 minutes. Then the plate was then thawed on ice and the lysis buffer present in each well was removed and placed in eppendorfs. The samples were sonicated for 10 seconds then on ice for 10 seconds (repeated six times) and then centrifuged (4°C, 14000g, 10 minutes). The supernatant was then transferred to a new eppendorf and frozen or used.

When samples were quantified via AlphaLISA the lysis buffer used contained 1% Triton X100 in PBS pH7.6 + Phosphostop + Protease inhibitors instead of RIPA.

3.6 Western Blot

After cell lysis and protein quantification, 5 or 10µg of protein from each sample were loaded on Criterion™ Precast Gel 4-12% Bis-Tris and run in MOPS or MES SDS running buffer. Trans-Blot® Turbo™ Transfer System was used to transfer proteins from the

polyacrylamide gel onto the nitrocellulose membrane. After transfer, the membrane was blocked in 5% Blotto milk in TBS-T (1M Tris, 150nM sodium chloride and 0.05% Tween-20, pH 8.5) for 1 hour. The membrane was incubated with the primary antibody diluted in 5% Blotto milk or 5% BSA in TBS-T overnight at 4°C. Before incubating with secondary antibody diluted in TBS-T the membrane was washed 3 times in TBS-T for 5 minutes each. Protein detection was done with SuperSignal West Dura Chemiluminescent Substrate kit or SuperSignal West Femto Chemiluminescent Substrate kit. Signals were captured and quantified by the G:BOX Chemi system. For reprobing, membranes were stripped of secondary antibody with Restore™ Western Blot Stripping Buffer for 10min with agitation at RT. Before incubation with primary antibody the membranes were washed 3 times 5 minutes in TBS-T and blocked 30 minutes in 5% Blotto milk in TBS-T.

When detecting labeled proteins with HaloTag TMR ligand the protocol used was the same, except after transfer the membranes were dry and then measured and quantified by the Typhoon scanner that detects the fluorescence of this ligand. To quantify the control protein, the membrane was washed again in TBS-T and all the protocol is the same as previous.

3.7 AlphaLISA

The AlphaLISA bead-based technology (exclusive Amplified Luminescent Proximity Homogeneous Assay) uses a luminescent oxygen-channeling chemistry. No washes and smaller sample sizes are some examples of the differences between this technology and ELISA.

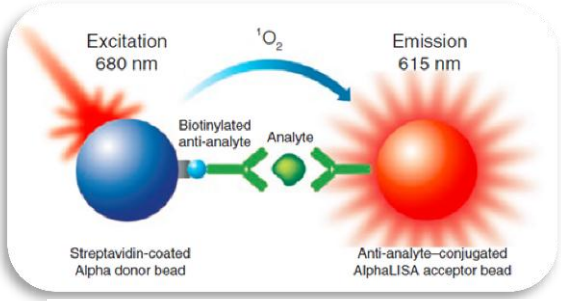

Figure 10 - Principle of the AlphaLISA technology

On this assay two antibodies that bind to different epitopes in the protein of interest are required. The first (biotinylated) antibody binds to the analyte as well as a streptavidin-coated donor bead. The second antibody is directly conjugated to AlphaLISA acceptor beads. In the presence of the analyte, the two beads come into close proximity what will allow the adjuvant reaction. Excitation of the donor beads at 680 nm generates single

oxygen molecules that trigger a series of chemical reactions in the acceptor beads resulting in a sharp peak of light emission at 615 nm (Figure 10).

After cell lysis, a dilution curve for each sample was made, and 5µl of each dilution was added to the OptiPlate™ – 384 or 96 well plate along with 20µl of Biotinylated AB-Acceptor Bead conjugated AB mix. Plates were incubated of 2 hrs at RT. After the incubation 25µl of Donor Beads were added and plates were incubated for another 30 minutes. At the end of the incubation the plate was read with Envision® 2102 Multilabel Reader or Envision® Multiplate Reader.

In our lab different antibodies are used to detect the aggregates of tau as well as total tau. The most used antibody to analyze the total amount of tau present in the sample is the biotinylated HT7 together with acceptor bead conjugated hTau10. Related with the aggregates quantification a diverse range of antibodies are possible but in this project only the complex hTau10/hTau10 and pTX/pTX were used.

3.8 Immunocytochemistry

QBI cells were seeded in a 96 µClear bottom plate at a density of 8000 cells per well. 2 days after the seeding the cells were washed with PBS at RT and a 4% paraformaldehyde (PFA) fixation or a 4% PFA 1% Triton fixation was done (Guo and Lee 2011). After the washes 4% PFA or 4% PFA 1% Triton was added and an incubation of 10 minutes at RT took place. The cells were washed 3 times with PBS and the quenching was done. To do this 100µL of 50mM NH4Cl were added to each well for 30 minutes at RT. The cells were washed again (3x) and they were ready to stain.

The staining protocol was the same for both fixations. First the blocking was done with 5% BSA (bovine serum albumin) in PBS for 30 minutes at RT. After this step the primary antibody (AT8 to the aggregates and HT7 to the total) in PBS-0.1% BSA was added for 1-2hr at RT. The cells were washed again in PBS and the secondary antibody (alexafluor 555) was added overnight at 4°C. After 3 washes the nucleus were labeled with DAPI for 10 minutes and the plates were analyzed.

Pictures were taken using a Zeiss Axiovert 135 fluorescence microscope equipped with a Zeiss Axiocam ICc1 camera and Zeiss Axiovision 4.8 software using 40x objective.

3.9 Imunoprecipitation

Dynabeads® Protein G were vortexed and 200µl were washed with RIPA. Dynabeads® were incubated at RT for 30 minutes, rotating, with 500µl RIPA containing 20µg of HT7 antibody to bind the antibody with the beads and then washed 3 times again with RIPA. A chemical coupling was done to covalently bind the beads and the antibody. In this step the Dynabeads® Protein G-Ig complex was washed twice in 1mL 0.2M triethanolamine, pH8.2 and resuspended in 1mL of 20mM DMR (dimethyl pimelimidate x 2HCl) and other incubation of 30 minutes at 20°C toke place. The supernatant was removed and the reaction was stopped with 1mL 50mM Tris, pH7.5 for 15 minutes while samples were rotating. The supernatant was discarded again and the complex was washed 3 times with RIPA. 100µg of sample were diluted into 500µl of RIPA containing phosphatase and protease inhibitors. 50µl of antibody- Dynabeads® complex were wash with RIPA containing inhibitors and to bind the antibody with our protein of interest from our samples, these solutions were mix and incubated overnight with rotation at 4°C. After this incubation the mix was washed 3 times with RIPA containing inhibitors and a gel electrophoresis toke place. To detach the beads 6.5 parts of RIPA to 3.5 parts of reducing buffer were added to samples for a total of 25µl and the mix was heated at 75°C for 10 minutes. Therefore the samples were cooled on ice for 5 minutes and centrifuged for 2 minutes at 10000g. The samples were placed on magnet to remove the beads and the samples were loaded on a 4-12% Tris-Glysine gel and run in MOPS running buffer. The proteins present in the polyacrylamide gel were transferred onto the nitrocellulose membrane and all remaining procedure is identical to that described in the western Blot protocol.

3.10 Clonning

To evaluate the effect of ubiquitination on tau degradation and clearance of tau aggregates, we mutated either 3 or 5 of the proposed tau ubiquitinated sites of full-length P301L 2N4R Tau. The mutations involved changing the lysines that are proposed to be ubiquitinated to arginies to prevent ubquitination at these sites. Constructs were cloned

into XhoI, NHEI (Non-Tagged) or XhoI, HindIII (HaloTag) sites of NonTagged-P301L or HaloTag-P301L vector, respectively.

For replication, plasmids were transformed into e.coli TOP10 cells. For transduction, 1µl of plasmid (100pg/µl) in DNA-free water was added to TOP10 cells. Cells were placed no ice for 30 minutes, followed by 2 min of heating at 42°C and then again placed on ice. 250µl of S.O.C medium was added to the cells, after which cells were placed in the incubator at 36°C rotating at 225rpm for 60 minutes. After this incubation the cells should be plated onto agarose plate with 100µg/mL ampicillin where they should grow overnight (in the incubator) or during the week-end at RT. Colonies were picked and added to Luria Broth medium with Ampicillin and incubated at 36°C at 300 rpm overnight or all day. At the end of this time a QIAprep® Spin Miniprep Kit was used to obtain DNA.

For excision of DNA from vectors, 4µg of each vector DNA was added to 10µL of 10X Buffer, 2µL of restriction enzymes of interest and water, and incubated for 30 minutes at 37°C. To obtain a maximum result in the cloning process the vectors were dephosphprylated. After ligation, DNA was separated on an agarose gel (1g) with 1:20,000 Ethidium Bromide at 100 V for 30 minutes. The bands of interest were cut out and DNA extraction was done with a Qaigen kit. After a plasmid ligation the TOP10 cells were transformed again, this time 25 µl of Kanamicin stock (100x) was used. Cell growth, colonies picked and DNA extraction, DNA quantification were the steps that were done before the confirmation of our result. The cloning process was confirmed through the use of BamHI and BstEII (Non-Tagged) and XbaI and BstEII (HaloTag).

3.10.1 Degradation of tau protein

The WT QBI cells were transfected with 0.25µg/well plasmids containing P301L-tau binding to the halotag. One day later, fibrils were added along with 250nM of fluorescent halotag ligand TMR (4hr after) and allowed 2 days to incorporate during the aggregate formation. Two days after, TMR/fibril-containing medium was replaced with 200nM coumarin-containing medium to prevent further TMR incorporation into newly made tau. At this point, 'time 0' samples were lysed (Figure 11.A).

To measure tau-halotag loss in the absence of fibrils/aggregation, on the day after transfection 100nM of TMR-containing medium was added to the cells and one day after TMR-containing medium was replaced with 400nM coumarin-containing medium and the desired concentration of the drug of interest. At this point, 'time 0' samples were lysed (Figure 11.B)

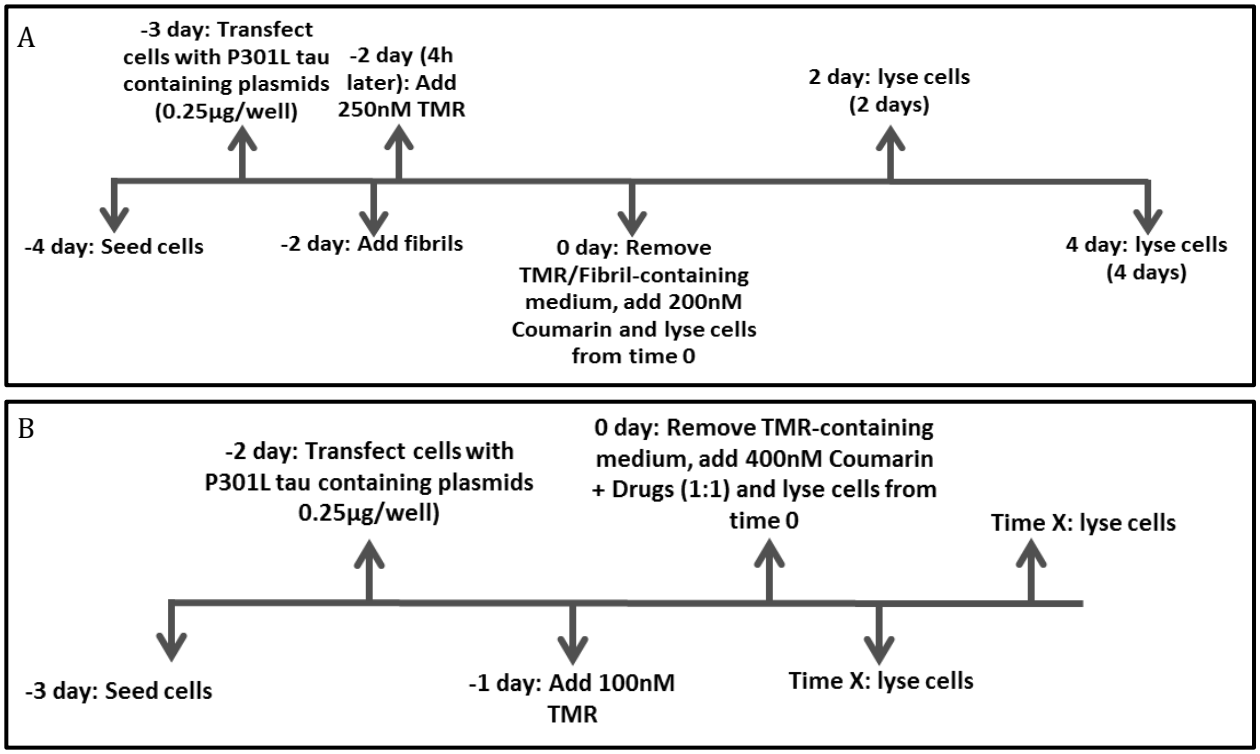

Figure 11 – schematic representation of strategy used so evaluate the degradation of Tau protein. (A) Protocol used when we want to induce aggregation. (B) Protocol used when aggregation was not necessary.

3.10.2 Synthesis of tau

The WT QBI cells were transfected with the plasmids containing 0.25µg/well of P301L-tau binding to the halotag. The next day, 200nM of fluorescent halotag ligand Coumarin-containing medium was added to the cells. One day later, coumarin-containing medium was replaced with 200nM TMR-containing medium and the desired concentration of the drug of interest was added to cells, allowing TMR-haloligand to now be incorporated into only newly synthesized tau and evaluate whether the drug altered tau synthesis. At this point, time '0' cells were treated as follows: 2.5 µl of TMR was diluted in 0.5 ml medium (5x

TMR) and 600 µl of medium from each well was removed (from the 1 ml in each well) and replaced with 100 µl of 5X diluted TMR. After 15 minutes 'time 0' samples were lysed (Figure 12).

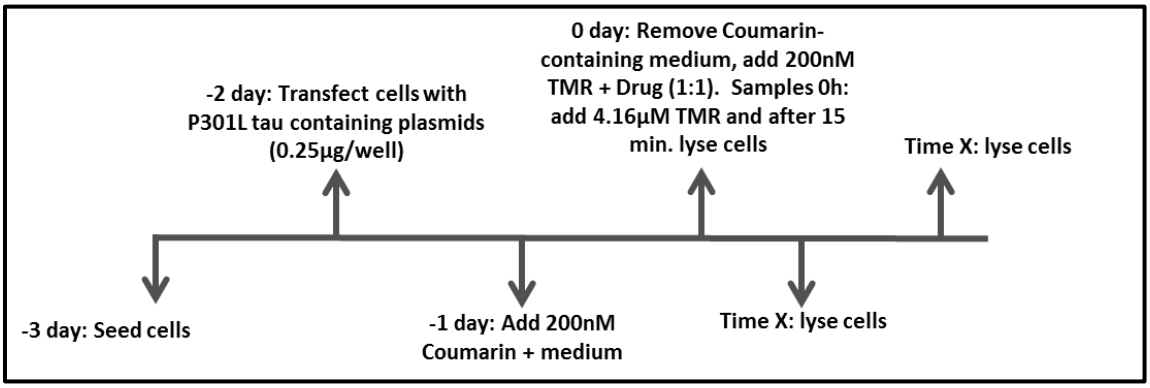

Figure 12 – Schematic representation of strategy used so evaluate the synthesis of Tau protein.

3.11 Statistical analysis

All quantitative results are expressed as means ± SEM. Statistical analysis were performed using ANOVA and t-test. AlphaLISA results as well as protein synthesis and degradation quantifications with the exception of Rapamycin experiments were analyzed using two-way ANOVA with alpha = 0.05. Relatively to the ratios between aggregates signal and total tau signal from AlphaLISA results, these were analyzed using t-test analyzes using the Holm-Sidak post-hoc analysis, with alpha=5.000%.

All statistical analysis was performed with GraphPad Prism 6 (GraphPad Software).

3.12 Dose response experiments

QBI WT or QBI inducible cells, depending on the goal of the experiment, were exposed to different concentrations of MG-132, Leupeptin, E64 and Rapamycin during different period of time. On time 0 and after each 24 hours the cells were observed under microscope and the cells were count to see if they were starting look different and if they were staring dying.

Results

4.1 Evaluate the effect of ubiquitination on soluble and aggregated tau levels.

4.1.1 Cloning of tau plasmid containing the P301L mutation and 3 or 5 ubiquitination site mutations.

To evaluate the effect of ubiquitination on normal tau turnover and aggregated tau turnover we designed a vector in which either 3 (3xKR) or 5 (5xKR) of the putative lysine ubiquitination sites of tau were mutated to arginine in a standard TauP301L vector, or a vector containing TauP301L fused at the c-terminal with the Halotag protein.

After cloning, we verified that the ligation worked appropriately by excising portions of the cloned gene and confirming their appropriate size (Figure 13). Once confirmed, plasmids were sent for sequencing for further verification (appendix Figure 38 for sequences).

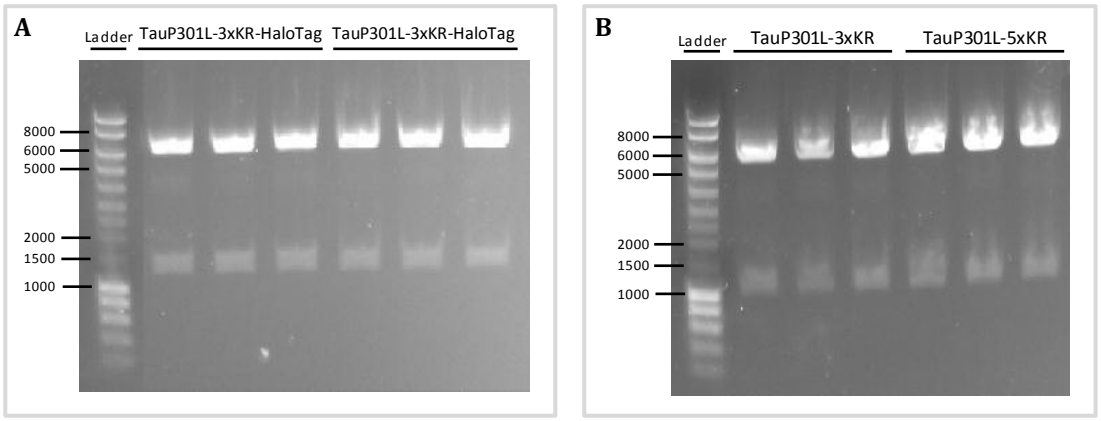

Figure 13 - Cloning of plasmids with three, five or no mutations. (A) and (B) Cloning confirmation: after cloning a digestion with BamHI and BstEII (A) and XbaI and BstEII (B) was done to confirm that the result of the cloning was the expected.

4.1.2 Quantitative analysis of tau aggregation by P301L tau, 3xKR-P301L tau and 5xKR-P301L tau.

The WT QBI cells were transfected with either control P301L tau, 3xKR-P301L tau or 5xKR-P301L tau plasmids, and treated with K18 fibrils to induce tau aggregate formation as described above. Transfected cells without added fibrils served as a negative control for aggregated tau (hT10/hT10). Nontransfect cells served as a negative control for tau expression. AlphaLISA was performed to analyze differences in total and aggregated tau protein.

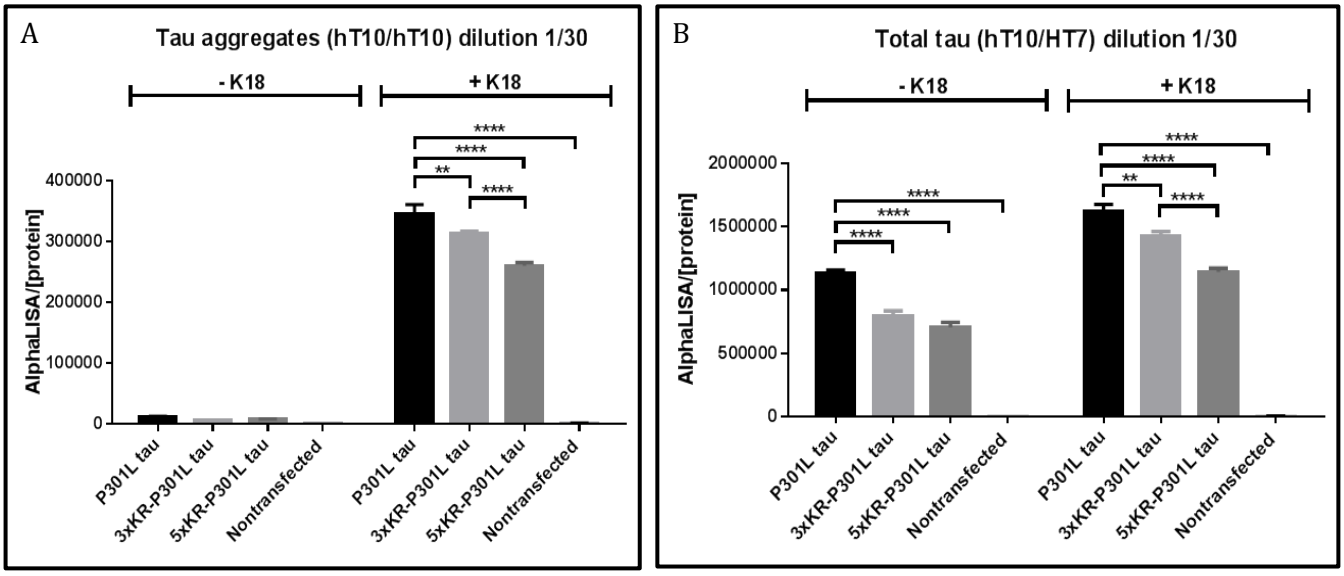

Figure 14 - AlphaLISA's results from cells non transfected or transfected with the plasmid without or with 3 or 5 mutation. (A) Tau aggregates quantification using hT10/hT10 antibodies combination with samples diluted 1/30. Results' normalization was done with the initial protein concentration of each sample. (B) Total Tau quantification using hT10/HT7 antibodies combination with samples diluted 1/30. Results' normalization was done with the initial protein concentration of each sample. Each data point is the mean ±S.E.M of 6 biological and 3 mechanic repetitions. A two-ways ANOVA analysis was performed (*P < 0.05).

Total tau hT10/HT7 signal (Figure 14.B) was significantly lower in cells that were not treated with fibrils than in fibril-treated cells ($F (1, 24) = 275.2$, $p < .0001$). Regardless of whether cells were treated with fibrils or not, 3xKR-P301L tau and 5xKR-P301L tau-transfected cells had a lower level of hT10/HT7 signal than P301L transfected controls cells ($F (2, 24) = 70.28$, $p < .0001$). Under fibril treated conditions, 3xKR-P301L tau-transfected cells, had higher hT10/HT7 signal than 5xKR-P301L tau-transfected cells ($P<0.05$).

As expected, cells not treated with fibrils had negligible levels of aggregated tau levels, that were significantly lower than fibril-treated cell, resulting in a significant effect of fibril addition ($F (1, 21) = 2061$, $p < .0001$) (Figure 14.A). Nontransfected cells had undetectable levels of aggregated or total tau (Figure 14.A and B). In fibril-treated cells, aggregated tau signal was significantly lower in cells expressing 3xKR-P301L tau and 5xKR-P301L tau than P301L tau control cells ($p<0.05$). 5xKR-P301L tau transfected cells had a lower hT10/hT10 signal than cells transfected with 3xKR ($p<0.05$). There was as a main effect of vectors used, $F (2, 21) = 15.56$, $p < .0001$ as well as a significant fibril x construct interaction ($F (2, 21) = 12.86$, $p = .0002$), primarily due to a difference in hT10/hT10 signal between fibril and nonfibril-treated 3xKR-P301L-tau transfected cells.

The AlphaLISA results with all dilutions used are present in the Figure 39 in appendix.

4.1.3 Quantifying normal and pathological tau protein degradation of P301L tau, 3xKR-P301L tau and 5xKR-P301L tau with and without K18P301L fibrils.

To determine the effect of ubiquitination on degradation of soluble and aggregated tau, WT QBI cells were transfected with the P301L, 3xKR-P301L tau or 5xKR-P301L tau containing a C-terminal Halotag and loss of a halotag-bound ligand signal was followed over time in a pulse-chase experiment, as described in the methods section.

Figure 15.A contains a representative scan of the fluorescent TMR ligand bound to the tau-halo complex after western blotting. Note, only the samples where K18 was added have two tau bands (the insoluble upper band and the soluble lower band).

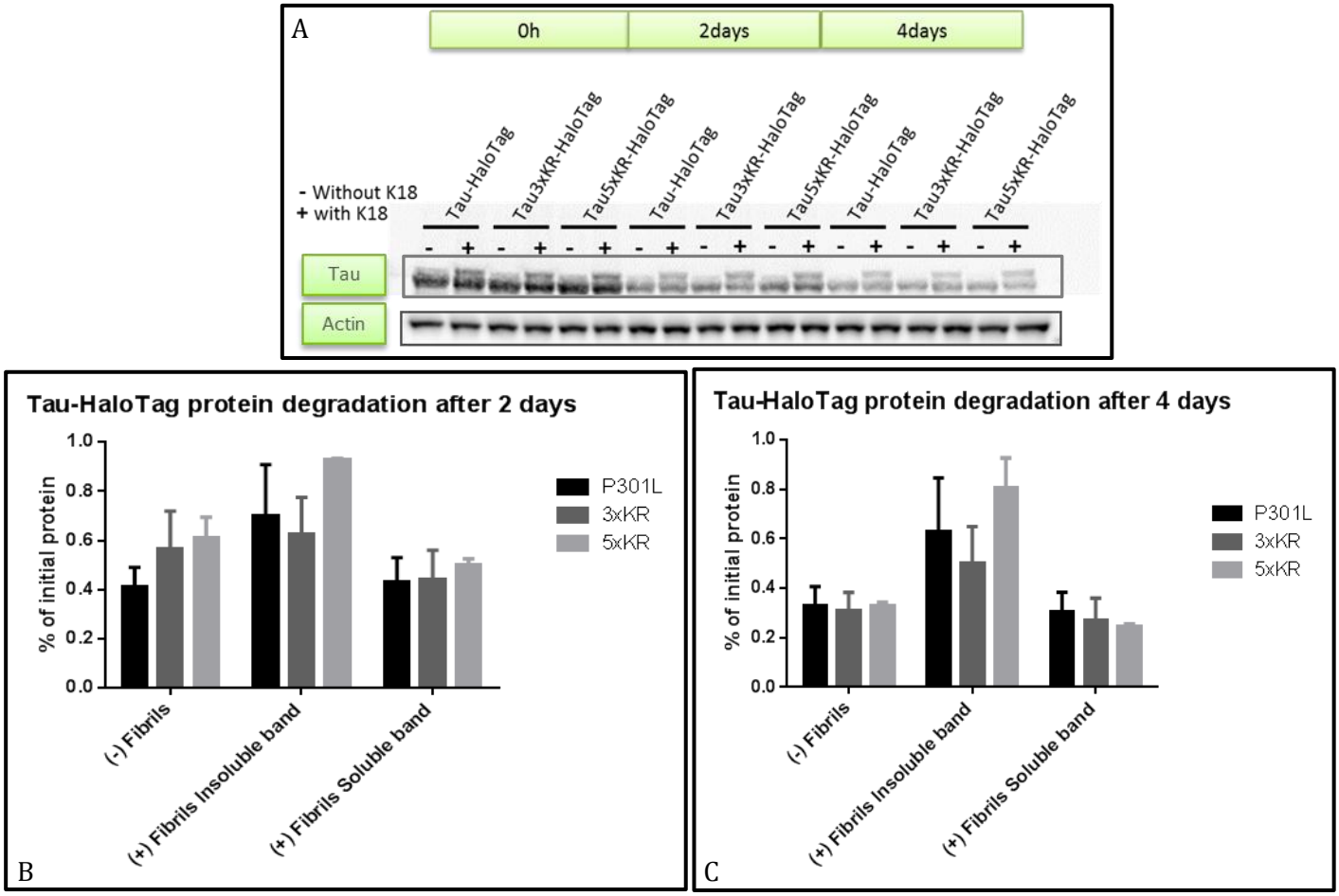

Figure 15 - TauP301L-HaloTag protein degradation after 2 and 4 days. (A) Western Blot analysis of Tau-Halotag protein degradation with and without K18 at time 0, 2 and 4 days. The analysis was done between the cells with Tau-HaloTag, Tau3xKR-HaloTag and Tau5xKR-HaloTag. (B) Quantification of initial protein present in the cells after 2 days. Time 0 was assumed as 100% of protein and all the results were compared with them. (C) Quantification of initial protein present in the cells after 4 days. Time 0 was assumed as 100% of protein and all the results were compared with them. Each data point is the mean ±S.E.M of 3 biological repetitions. A two-ways ANOVA analysis was performed (*P < 0.05).

Bands were quantified, normalized to actin levels and these results are presented in Figure 15.B and C. The quantification was done comparing the results of each condition with the time 0 of the same condition assuming the time 0 as 100% of tau protein.

In general, about half of the TMR signal in the soluble band (+ or – fibrils) was lost by day 2 (Figure 15.B) and about 70% was gone by day 4 (Figure 15.C). However, there were no statistically different in signal loss between our mutants. In contrast, only 10-40% of the insoluble band was lost by day 2 and 20-50% on day 4, suggesting a slower loss of the insoluble tau over time. While there was a tendency for what appears to be slower loss of 5xKR-tau in the insoluble band compared to P301L tau or 3xKR-P301L tau, this was not statistically significant.

4.1.4 Ubiquitination sites mutations confirmation.

To determine whether ubiquitin could be detected conjugated to tau, and whether our mutations impacted this, an immunoprecipitation was performed on 100µg of cell lysate. To increase the possibility of detection the proteasome inhibitor MG-132 (0, 300 and 1000nM) was added to the cells. After 7 hours of MG-132 exposure, tau from 100µg of immunoprecipated cellular lysate was western blotted and detected with anti-ubiquitin antibody (Figure 16.A). To confirm the efficiency of the IP the same membrane was incubated with anti-tau antibody, and analyzed (Figure 16.B). Finally, to confirm the activity of the MG-132 cell lysates were run in a gel that was incubated with anti-ubiquitin antibody, and analyzed (Figure 16.C).

In the membrane blotted for anti-ubiquitin, there was no clear indication of ubiquitinated tau species, in P301L tau, P301L-3xKR tau and P301L-5xKR tau transfected cells nor after MG-132 treatment (Figure 16.A). Also, in the tau immunostained blot, there was no indication of higher MW tau species with any of the constructs, nor was there an apparent increase in un-ubiquitinated or ubiquitinated tau upon MG-132 treatment (Figure 16.B). The anti-ubiquitin blot of whole cell lysates did however show, an increase of ubiquitinated proteins was detected after MG-132 treatment (Figure 16.C) indicating proteasome inhibition was achieved.

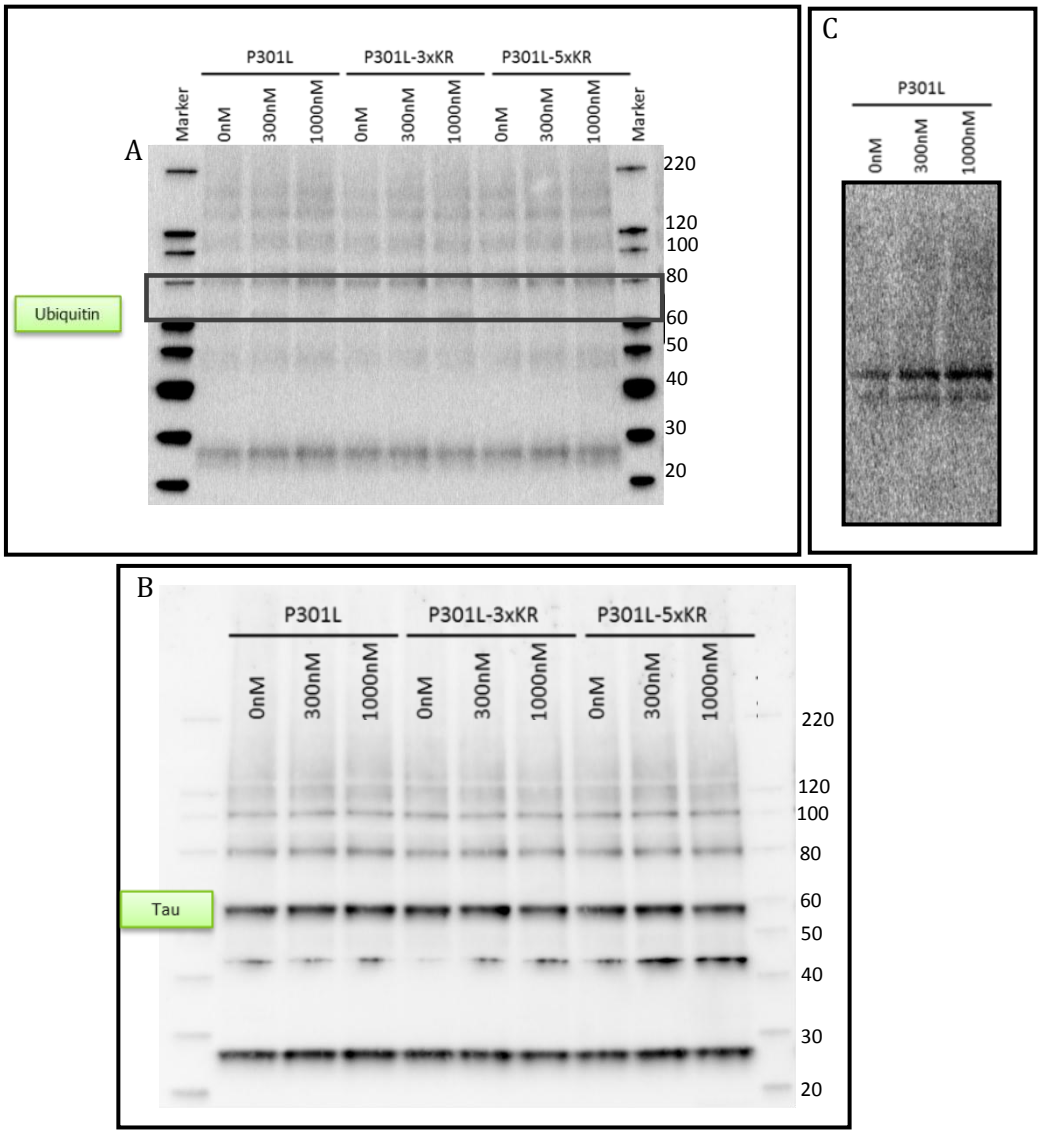

Figure 16 - Western blotting analysis of IP samples. P301L, P301L-3xKR and P301L-5xKR transfected cells exposed to a 0, 300 and 1000nM of MG-132 submitted to an IP protocol. (A) The membrane was labeled with anti-ubiquitin antibody. (B) The same membrane was labeled with anti-tau antibody. (C) Western blot done with P301L transfected cell lysate and labeled with anti-ubiquitin antibody.

4.2 Evaluate the effect of overexpression of USP5, USP7, USP9x and OTUB1 on aggregation of tau protein.

In order to see the effect of different DUBs on the aggregation of tau protein clonal wild type QBI cells were transiently transfected with the expression vectors for USP5, USP7, USP9x and OTUB1 that were previously sequence verified. The cDNA concentrations used in these transfections were 0.25µg/well and 0.5µg/well when transfected in a 24 well plate and 0.08µg/well when transfected in a 96 well plate. The controls used in these experiments were: transfection of the cells with the same concentration of an empty vector

corresponding to the parental vector used to create the vectors containing the DUBs, as well as non-transfected cells. In all these conditions we had cells where K18 was added and cells where K18 was not added as a negative control.

4.2.1 Effect of overexpression of USP5 on soluble and aggregated tau levels.

4.2.1.1 Overexpression confirmation through western blot.

After the overexpression of USP5 a western blot was done to confirm the efficiency of the transfection (Figure 17). The samples were run and detected with USP5 antibody and the results were normalized to actin. Different concentrations of USP5 and empty vector plasmids were used: 0.25µg/well (Figure 17.A) and 0.5µg/well (Figure 17.B) where K18 was added or not K18.

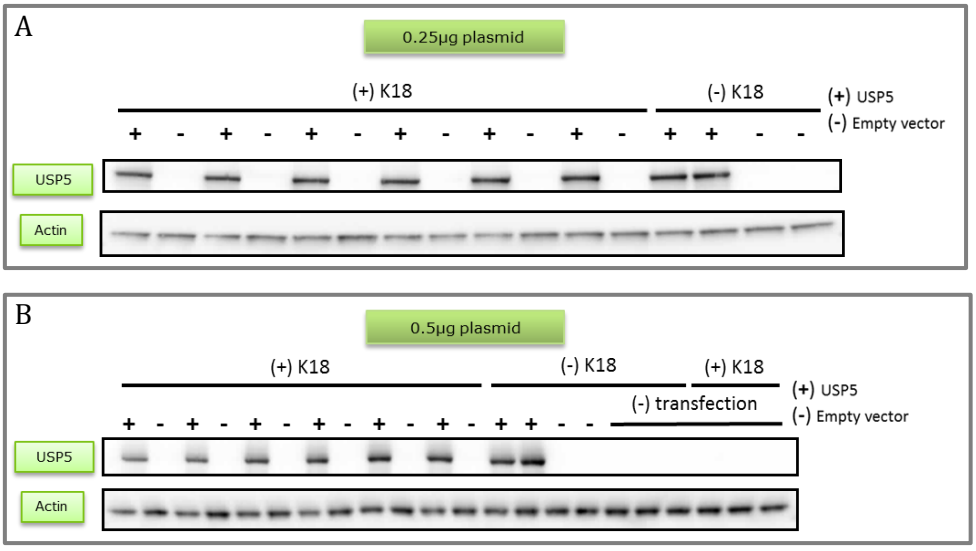

Figure 17 - Wetern blotting analysis of overexpression with USP5 (+) and an empty vector (-) against USP5 and actin. (A) Samples transfected with 0.25µg of DNA. (B) Samples transfected with 0.5µg of DNA.

Levels of USP5 were detectable in cells transfected with 0.25µg/well (Figure 17.A) or with 0.5µg/well, but not in non-transfected cells.

4.2.1.1.1 Soluble and aggregated tau quantification through AlphaLISA.

We next evaluated whether aggregation of tau protein was altered by USP5 overexpression (0.25µg/well) in QBI cells with inducible tau expression (Figure 18). The AlphaLISA results with all the dilutions done are annexed in the appendix (Figure 40).

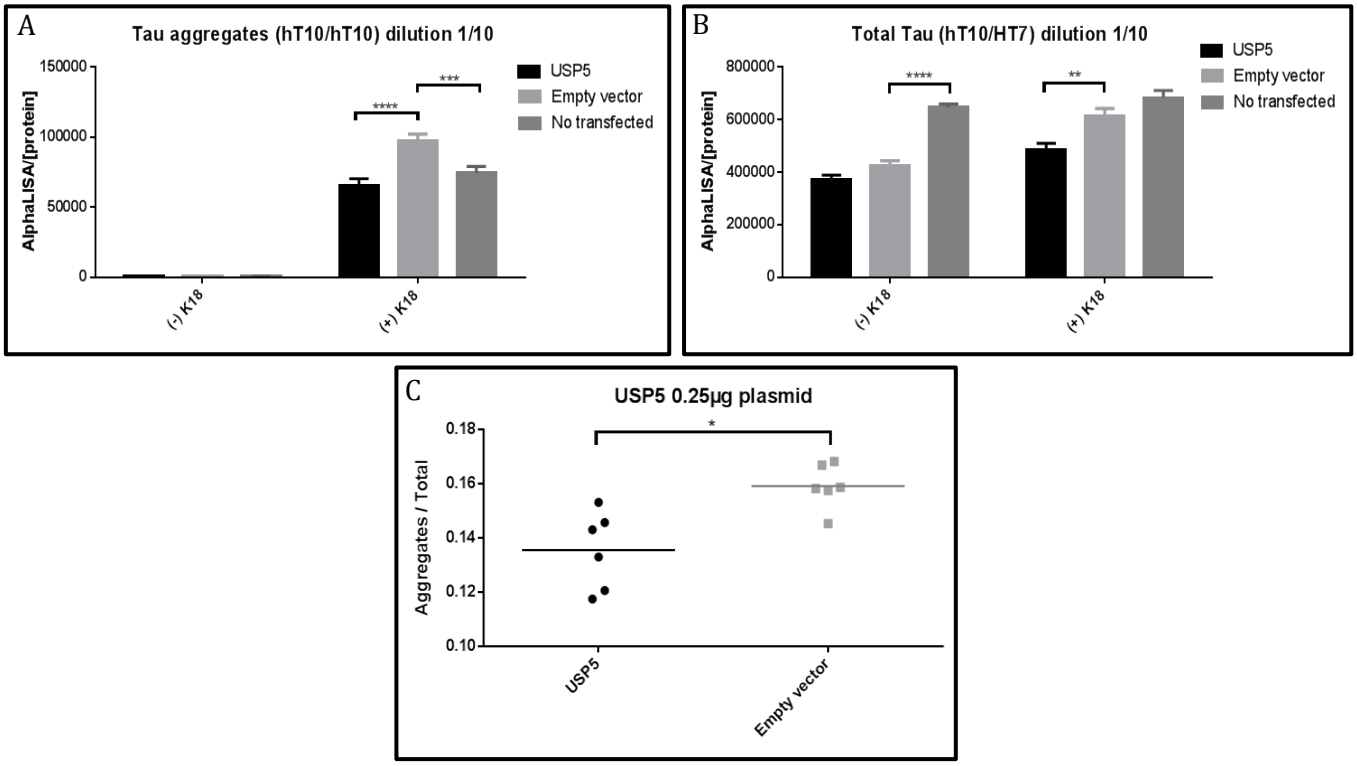

Figure 18 - AlphaLISA's results from overexpression of USP5 with 0.25µg of each plasmid. (A) Tau aggregates quantification using hT10/hT10 antibodies combination with samples diluted 1/10. (B) Total Tau quantification using hT10/HT7 antibodies combination with samples diluted 1/10. Data were corrected for the initial protein concentration of each sample. Each data point is the mean ±S.E.M of 6 biological and 3 mechanic repetitions. A two-ways ANOVA analysis was performed (*P < 0.05). (C) Ratio between the aggregates signal and total tau signal with K18 exposed samples where each data point is the mean ±S.E.M of 6 biological and 3 mechanic repetitions. A t-test analysis was performed (*P < 0.05).

The difference between hT10/HT7 signal from USP5 and empty vector transfected cells when in absence of fibrils was not significant. However, the total tau signal from empty vector transfected cells was lower than no transfected cells (Figure 18.B). A lower total tau hT10/HT7 signal in USP5 transfected cells after fibril addition when compared with empty vector-transfected cells appeared. Deriving from these differences a fibril x vector interaction ($F(2, 30) = 5.429$, $p = 0.0097$) was shown. As expected, cells not treated with fibrils had negligible levels of aggregated tau signal (Figure 18.A) which were significantly lower than in fibril-treated cells ($F(1, 30) = 798.6$, $p < .0001$). In fibril-treated cells, aggregated tau signal was significantly lower in cells transfected with the USP5 than in empty vector-transfected and non-transfected cells ($F(2, 30) = 11.63$, $p = 0.0002$). Total tau hT10/HT7 signal was significantly reduced in fibril-treated cells ($F(1, 30) = 35.04$, $p < .0001$) and in USP5 and empty vector-transfected cells vs. non-transfected cells ($F(2, 30) = 53.35$, p

< .0001) (Figure 18.B). Because total tau hT10/HT7 signal was altered by transfection, and total tau levels may impact the amount of tau available for aggregation, we tested whether the ratio of hT10/hT10 signal to HT7/hT10 signal (i.e. aggregated/total tau) was significantly altered by USP5 overexpression vs. empty vector transfection (Figure 18.C). In this case, USP5 transfected cells still had a lower aggregated/total tau ratio ($p < 0.05$).

To confirm the above results, in the same cell model transfected with 0.5 µg/well of USP5 and empty vector/well instead of 0.25 µg/well (Figure 19). Total tau signal from empty vector transfected cells was significantly lower than no transfected cells when in absence of fibrils. USP5-transfected cells present a lower total tau level than empty vector-transfected cells equally in absence of seeding. Total tau hT10/HT7 signal did not present any statistical difference between USP5, empty vector and no transfected cells when in presence of fibrils. Total tau hT10/HT7 signal was significantly reduced in fibril-treated cells compared to nontreated cells ($F (1, 30) = 19.06$, $p < .0001$) and a significant difference was shown too depending on the vectors that was used ($F (2, 30) = 21.56$, $p < .0001$) (Figure 19). As

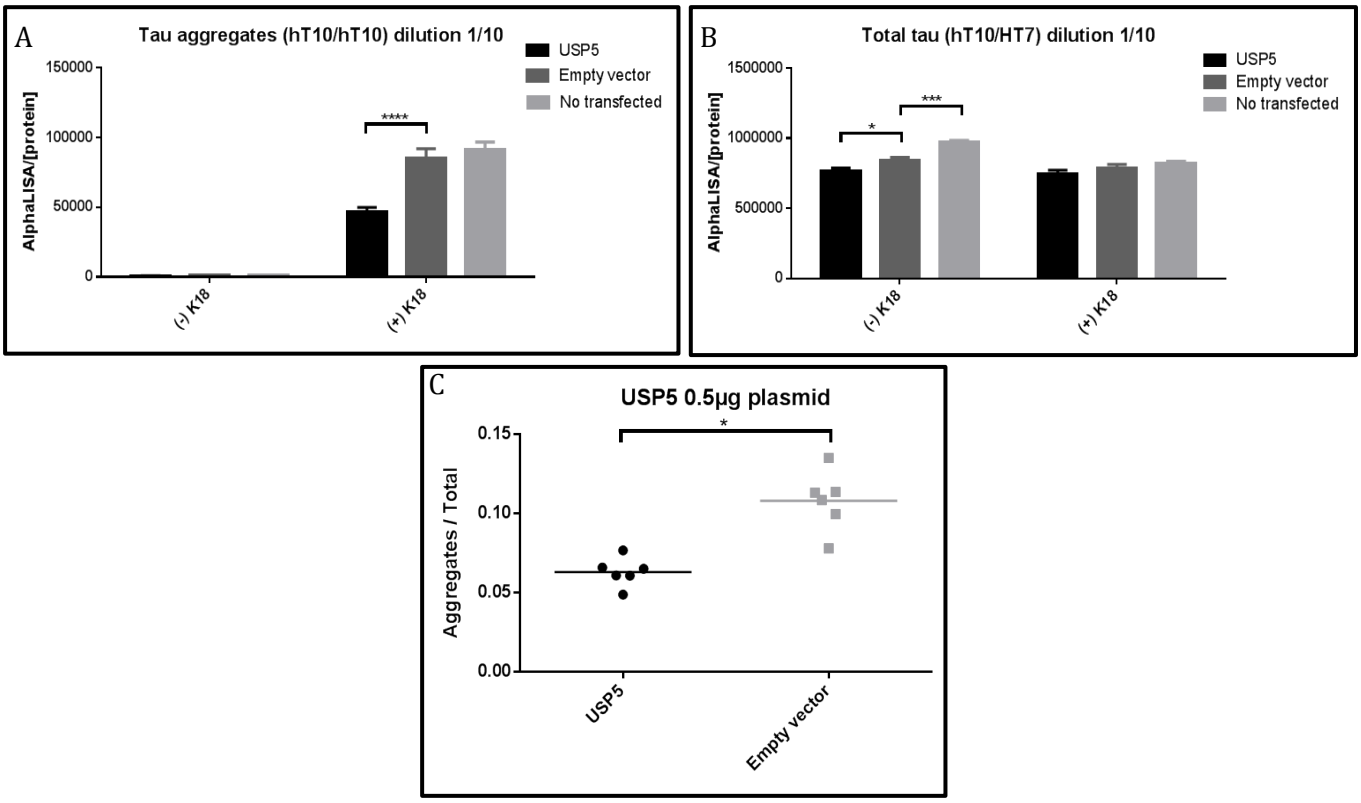

Figure 19 - AlphaLISA's results from overexpression of USP5 with 0.5µg of each plasmid. (A) Tau aggregates quantification using hT10/hT10 antibodies combination with samples diluted 1/10. (B) Total Tau quantification using hT10/HT7 antibodies combination with samples diluted 1/10. Results' normalization was done with the initial protein concentration of each sample. Each data point is the mean ±S.E.M of 6 biological and 3 mechanic repetitions. A two-ways ANOVA analysis was performed (*P < 0.05). (C) Ratio between the aggregates signal and total tau signal with K18 exposed samples where each data point is the mean ±S.E.M of 6 biological and 3 mechanic repetitions. A t-test analysis was performed (*P < 0.05).

expected, cells not treated with fibrils had negligible levels of aggregated tau signal (Figure 19.A) which were significantly lower than in fibril-treated cells ($F(1, 30) = 602.5$, $p < .0001$). In fibril-treated cells, aggregated tau signal was significantly lower in cells transfected with USP5 than in cells transfected with the empty vector ($F(2, 30) = 22.39$, $p < 0.0001$) (Figure 19.A).

In general, vector transfection impacted HT7/hT10 total tau levels less in this experiment, nonetheless, we evaluated the hT10/hT10 signal to HT7/hT10 signal ratio. In this case the ratio of aggregated tau signal to total tau signal was still significantly lower in USP5 overexpression cells compared to empty vector transfected cells ($p < 0.05$).

The AlphaLISA results' with all the dilutions done were annexed in the appendix (Figure 43).

4.2.2 Effect of overexpression of USP7 soluble and aggregated tau levels.

4.2.2.1 Overexpression confirmation through western blot.

After the transfection of USP7 a western blot was done to confirm the efficiency of the transfection (Figure 20). The samples were run and detected with USP7 antibody and the results were normalized to actin. Different concentrations of USP7 and empty vector plasmids were used: 0.25µg/well (Figure 20.A) and 0.5µg/well (Figure 20.B) where added with or without K18. The results obtained in the western blot were quantified and the graph is presented in the Figure 20.C.

In Figure 20 we could see that USP7 transfected cells had elevated USP7 protein levels when compared with the endogenous levels of USP7 on empty vector or non-transfected cells when transfected with 0.5µg/well (Figure 20.B and C).

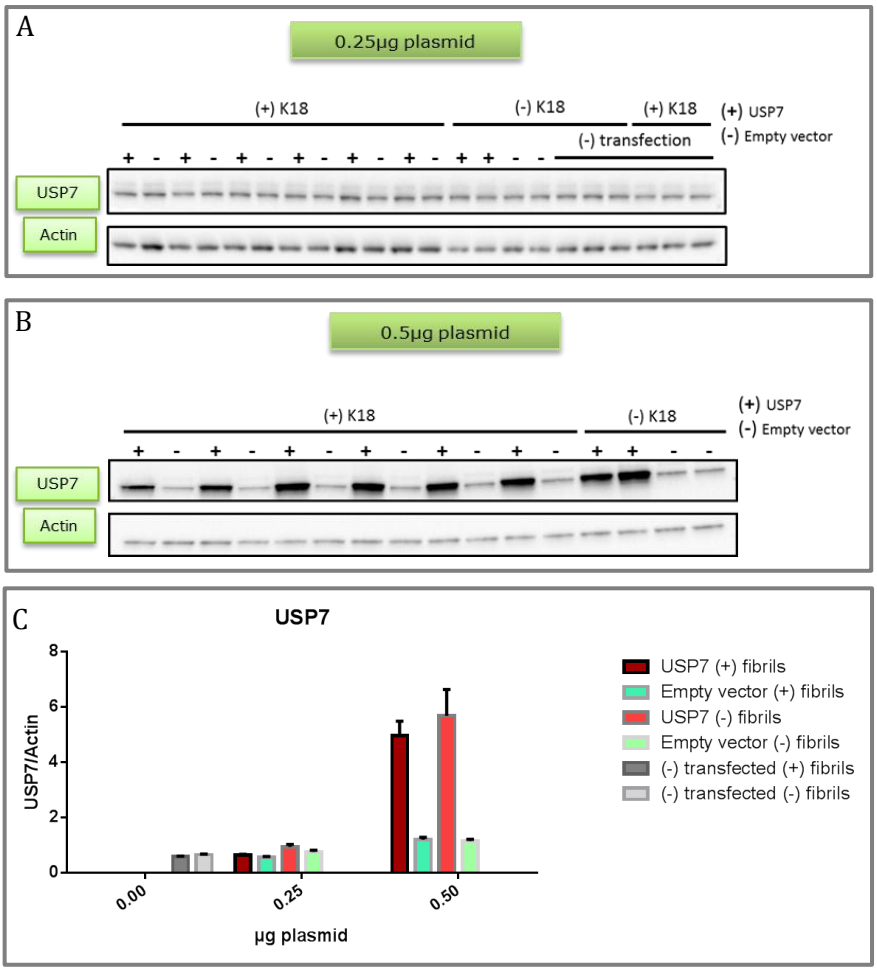

Figure 20 - Western blotting analysis of overexpression with USP7 (+) and an empty vector (-) against USP7 and actin. (A) Samples transfected with 0.25µg of DNA. (B) Samples transfected with 0.5µg of DNA (C) Graph of results quantification and normalized with actin. Each data point is the mean ±S.E.M of 6 biological repetitions.

However when transfected with 0.25µg/well the levels of USP7 remains the same (Figure 20.A and C).

4.2.2.1.1 Aggregation quantification through AlphaLISA.

We next evaluated whether USP7 overexpression (0.5µg/well) altered tau aggregation in the samples that were previously analyzed through western blot (Figure 21).

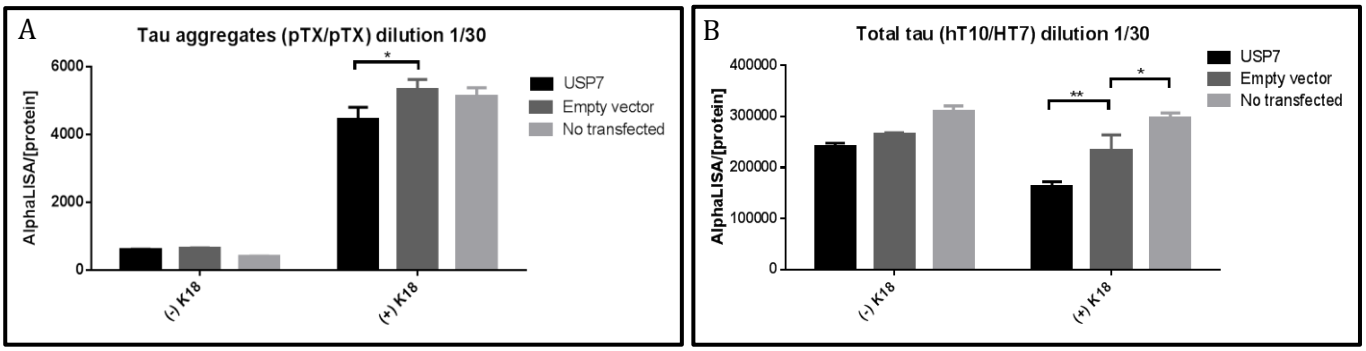

Figure 21 - AlphaLISA's results from overexpression of USP7 with 0.5µg of plasmid. (A) Tau aggregates quantification using pTX/pTX antibodies combination with samples diluted 1/30. (B) Total Tau quantification using hT10/HT7 antibodies combination with samples diluted 1/30. Results' normalization was done with the initial protein concentration of each sample. Each data point is the mean ±S.E.M of 6 biological and 3 mechanic repetitions. A two-ways ANOVA analysis was performed (*P < 0.05).

Signal from total soluble tau did not present any statistical differences between USP7, empty vector and non-transfected cells when no fibrils were added (Figure 21.B). Total tau levels were significantly lower in USP7 and empty vector transfected cells as compared to non-transfected cells, when in presence of fibrils, resulting in on overall vector effect ($F(2, 30) = 24.02$, $p < .0001$). Total tau hT10/HT7 signal was slightly, but significantly lower in fibril treated cells vs. non-treated cells ($F(1, 30) = 11.87$, $p = 0.0017$). In the presence of fibrils, USP7 transfected cells had significantly lower total tau hT10/HT7 signal than empty vector transfected cells ($p < 0.05$) (Figure 21.B).

Consistent with previous experiments, cells not treated with fibrils had very low levels of aggregated tau (pTX/pTX) signal (Figure 21.A) which were significantly lower than in fibril-treated cells ($F(1, 30) = 641.8$, $p < .0001$). In fibril-treated cells, aggregated tau signal was significantly lower in USP7-transfected than empty vector-transfected cells ($F(2, 30) = 2.367$, $p > 0.1$) (Figure 21.A).

The original results containing all the dilutions done are presented in annex (Figure 42).

4.2.2.2 Aggregation qualification through immunocytochemistry.

To confirm the results obtained from AlphaLISA with the overexpression of USP7 and the empty vector an immunocytochemistry was done with the same conditions and with the concentrations adjusted to the 96 well plate (Figure 22.A).

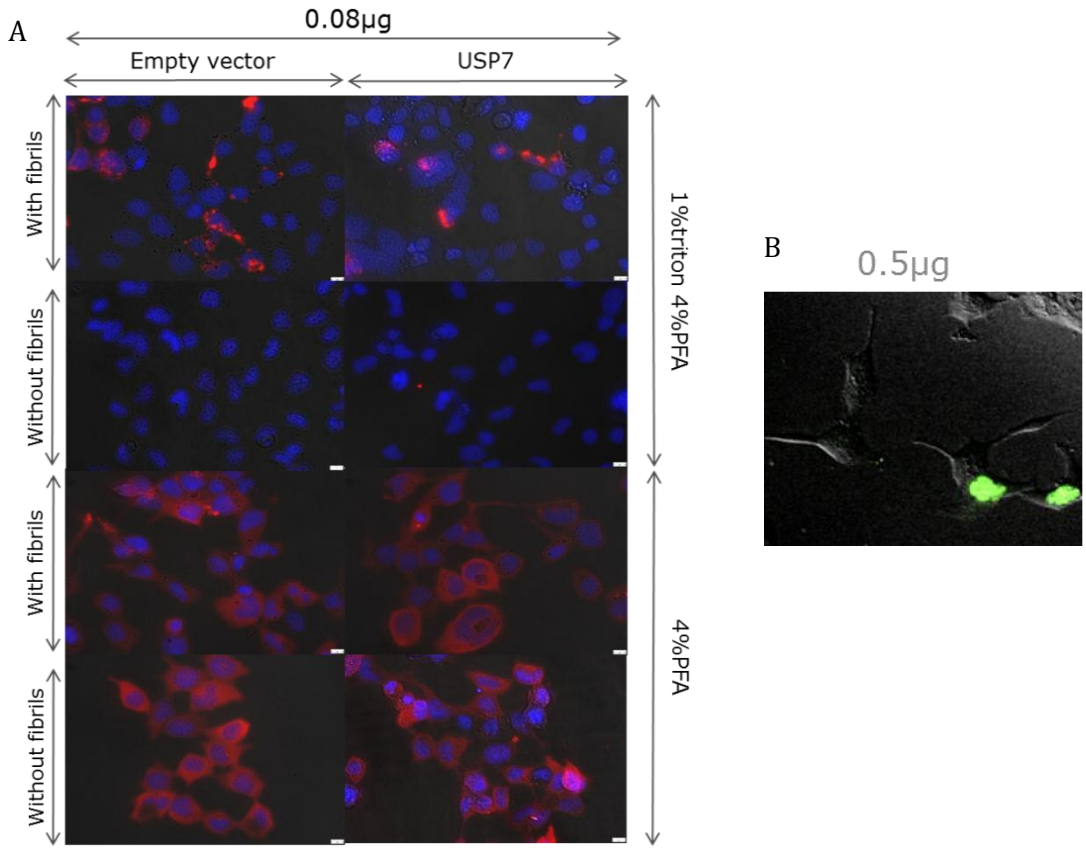

Figure 22 - Representation of overexpression of USP7. (A) Immunocytochemstry's representation of overexpression of USP7. The fixations preformed were 1%triton 4% PFA (tau aggregates) and 4% PFA (total tau) in cells transfected with 0.25 µg and 0.5 µg of empty vector and USP7 and in the presence and absence of fibrils. Red staining corresponds to tau protein and blue staining corresponds to nucleus. (B) Live imaging representation of overexpression of USP7. The cells were transfected with USP7-GFP.

To confirm the localization of USP7, USP7-GFP was used (Figure 22.B). On this picture we could clearly see that USP7 was preferentially located at the nucleus.

To see the aggregation of tau protein a 1% triton 4% PFA fixation was done and to see the total tau a 4% PFA fixation was done. On this representation we could see that in the aggregation condition (1%triton 4%PFA and with fibrils) and total tau condition (4%PFA and with and without fibrils) the red signal emitted from tau protein, from the 0.08µg USP7 transfected cells was preferentially located at the cytosol as well as the signal emitted from the empty vector transfected cells.

4.2.3 Effect of overexpression of USP9x on aggregation of tau protein.

4.2.3.1 Overexpression confirmation through western blot.

A western blot was done to confirm the efficiency of the USP9 transfection (Figure 23). The samples were run and detected with USP9x antibody and the results were normalized to actin. Different concentrations of USP9x and empty vector plasmids were used: 0.25µg (Figure 23.A) and 0.5µg (Figure 23.B) in the presence or absence of K18. The results obtained in the western blot were analyzed and the graph is presented in the Figure 23.C.

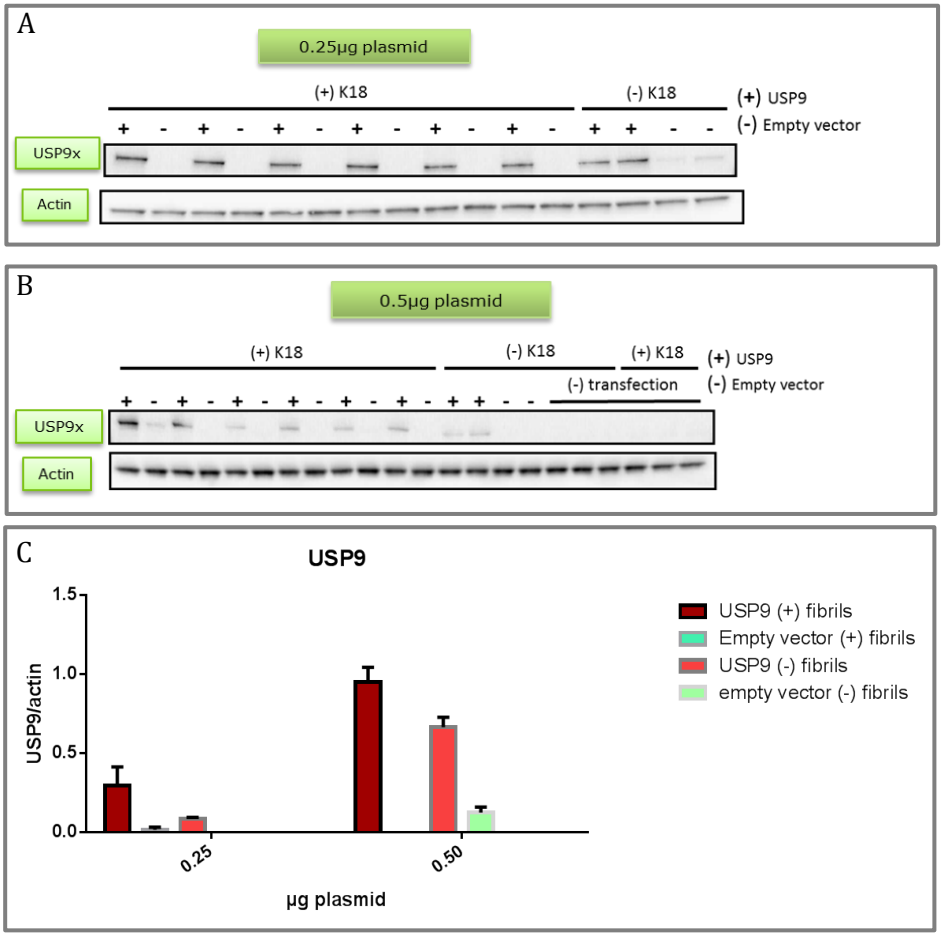

Figure 23 - Wetern blotting analysis of overexpression with USP9x (+) and an empty vector (-) against USP9x and actin. (A) Samples transfected with 0.25µg of DNA. (B) Samples transfected with 0.5µg of DNA (C) Graph of results quantification and normalized with actin. Each data point is the mean ±S.E.M of 6 biological repetitions.

Figure 23 shows that cells transfected with 0.25µg/well or 0.5µg/well USP9 have an increase on USP9 levels when compared with empty vector or non-transfected cells. However when transfected with 0.25µg/well the increase in USP9x levels was not as significant as when transfected with 0.5µg/well.

4.2.3.1.1 Aggregation quantification through AlphaLISA.

We next tested whether USP9x overexpression altered tau aggregation in the samples that were previously analyzed through western bolt (Figure 24).

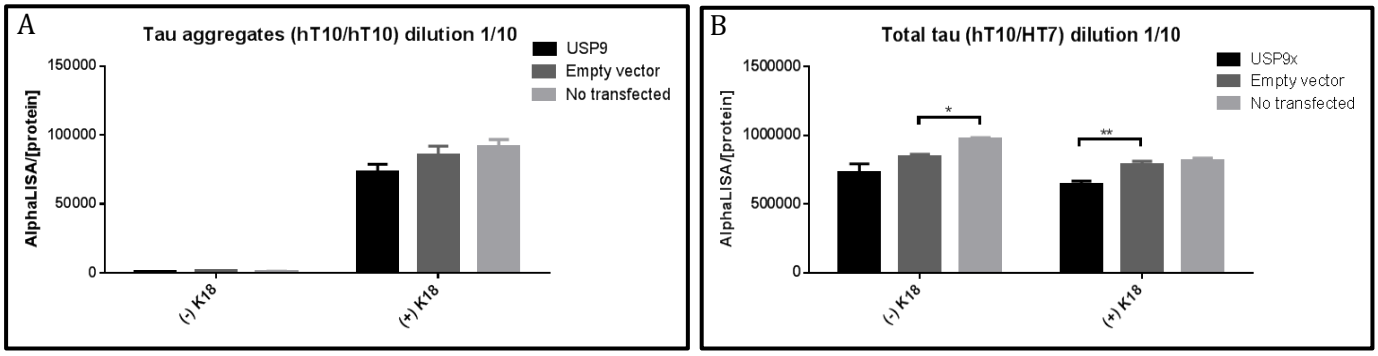

Figure 24 - AlphaLISA's results from overexpression of USP9 with 0.5µg of plasmid. (A) Tau aggregates quantification using hT10/hT10 antibodies combination with samples diluted 1/10. (B) Total Tau quantification using hT10/HT7 antibodies combination with samples diluted 1/10. Results' normalization was done with the initial protein concentration of each sample. Each data point is the mean ±S.E.M of 6 biological and 3 mechanic repetitions. A two-ways ANOVA analysis was performed (*P < 0.05).

Total tau signal was lower in empty vector transfected cells, not treated with fibrils, than in no transfected cells (Figure 24.B). When the cells were treated with fibrils USP9x transfected cells were presenting lower total tau signal than empty vector transfected cells (Figure 24.B). Total tau hT10/HT7 signal was slightly, but significantly lower in fibril treated cells vs. non-treated cells ($F(1, 30) = 14.78$, $p = 0.0006$). There was also a trend for total tau hT10/HT7 signal to be significantly lower in USP9x and/or empty vector transfected cells as compared to non-transfected cells, resulting in on overall vector effect ($F(2, 30) = 21.89$, $p < .0001$) (Figure 24.B). Total tau hT10/HT7 signal was lower in USP9x transfected cells compared to empty vector transfected cells in the presence of fibrils ($p < 0.05$). As observed in previous experiments, cells not treated with fibrils had very low levels of aggregated tau (hT10/hT10) signal (Figure 24.A) which were significantly lower than in fibril-treated cells ($F(1, 30) = 603.5$, $p < .0001$). In fibril-treated cells, aggregated tau signal was not significantly different between USP9x-transfected and empty vector-transfected ($p < 0.05$) (Figure 24.A).

The original results containing all the dilutions done are presented in annex (Figure 41).

4.2.4 Effect of overexpression of OTUB1 on aggregation of tau protein.

4.2.4.1 Overexpression confirmation through western blot.

OTUB1 was overexpressed in QBI cells, and a western blot was done to confirm the transfection efficiency (Figure 25). The samples were detected with an anti-HA antibody (the OTUB1 has an HA-tag in the N-terminal) and the results were normalized with actin. Different concentrations of OTUB1 and empty vector plasmids were used: 0.25µg (Figure 25.A) and 0.5µg (Figure 25.B) in the presence or absence of K18.

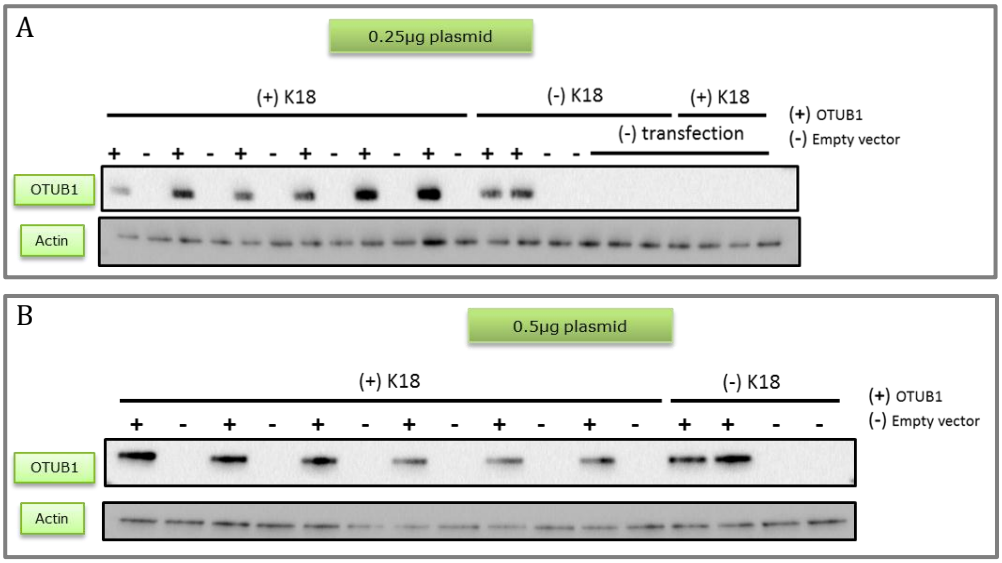

Figure 25 - Wetern blotting analysis of overexpression with OTUB1 (+) and an empty vector (-) against HA and actin. (A) Samples transfected with 0.25µg of DNA. (B) Samples transfected with 0.5µg of DNA.

OTUB1 transfected cells have an increase in OTUB1 levels when compared with empty vector or non-transfected cells either when transfected with 0.25µg or 0.5µg (Figure 25.A and B).

4.2.4.1.1 Aggregation quantification through AlphaLISA.

To evaluate whether OTUB1 overexpression altered tau aggregation we analyzed total and aggregated to via AlphaLISA in the samples that were previously analyzed by western bolt (Figure 26).

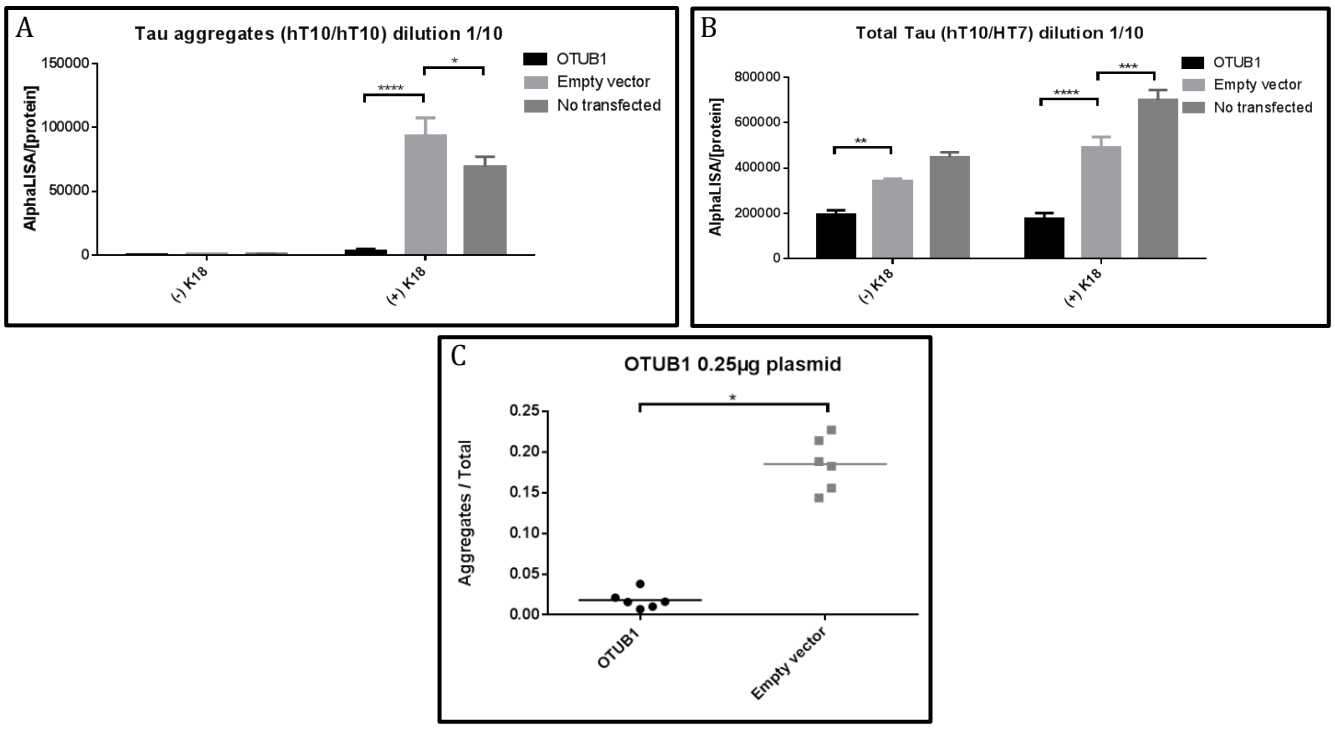

Figure 26 - AlphaLISA's results from overexpression of OTUB with 0.25µg of plasmid. (A) Tau aggregates quantification using hT10/hT10 antibodies combination with samples diluted 1/10. (B) Total Tau quantification using hT10/HT7 antibodies combination with samples diluted 1/10. Data were corrected for the initial protein concentration of each sample. Each data point is the mean ±S.E.M of 6 biological and 3 mechanic repetitions. A two-ways ANOVA analysis was performed (*P < 0.05).

Total tau hT10/HT7 signal was consistently and significantly lower in all fibril treated groups compared to non-treated groups resulting in a main effect of fibrils ($F(1, 30) = 24.36$, $p < .0001$). OTUB1 transfected cells have lower hT10/HT7 signal than empty vector transfected cells when fibrils were no added (Figure 26.B). Total tau hT10/HT7 signal was consistently significantly lower in OTUB1 transfected cells, intermediate in empty vector-transfected cells and highest in non-transfected cells, resulting in on overall vector effect ($F(2, 30) = 75.96$, $p < .0001$) (Figure 26.B).

As observed in previous experiments, cells not treated with fibrils had very low levels of aggregated tau (hT10/hT10) signal (Figure 26.A) which was significantly lower than in fibril-treated cells ($F(1, 30) = 99.64$, $p < .0001$). In fibril-treated cells, aggregated tau signal was significantly lower in OTUB1-transfected cells than empty vector-transfected or non-transfected cells ($F(2, 30) = 24.49$, $p < 0.0001$).

The ratio of hT10/hT10 signal to HT7/hT10 signal was calculated and is shown in Figure 26.C. A significant difference was detected when comparing the OTUB1 transfected

cells with the empty vector transfected cells, where the first presented a lower ratio ($p < 0.05$).

To next confirmed whether the results obtained above were repeatable by analyzing total and aggregated tau in the cells that were transfected with 0.5 μg of OTUB1 (Figure 27).

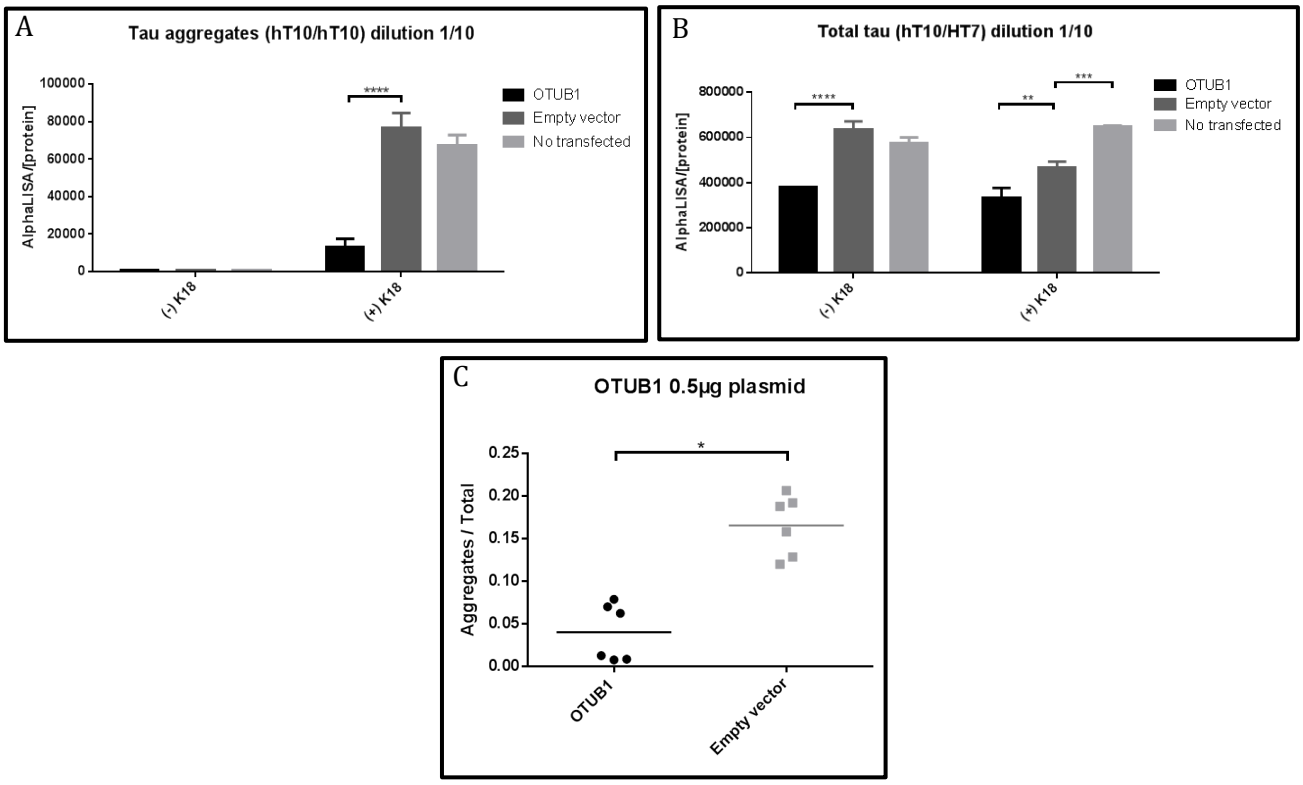

Figure 27 - AlphaLISA's results from overexpression of OTUB with 0.5µg of plasmid. (A) Tau aggregates quantification using hT10/hT10 antibodies combination with samples diluted 1/10. (B) Total Tau quantification using hT10/HT7 antibodies combination with samples diluted 1/10. Results' normalization was done with the initial protein concentration of each sample. Each data point is the mean ±S.E.M of 6 biological and 3 mechanic repetitions. A two-ways ANOVA analysis was performed (*P < 0.05).

Results from cells transfected with 0.5 μg/well OTUB1 replicated those from cells transfected with 0.25 μg/well OTUB1 above. That was, a significant decrease in total tau signal in OTUB1 transfected cells when compared with empty vector transfected cells whether in presence or absence of fibrils and a decrease in total tau signal from empty vector transfected cells when compared with no transfected cells, in the presence of fibrils (Figure 27.B). Aggregated tau (hT10/hT10) signal was dramatically lower in OTUB1 transfected cells than in empty vector transfected cells in the presence of fibrils ($F(2, 30) = 31.97$, $p < 0.0001$) (Figure 27.A) even though total tau signal was significantly lower in OTUB1 transfected cells compared to empty vector transfected cells (Figure 27.B, vector effect $F(2, 30) = 46.37$, $p < .0001$), the ratio of aggregated tau signal: total tau signal was

significantly lower in OTUB1 transfected cells compared to empty vector controls ($P < 0.05$) suggesting a significantly lower proportion of total tau accumulated in aggregates.

4.3 Explore the role of the proteasome and autophagy pathways on aggregation, degradation and synthesis of tau protein.

To evaluate tau synthesis and degradation, QBI cells were transfected with P301L tau tagged at the C-terminal with the halotag protein which can be irreversibly labelled with a fluorescent halo-ligand to follow its accumulation or loss over time. This method has been previously used in our lab and found to give similar degradation rates for tau (about 18-24 hours) when compared to another nonradioactive labeling techniques (replacing methionine in proteins with the noncanonical amino acid L-Homopropargylglycine) (results not shown).

4.3.1 Observation of effect of proteasome inhibition on tau protein degradation and synthesis through the use of MG-132.

The used drug to inhibit the proteasome activity was the MG-132 in different concentrations that were chose after a toxicity analysis.

4.3.1.1 Toxicity analysis with MG-132 on QBI WT cells

To have an idea of which concentrations of MG-132 and for how long we could use these concentrations, a toxicity analysis was done through the counting of number of cells (Figure 28) and their visualization under microscope (data not shown).

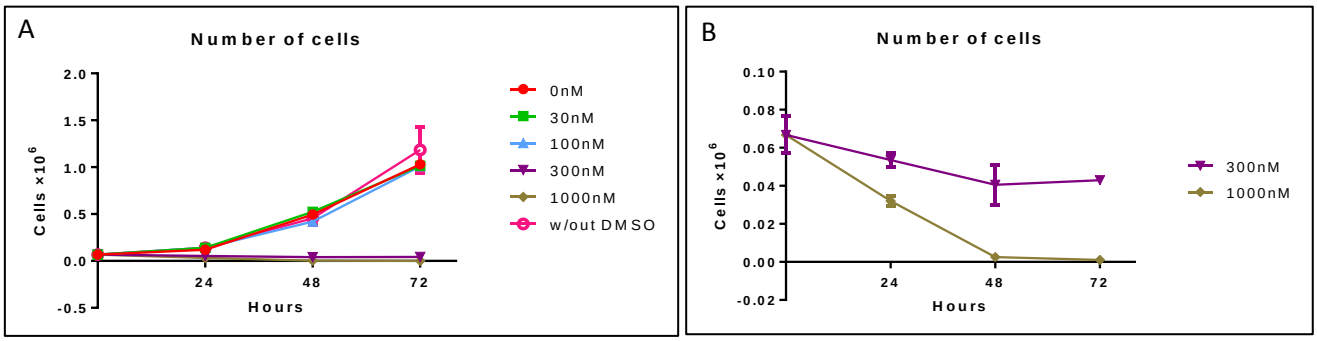

Figure 28 – Quantification of number of cells after an exposure to no DMSO, 0nM, 30nM, 100nM, 300nM and 1000nM of MG132 on time 0, after 24, 48 and 72 hours. (A) All data obtained. (B) Number of cells of 300nM and 1000nM exposure cells after 0, 24, 48 and 72 hours. Each data point is the mean ±S.E.M of 4 biological repetitions.

Based on the results from the cells counting we can see that all the conditions with the exception of 300nM and 1000nM treated cells presented approximately the same number of cells as the control (0nM) (Figure 28.A). In the Figure 28.B was visible that cells treated with 300nM and 1000nM were starting to die even after 24 hours.

A western blot was done with samples treated with 0, 100 and 300nM of MG-132 for 0 and 24 hours and the result is present in Figure 29.

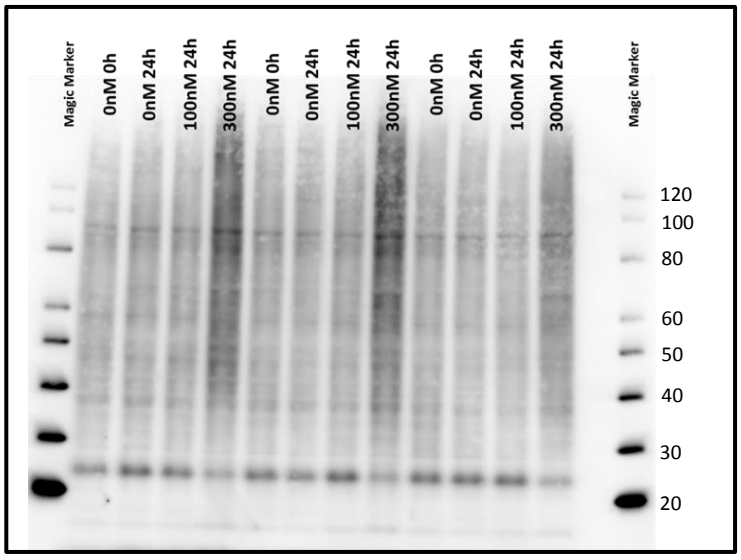

Figure 29 – Western blotting analysis of cells exposed to 0, 100 and 300nM of MG-132 for 0 and 24h.

Based on the western blot, 100 nM MG132 did not result in a noticeable increase in protein ubiquitination whereas there was a clear increase in ubiquitin signal in cell treated with 300 nM MG-132. Based on unpublished data from our lab, 100 and 1000 nM MG-132 inhibit proteasome activity by 60 and 90% respectively (data not shown), implying that more that 60% of proteasomal inhibition is required for accumulation of ubiquitinated protein.

4.3.1.2 Effect of proteasome inhibition on tau protein synthesis.

In addition to using the halotag as a means to label tau and measure protein degradation via pulse-chase, we also evaluated whether it could be used as a simple nonradioactive means to measure rates of tau synthesis. Compounds that decrease total tau levels could do so simply by decreasing tau synthesis. In this experiment, a western blot was done with these samples (Figure 30.A) that was then quantified (Figure 30.B).

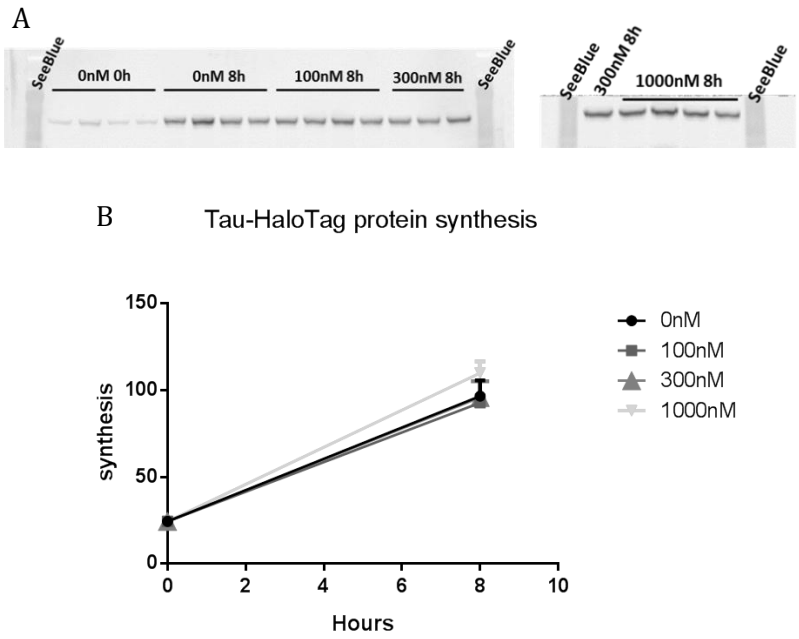

Figure 30 - TauP301L-HaloTag protein synthesis after the exposition to a 0, 100 and 300nM of MG-132 for 8 hours. P301L tau-halotag transfected cells were exposed to coumarin haloligand to block all halotag sites time 0, when the tracer ligand, TMR, was added along with MG-132. (A) Western Blot analysis of Tau-Halotag protein synthesis without K18. (B) Quantitative analysis of Tau-HaloTag protein accumulation in the same conditions. Each data point is the mean ±S.E.M of 4 biological repetitions.

Tau synthesis after 8 hours seemed to be the equal in the conditions where cells were exposed to 0,100, 300 and 1000 nM of MG-132 (Figure 30).

4.3.1.3 Effect of proteasome inhibition on normal tau protein degradation.

If proteasomal degradation is a significant pathway for tau degradation, then proteasomal inhibition should slow the rate of tau degradation. To test this, cells were transfected with the P301L-tau-halo plasmid, labelled with fluorescent halo ligand, and lysed at various times after MG-132 addition. A western blot was done with these samples (Figure 31.A) and the amount of fluorescent label was quantified (Figure 31.B).

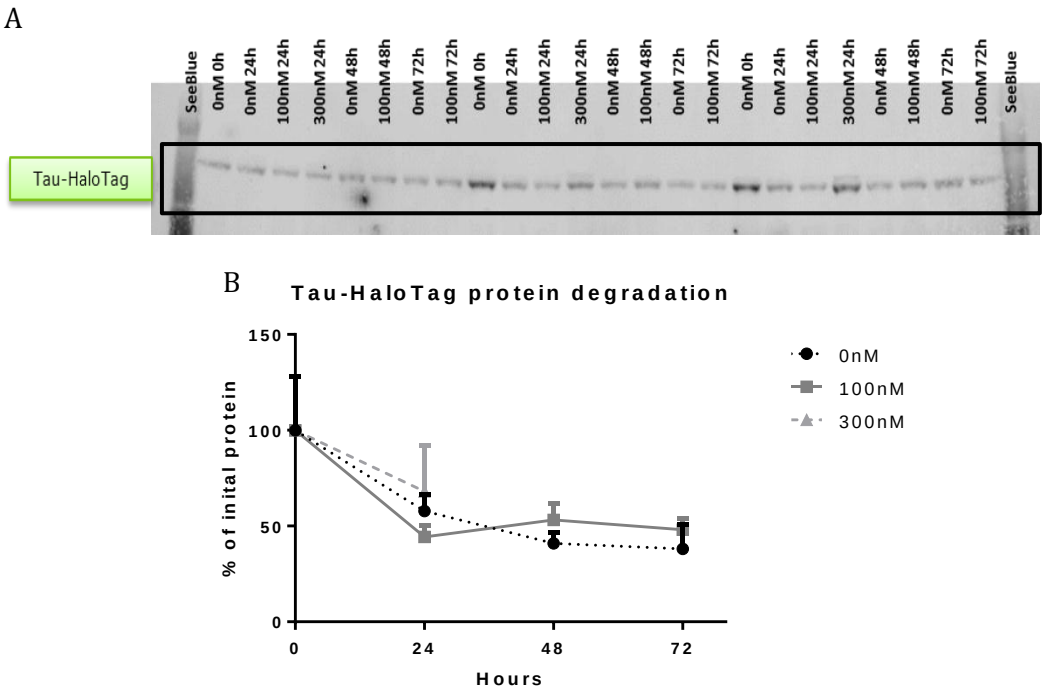

Figure 31 - TauP301L-HaloTag protein degradation after the exposition to a 0, 100 and 300nM of MG-132 for 24, 48 and 72 hours. (A) Western Blot analysis of Tau-Halotag protein degradation without K18. (B) Quantitative analysis of Tau-HaloTag protein degradation in the same conditions where the initial amount of protein was considered as 100%. Each data point is the mean ±S.E.M of 6 biological repetitions.

The signal of 0nM 0h was considered as 100% of initial protein when the results were analyzed (Figure 31). After 24 hours the amount of protein decreased to half of the initial amount and at 48 and 72 hours the decrease was not so significant (Figure 31.B). MG-132 addition did not significantly slow the loss of TMR-ligand in the tau band at any time points, suggesting proteasomal inhibition at 100 or 300 nM did not slow tau degradation.

4.3.2 Observation of effect of autophagy on tau protein degradation, synthesis and aggregation.

We next used E64 and Leupeptin to inhibit autophagy activity, and Rapamycin to enhance autophagy and evaluated their effects on tau degradation and synthesis at concentrations that were not cytotoxic.

4.3.2.1 Toxicity analysis of Leupeptin, E64 and Rapamycin on QBI WT cells.

To have an idea of which concentrations of Leupeptin, E64 and Rapamycin would be better and for how long these concentrations could be used, a toxicity analysis was done through the counting of number of cells (Figure 32) and their visualization under microscope (data not shown).

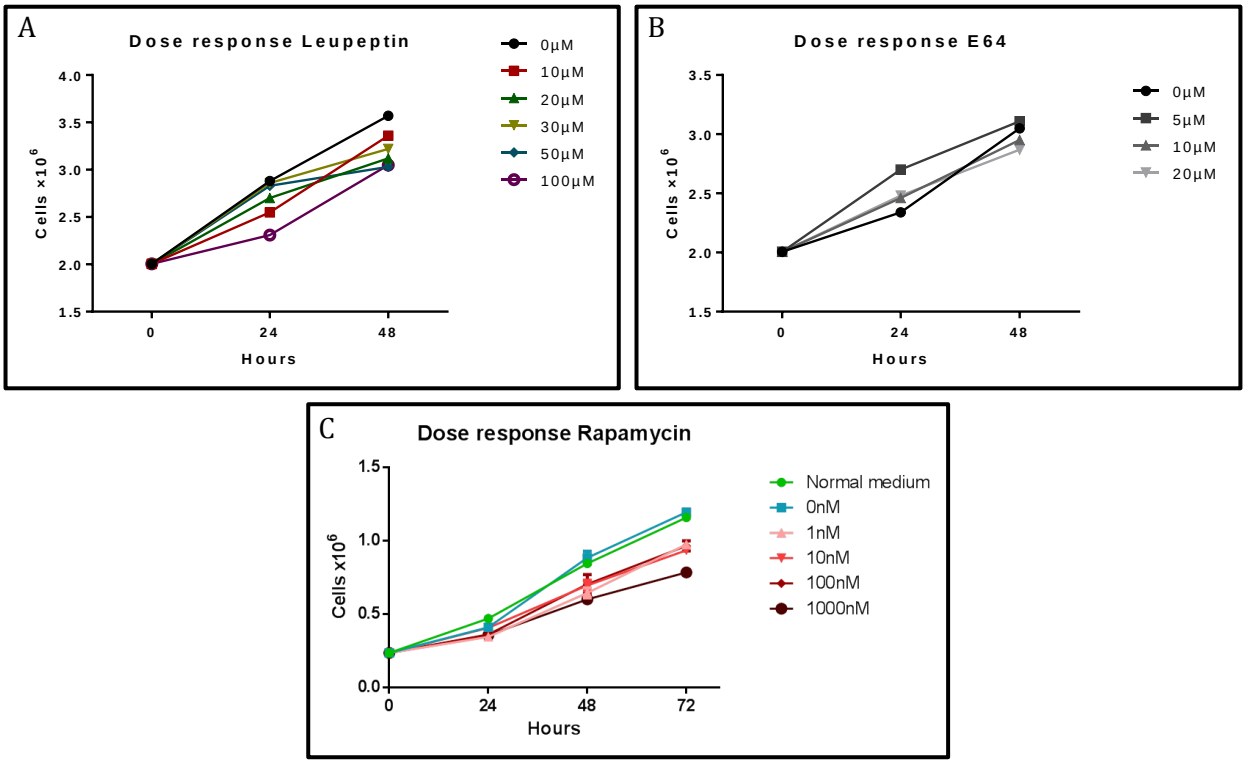

Figure 32 - Quantification of QBI WT number of cells after an exposure to different concentrations of Leupetin, E64 and Rapamycin on time 0, after 24, 48 and 72 hours (Rapamycin). (A) Dose response with Leupeptin treated cells. (B) Dose response with E64 treated cells (C) Dose response with Rapamycin treated cells. Each data point is the mean ±S.E.M of 2 biological repetitions.

Based on the results from the cells counting we could see that all the conditions presented approximately the same number of cells as the control (0nM) (Figure 32) and that there was no major cell death overtime like with MG-132 treatment.

4.3.2.2 Effect of Lysosome inhibition on tau protein degradation and synthesis through the use of E64 and Leupeptin drug.

4.3.2.2.1 Effect of lysosome inhibition on tau protein degradation.

Tau-HaloTag transfected cells (0.25µg) were treated with 50µM of Leupeptin or 5µM of E64 and lysed after 12 and 24 hours. Samples were western blotted (Figure 33.A), visualized via fluorescent scanner and bands quantified (Figure 33.B)

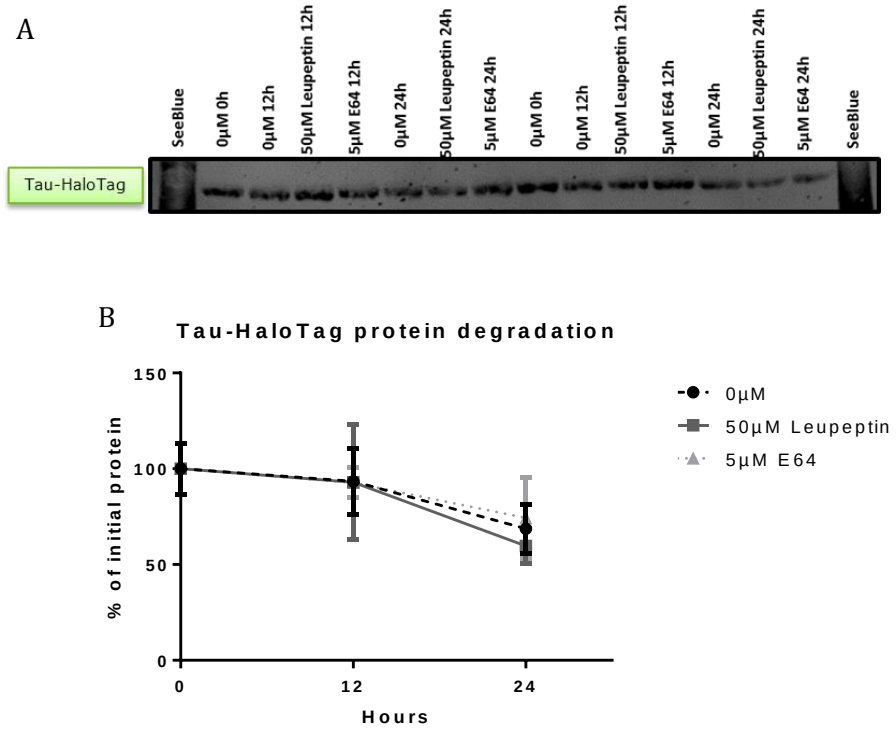

Figure 33 - TauP301L-HaloTag protein degradation after the exposition to a 50µM of Leupeptin and 5µM of E64 for 12 and 24 hours. Cells were transfected with P301L tau-halotag and exposed to TMR-haloligand to label tau. At time 0, TMR ligand was replace by coumarin halo-ligand, and Leupeptin or E64 were added. TMR ligand in tau bands was quantified by fluorescent scanner after western blotting. (A) Western Blot analysis of Tau-Halotag-TMR ligand protein degradation without K18. (B) Quantitative analysis of Tau-HaloTag protein degradation with the same conditions where the initial amount of protein was considered as 100%. Each data point is the mean ±S.E.M of 4 biological repetitions.

A decrease in the tau band fluorescent signal was seen by 24 hrs (Figure 33.A and B). Leupeptin and E64 did not significantly reduce the amount of fluorescent signal at 24 hrs suggesting they did not enhance tau degradation. Between 0h and 12h no difference was shown either in Figure 33.A and B.

4.3.2.2.2 Effect of lysosome inhibition on tau protein synthesis.

To confirm that Leupeptin and E64 did not alter tau synthesis rates, we measured the accumulation of Tau-halotag protein over time, as described previously. Tau-HaloTag transfected cells were treated with and 50µM of Leupeptin and 5µM of E64 and lysed after 2, 4 and 8 hours. A western blot was done with these samples (Figure 34.A) that was then quantified (Figure 34.B).

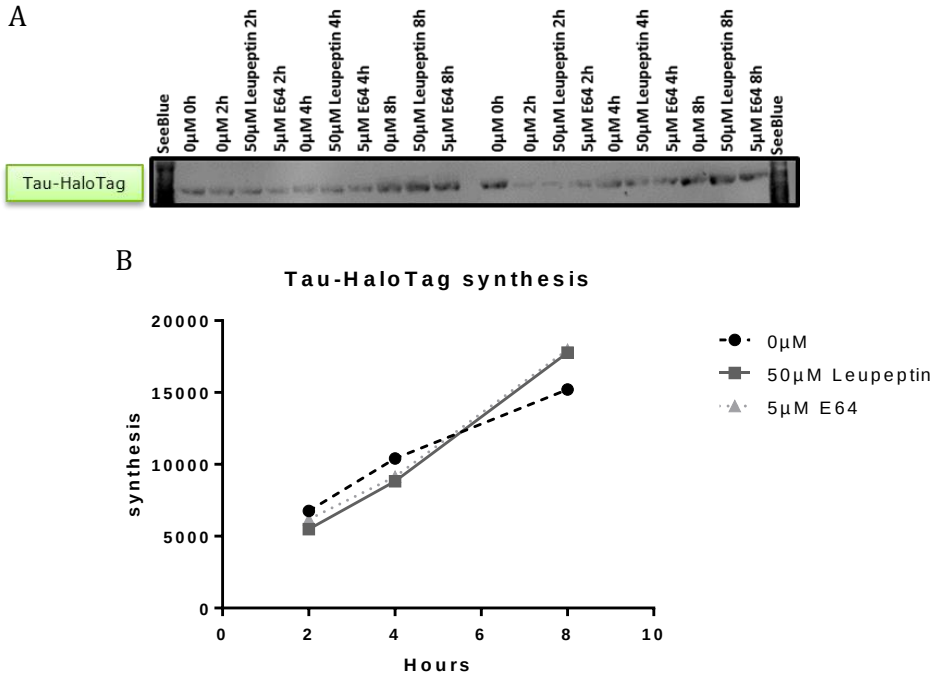

Figure 34 - TauP301L-HaloTag protein synthesis after the exposition to a 50µM of Leupeptin and 5µM of E64 for 2, 4 and 8 hours. (A) Western Blot analysis of Tau-Halotag protein synthesis without K18. (B) Quantitative analysis of Tau-HaloTag protein degradation with the same conditions. Each data point is the mean ±S.E.M of 4 biological repetitions.

There was a linear increase in the amount of fluorescent signal in the tau band from 2 to 8 hrs, which as not altered by addition of Leupeptin or E64 (Figure 34.B).

4.3.2.3 Effect of the autophagy inducer Rapamycin on tau protein degradation.

To evaluate whether the autophagy enhancer rapamycin altered tau degradation or aggregation, Tau-HaloTag transfected cells were treated with 0, 1, 10, 100 or 1000nM of

Rapamycin. Aggregation was induced via fibril addition and cells were lysed after 2 and 4 days.

4.3.2.3.1 Effect of increase of autophagy function on normal and pathological tau protein degradation.

A western blot was done with the samples previously described in 4.3.2.2 (Figure 35.A) that was then quantified (Figure 35.B and C).

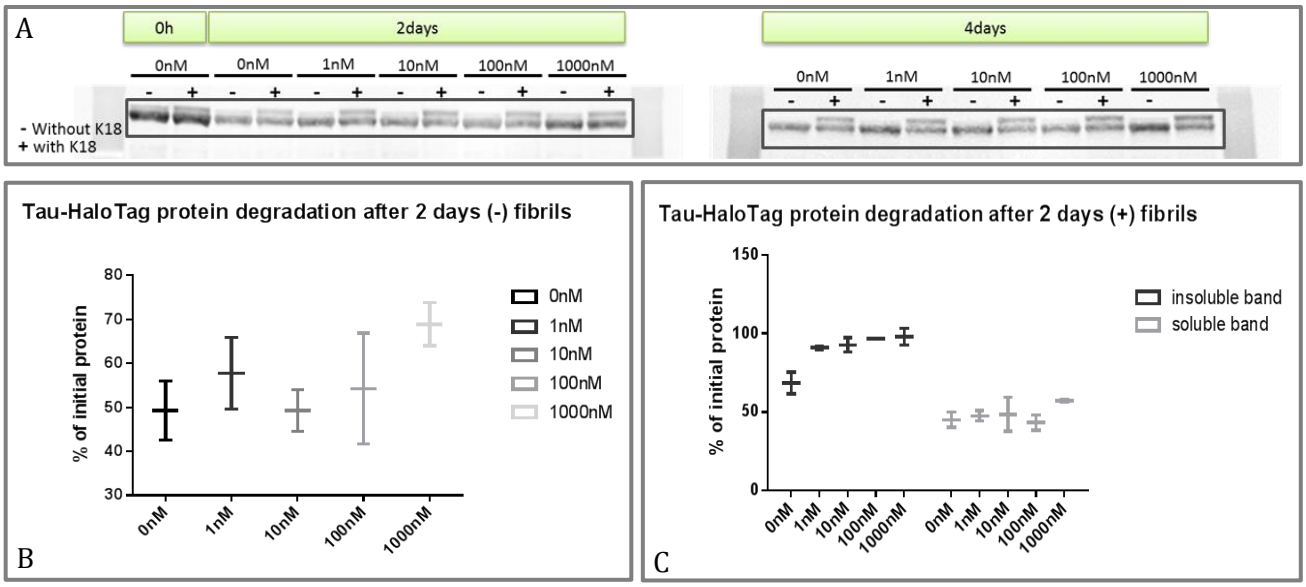

Figure 35 - TauP301L-HaloTag protein degradation after the exposition to a 0, 1, 10, 100 or 1000nM of Rapamycin for 2 and 4 days. (A) Western Blot analysis of Tau-Halotag protein degradation with and without K18. (B) Quantitative analysis of Tau-HaloTag protein degradation of soluble band (without K18) where the initial amount of protein was considered as 100%. (C) Quantitative analysis of Tau-HaloTag protein degradation of soluble and insoluble band where the initial amount of protein was considered as 100%. Each data point is the mean ±S.E.M of 2 biological repetitions.

In Figure 35.A a notable decrease of fluorescent signal was observed between 0h and 2 or 4 days. A second band appeared when K18 fibrils was added, corresponding to the sarkosyl insoluble tau band, while the consistent band was representing soluble tau (Figure 35.A and B). It was not possible to do a statistical analysis due to inadequate replicates, however the bands were quantified (Figure 47 in annex) and the only time point where some differences could be observed was on day 2 (Figure 35.B and C). When compared with 0nM control cells it seemed that 1000nM exposed cells had a higher percentage of initial protein in the absence of K18, however the results need to be confirmed (Figure 35.B). When we look to the Figure 35.C it seemed that when cells were exposed to K18 fibrils and some

concentration of drug different from 0nM the percentage of initial protein was higher than 0nM exposed cells. Related with the quantification of percentage of initial protein in the insoluble band, no significant differences seemed to be appearing.

4.3.2.3.2 Effect of rapamycin on tau protein aggregation.

In the same samples from day 2 above Figure 35.B an AlphaLISA was done to see the tau aggregation and the total tau (Figure 36).

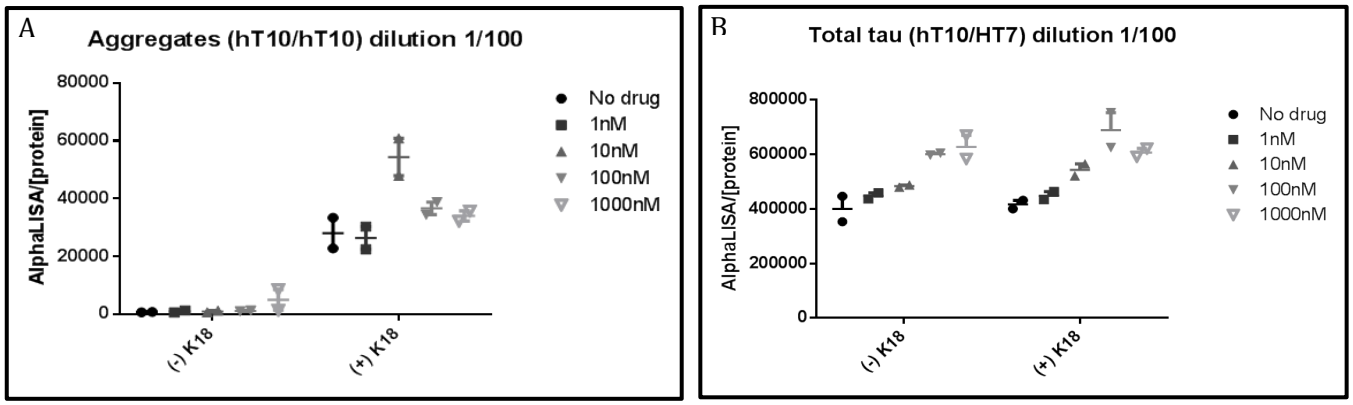

Figure 36 - AlphaLISA's results from autophagy enhance through Rapamycin. (A) Tau aggregates quantification using hT10/hT10 antibodies combination with samples diluted 1/100. (B) Total Tau quantification using hT10/HT7 antibodies combination with samples diluted 1/100. Results' normalization was done with the initial protein concentration of each sample. Each data point is the mean ±S.E.M of 2 biological and 3 mechanic repetitions.

In Figure 36 are represented the results from the AlphaLISA assays, preformed with the samples previously analyzed diluted 1/100. When we looked to total tau hT10/HT7 signal graph (Figure 36.B) we could see that in the absence of K18 100nm and 1000nm exposed cells presented a higher level of hT10/HT7 signal when compared with 0nM exposed cells. In the samples that were exposed to K18 the same effect was happening. In the tau aggregates graph (Figure 36.A) the results from the samples without K18 were negative (ns). When we analyzed the samples were K18 was added it seemed that 10nM exposed present a higher level of hT10/hT10 signal when compared with 0nM exposed transfected cells.

4.3.2.3.3 Confirmation of autophagy activity on the samples used.

To confirm the activity of the autophagy in the samples those were use in the previous step (day 2) we western blotted the lysates and detected them with LC3 antibody and normalized to actin (Figure 37).

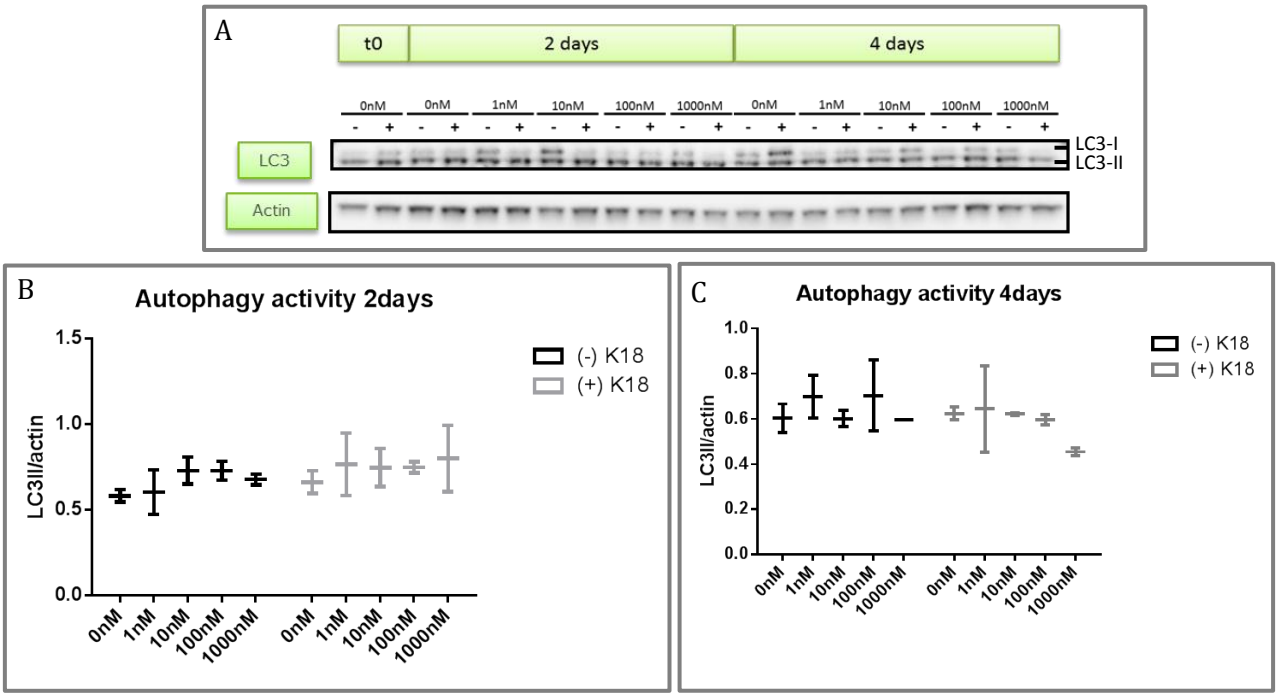

Figure 37 – Autophagy activity after the exposition to a 0, 1, 10, 100 or 1000nM of Rapamycin for 2 and 4 days. (A) Western Blot analysis of LC3-II with and without K18 and with different concentrations of drug. (B) Quantitative analysis of LC3-II with (+) K18 and without (-) K18 for day 2 normalized to actin. (C) Quantitative analysis of LC3-II with (+) K18 and without (-) K18 for day 2 normalized to actin. Each data point is the mean ±S.E.M of 2 biological repetitions.

The bottom LC3 band (LC3-II) in Figure 37.A was normalized to actin and is presented in Figure 37.B and C. However the quantification of the samples confirmed that no significant differences were found either in the presence or in absence of K18.

Discussion

Alzheimer's disease is the most common neurodegenerative disease, having more than 36 million newly diagnosed people per year worldwide what makes the study of the mechanisms involved in this disease really important. As referred above, tau protein aggregation is present in several neurodegenerative diseases as AD and other Taupathies and is correlated with the severity of memory deficit in AD (Wang and Mandelkow 2012). In this project we tried to find possible ways to decrease tau aggregate formation or increase its degradation.

Previous students, as Sara Calafate and Bruno Vasconcelos (thesis Bruno Vasconcelos 2011, and Sara Calafate 2012), showed that QBI cells are a good model to study specific genes and pathways in the buildup, spreading and clearance of tau aggregates. For these reasons and because it is easier to work with them more than with neurons, we could obtain results faster, the QBI WT and the QBI inducible cells were used during this entire project.

Ubiquitinated tau is reported to be a component of NFTs. Ihara's group showed that insoluble PHF-tau isolated from an AD brain were ubiquitinated at tau residues Lys^{254}, Lys^{257}, Lys^{311} and Lys^{317} (Morishima-Kawashima, Hasegawa et al. 1993). Moreover Cripps showed that soluble PHF-tau from AD brains was ubiquitinated at Lys^{254}, Lys^{311} and Lys^{353} (Cripps, Thomas et al. 2006). In addition, Kandimalla, et al. reported that there is a higher level of ubiquitin in subjects with AD and a significant positive correlation between ubiquitin and tau (Kandimalla, Anand et al. 2014). Although tau has been shown to be degraded by multiple pathways in vitro (20S proteasome, 26S proteasome, autophagy), the role of these pathways under normal physiological and pathophysiological conditions is less clear, as is their role on tau aggregate formation. We therefore chose to remove all reported ubiquitination sites from P301L tau via a lysine to arginine mutation and evaluate its effect on aggregation and degradation of tau protein (Lee, Lee et al. 2013).

After the cloning and sequence confirmation, we evaluated whether deletion of ubiquitination sites on P301L tau altered levels of tau protein or aggregates after the addition of fibrils (Figure 14). Regardless of fibril addition, total tau levels were consistently lower in cells expressing the 3xKR and 5xKR mutations. It was not clear whether this was due to altered synthesis or degradation. However, if ubiquitination played an obligatory role

in tau degradation in QBI cells one would expect elevated and not reduced levels of total tau. If ubiquitin did play a role in tau degradation in QBI cells, it must have been via ubiquitination of alternative unidentified ubiquitinated lysines or acting via other proteins. Aggregated tau signal was also lower in cells expressing the 3xKR and 5xKR mutations than in control cells, however as the proportion of aggregated to total tau levels was equal between all three groups, the difference was likely driven by total tau levels (i.e. less total tau means less tau to aggregate). Nevertheless, if ubiquitination of tau has an important role in preventing the buildup or enhancing the clearance of aggregates in this model, aggregated tau levels should have been elevated in 3xKR or 5xKR expressing cells rather than reduced.

To evaluate whether clearance is altered by the 3xKR or 5xKR mutations we estimated tau degradation by measuring the loss of fluorescent signal when was bound to the tau-halotag (Figure 15). There was approximately 50% loss in signal in the main soluble tau band 2 days after fibril addition in the control group as well as 3xKR and 5xKR groups, suggesting a half-life of 2 days under these conditions. This was slightly longer than previously observed in our lab (~18-24 hrs half-life), however, the cells in this experiment were older and more confluent than in previous experiments. Cell growth or cell division could have biased the half-life by diluting the signal. Tau half-life has been estimated to be anywhere from 6 to 72 hours depending on the model and methodology used (Poppek, Keck et al. 2006). The loss of signal in the band representing insoluble tau was variable and not statistically different between groups. However we should have seen if the synthesis of tau was affected by these mutations. The absence of differences between the mutants could also have been explained by the clearance of tau through 20S proteasome subunit without a requirement for ubiquitination (David, Layfield et al. 2002, Grune, Botzen et al. 2010) or by the clearance of tau through autophagy.

To evaluate whether we could detect ubiquitinated tau species and whether these were reduced in the 3xKR and 5xKR mutants, we immunoprecipitated tau in control and proteasome inhibited cells (Figure 16). Different concentrations of MG-132 were used to increase the amount of ubiquitinated protein to facilitate the detection. (You and Park 2011, Park and Kim 2012). We have previously observed that 300 nM MG-132 was necessary and sufficient to enhance overall protein ubiquitination in western blots (Figure 29). We detected a weak anti-ubiquitin labelling against cell lysates due to a low amount of protein

available. No ubiquitin labelling of tau was detected. When tau was immunoblotted, there was no visible difference in tau protein between control and 3xKR or 5xKR lanes, further confirming that these mutations did not result in an accumulation of tau in the cell. There was also no visible difference in anti-tau bands (or smears) above 60 kDa which are indicative of ubiquitinated tau accumulation or lack thereof. These results were consistent with Babu et al 2005, who observed ubiquitinated tau only if tau was co-transfected with a HA-ubiquitin, and confirmed that detecting ubiquitinated tau without the use of mass spectrometery is extremely difficult. A possible solution to this problem should be to do an IP labeling ubiquitinated protein and detect tau protein, or do a mass spectrometry and isolate and quantify the ubiquitinated tau.

The physiological importance of DUBs in neurodegenerative diseases remains to be determined. However some mutations in DUBs, as UCH-L1 and Ataxin-3, have been proposed to have a role in various neurodegenerative diseases including AD and Parkinson (Lee, Lee et al. 2013). Furthermore, the first evidence for the pathological relation between tau and UPS appeared from the frequent co-localization and accumulation of Ub in PHFs and NFTs (Lee, Lee et al. 2013). So as one of the most important goals of this project we wanted to know if the overexpression of DUBs: USP5, USP7, USP9x and OTUB1 could alter the levels of tau. These DUBs have been observed to co-immunoprecipiate with tau derived from mouse brain as quantified by iTRAQ MS quantification. Because of this observed interaction with tau, we evaluated whether overexpression of these DUBs could alter tau aggregation.

We examined whether overexpression of USP5 (at 2 different construct concentrations) altered tau aggregation in our QBI model. USP5 overexpression without fibrils resulted in either a small or no decrease in total tau levels. After fibril addition, aggregated tau signal was consistently lower in USP5 overexpressing cells than in empty vector transfected cells. The proportion of aggregated tau to total tau signal was calculated under fibrils conditions to correct for levels of total tau, and this was also consistently lower after USP5 overexpression compared to control vector in both experiments.

As mentioned above, besides having been observed to colocalize with tau, we had no biological explanation as to why USP5 overexpression lowers aggregated tau preferentially.

USP5 is responsible for recycling unanchored polyubiquitin from proteasomes back to free ubiquitin (Fan, Huang et al. 2014), whether overexpressing USP5 significantly enhances free ubiquitin is unknown. This process can help the labeling of new protein to degradation since the amount of free ubiquitin will increase. Since USP5 is believed not to prematurely deubiquitinate a polyubiquitinated protein (Reyes-Turcu, Ventii et al. 2009), its interaction with tau is not likely one of deubiquitination, and likely a more complex protein-protein interaction.

Although we overexpressed USP7 in QBI cells (Figure 21), this overexpression only resulted in a small decrease in aggregated tau signal, which was accompanied with a decrease in total tau signal. However, there was no indication that USP7 overexpression preferentially lowered aggregated tau levels. Furthermore there was also a trend towards a lowering of total Tau levels in the USP7 versus empty vector transfected cells in the absence of the seed, suggesting USP7 overexpression primarily altered levels of total tau rather than buildup or clearance of aggregates.

USP7 was located in the nucleus (Figure 22.B) and some of its substrates play roles in tumor suppression, immune responses, DNA repair, viral replication and epigenetic modulators, however its interaction with tau is unclear since tau is located in the cytosol. USP7 could be minority located in cytosol and then interacting with tau or could be regulating tau protein at nuclear level. Other possibility was that results from the interactome were derived from the breaking of membranes and the mixing of all complexes that would allow the binding of these proteins.

Like USP7, USP9x overexpression did not significantly alter aggregated tau levels, and any suggestion for a difference could be explained by a similar trend for a reduction on total tau levels, after fibrils.

USP9x is implicated in developing of CNS and when this is already mature USP9x is present just in neurogenic regions meaning that its principal role is involved in neurons maturation and its substrates show that is implicated in multiple physiological pathways including neurodevelopmental signaling pathways. However, its interaction with tau protein is not well known.

Overexpression of OTUB1 resulted in a significant and almost complete reduction in tau aggregate levels when comparing OTUB1 versus empty vector transfected cells. This was also apparent when the relative level of aggregated to total tau within a condition were measured. In contrast to the results obtained for Usp5, a significant OTUB1 mediated effect on total tau levels was observed. This was also observed when comparing OTUB1 to empty vector transduced cells in the absence of the seed (Figure 26 and 28). Whether OTUB1 overexpression exclusively lowers total tau levels or also directly affects aggregated tau levels requires further investigation. To evaluate this effect we could use a cell line present in our lab that is constantly expressing tau aggregates at the same level an overexpress OTUB1 as well as the correspondent empty vector in that cells and evaluate if some differences in the aggregates appear.

The effect on total tau levels was not due to a generalized effect of OTUB1 overexpression on protein expression. AlphaLISA results were normalized to total lysate protein concentration, so the result could not be attributed to a lowering of protein levels due to cellular toxicity. As mentioned, OTUB1 was observed to co-immunoprecipitate with tau, so it was perceivable that OTUB1 did play some role in controlling cellular levels of tau protein. If this was the case, it would imply that enhancing OTUB1 activity could be used as a means to lower total tau levels.

Some authors as Babu (2005, 2009) show that tau in pathological and non-pathological conditions are K63-ubiquitinated, even if the tau protein is degraded by UPS, however others authors as Morishima and Cripps detected K48-linked Ub chains in PHF-tau form from an AD brain (Morishima-Kawashima, Hasegawa et al. 1993, Babu, Geetha et al. 2005, Cripps, Thomas et al. 2006, Ramesh Babu, Lamar Seibenhener et al. 2008). OTUB1 has deubiquitinating activity to preferentially deubiquitinate K48-linked polyubiquitin chains and besides that preferentially also regulates synthesis of K63Ub in a non-canonical manner (Stanisic, Malovannaya et al. 2009). It was not clear if OTUB1 was regulating the degradation of tau/aggregates through one of these two ways and to know these more experiments have to be done, as evaluate the difference of amount of K48-linked polyubiquitin chains and K63-Ub after the overexpression of OTUB1.

UPS might be the mechanism more efficient and dominant, mediating tau clearance when the protein is monomeric. However, higher conformations as oligomers and aggregates are likely to be inaccessible to the narrow proteasome opening, so is expected that these species have much higher dependency on autophagy for degradation (Lee, Lee et al. 2013). This subject is still unclear so we wanted to understand more about the effect of changing the activity of the proteasome and the autophagy. With these changes we tried to evaluate the effect this mechanisms on aggregation, degradation and synthesis of tau.

MG-132 is a peptide aldehyde that effectively blocks the proteolytic activity of proteasome complex and it was for that reason that we chose it for this project. Rapamycin is an mTOR inhibitor which in turn negatively modulates autophagy. The use of Rapamycin was chosen in this project to enhance the activity of autophagy (Lee, Lee et al. 2013). Besides these drugs, Leupeptin and E64 (proteases inhibitors) were also chosen but in this case they were used to inhibit autolysosome formation and consequentially autophagy activity (Mizushima, Yoshimori et al. 2010).

Before evaluating whether proteasome inhibition could inhibit tau degradation or not, we tested the toxicity of MG-132 on QBI cells. MG-132 was cytotoxic. At 1 M it killed almost all cells within 2 days, and at 300nM it killed almost half of the cells. Only at 100nM MG-132 and below did cells grow normally. In agreement with the cell growth data, 300nM MG-132 was also the lowest concentration that caused polyubiquitinated protein accumulation when evaluated by western blotting. Based on a proteasome inhibition assay in our lab, we predict 300nM MG-132 to inhibit the proteasome by about 75%. Below this level of inhibition, it appeared QBI cells were able to cope with the reduced level of proteasome flux. To avoid proteotoxicity, selected concentrations (100 and 300nM) were used to evaluate the effect of proteasome inhibition on normal tau protein degradation (Figure 31). However no significant differences were found between the control (0nM) and 100nM and 300nM of MG-132 concentration meaning that the inhibition of proteasome by about 60% or more is not altering the degradation on tau protein in QBI cells. Whether tau is normally not degraded via the proteasome, or whether cellular adaptation occurred was not clear. UPS inhibition has been found increase autophagy activity and flux (Lee, Lee et al. 2013) However this might be explain by an increase in the autophagy activity, as it has been

observed that the UPS inhibition can result in an enhancement of autophagy flux, at least after 0.5µM of MG-132 in HCT116 cell line (Ding, Ni et al. 2007, Lee, Lee et al. 2013).

Proteasome inhibition lowers protein degradation, which reduces amino acid recycling and could result in amino acid starvation and inhibition of protein synthesis. When therefore tested whether acute MG-132 treatment altered tau synthesis, we found no change in accumulation of fluorescently labelled tau-halotag over time (Figure 30). However, this could be again due to autophagy compensation because if the tau degradation would be decreased the amino acids available to re-synthesis tau protein would decrease too.

Since proteasome inhibition did not alter tau degradation in our hands, we next tested whether autophagy inhibition could attenuate tau degradation (Figure 33) or tau synthesis (Figure 34) using Leupeptin and E64. The doses we chose were similar to those previously reported in the literature, and had much less impact on cell survival than the proteasome inhibitor MG-132. However the concentrations chosen to evaluate protein degradation had no impact on tau-halotag loss over 24 hr. Whether this was due to cellular compensation (Seiberlich, Goldbaum et al. 2012), or inadequate drug concentration was not clear.

Since enhancing autophagy has been proposed as a potential therapy for neurodegenerative disease (Lee, Lee et al. 2013) we performed a preliminary experiment, over a broad concentration range to evaluate whether rapamycin could alter tau aggregation or degradation in our QBI model. We wanted to evaluate the effect of autophagy pathway in tau degradation but since with the inhibition nothing was shown we tried to enhance autophagy activity with the use of different concentrations of Rapamycin, under normal and pathological conditions, without and with K18, respectively. After 4 days the differences between the conditions were not significant meaning that the autophagy system was already too damaged to do function (Lee, Lee et al. 2013) or the action of Rapamycin was already over. By 2 days after fibril addition, (Figure 30), aside from control cells, there was very little loss in the insoluble band at all rapamycin concentrations. Whether this is repeatable needs to be confirmed, but it would imply that rapamycin was

actually attenuating tau aggregate degradation. However, except for one rapamycin concentration, this did result in an increase in aggregated tau as measured by AlphaLISA. (Figure 36) Both in the presence and absence of fibrils, total tau hT10/HT7 signal increased with increasing concentrations of Rapamycin. This could means that under normal conditions ((-) K18), after 2 days, the total amount of tau was increasing with the increase of Rapamycin as well as under pathological conditions. However when we looked to hT10/hT10 signal the samples with higher signal were the samples with 10nM of Rapamycin. To confirm the activity of Rapamycin we measured the amount of LC3-II (Figure 37) present in the same samples previously analyzed and the ratio between LC-II signal and actin was done (Figure 37.B and C) (Mizushima and Yoshimori 2007, Mizushima, Yoshimori et al. 2010). However we were unable to confirm that rapamycin altered LC3-II levels, to confirm that it altered autophagy activity. Furthermore all the experiments involving Rapamycin have to be repeated.

Here we show that ubiquitination of tau at the known ubiquitinated lysine residues did not have an obligatory role in tau clearance, however the action of USP5 and OTUB1 were changing the same mechanism whether clearing soluble or aggregated tau. This could potentially be explained, as mentioned before, by the action of other unknown lysines involved in tau ubiquitination in our model, by the interference with ubiquitination of other proteins that could regulate the clearance of tau or that could change ubiquitination of proteins that link both systems, UPS and autophagy, like P62, enhancing the autophagy pathway (Seiberlich, Goldbaum et al. 2012) or could be explained by the enhancement in the activity of the DUBs that usually do not play an important role.

Concluding Remarks

Decreasing the amount of aggregates seems to be a good strategy to reduce the severity of memory deficit in AD.

Our studies provide no indication that ubiquitination on Lys^{254}, Lys^{257}, Lys^{311}, Lys^{317} and Lys^{353} played an obligatory role in either tau degradation, or in the buildup or clearance of aggregates in our cellular model. However the total amount of tau and consequently the aggregates of tau were decreased with these mutations.

The DUBs USP5, USP7, and OTUB1 were shown to interact with tau protein under normal condition and USP9x was showed to interact under pathological conditions. However, USP5 and OTUB1 were the only DUBs that decreased the aggregated tau protein upon overexpression, possibly by its degradation. However the mechanisms involved in this process are still unclear.

Inhibition of UPS up to doses that resulted in accumulation of polyubiquitinated proteins and were marginally cytotoxic did not alter tau degradation on our cellular model. Likewise, subsequently autophagy inhibition and activation did not have any effect on tau degradation. Whether these results are due to cellular compensation, inadequate drug concentrations or indicate alternative degradation mechanism was not clear.

Bibliography

Bibliography

Alonso, A. D., J. Di Clerico, B. Li, C. P. Corbo, M. E. Alaniz, I. Grundke-Iqbal and K. Iqbal (2010). "Phosphorylation of tau at Thr212, Thr231, and Ser262 combined causes neurodegeneration." J Biol Chem **285**(40): 30851-30860.

Babu, J. R., T. Geetha and M. W. Wooten (2005). "Sequestosome 1/p62 shuttles polyubiquitinated tau for proteasomal degradation." J Neurochem **94**(1): 192-203.

Bahar-Fuchs, A., L. Clare and B. Woods (2013). "Cognitive training and cognitive rehabilitation for mild to moderate Alzheimer's disease and vascular dementia." Cochrane Database Syst Rev **6**: CD003260.

Ballatore, C., V. M. Lee and J. Q. Trojanowski (2007). "Tau-mediated neurodegeneration in Alzheimer's disease and related disorders." Nat Rev Neurosci **8**(9): 663-672.

Behrends, C. and J. W. Harper (2011). "Constructing and decoding unconventional ubiquitin chains." Nat Struct Mol Biol **18**(5): 520-528.

Bennett, D. A., J. A. Schneider, Z. Arvanitakis, J. F. Kelly, N. T. Aggarwal, R. C. Shah and R. S. Wilson (2006). "Neuropathology of older persons without cognitive impairment from two community-based studies." Neurology **66**(12): 1837-1844.

Billingsley, M. L. and R. L. Kincaid (1997). "Regulated phosphorylation and dephosphorylation of tau protein: effects on microtubule interaction, intracellular trafficking and neurodegeneration." Biochem J **323 (Pt 3)**: 577-591.

Blennow, K. (2004). "CSF biomarkers for mild cognitive impairment." J Intern Med **256**(3): 224-234.

Blennow, K., H. Hampel, M. Weiner and H. Zetterberg (2010). "Cerebrospinal fluid and plasma biomarkers in Alzheimer disease." Nat Rev Neurol **6**(3): 131-144.

Blennow, K., A. Wallin, H. Agren, C. Spenger, J. Siegfried and E. Vanmechelen (1995). "Tau protein in cerebrospinal fluid: a biochemical marker for axonal degeneration in Alzheimer disease?" Mol Chem Neuropathol **26**(3): 231-245.

Borchelt, D. R., M. K. Lee, V. Gonzales, H. H. Slunt, T. Ratovitski, N. A. Jenkins, N. G. Copeland, D. L. Price and S. S. Sisodia (2002). "Accumulation of proteolytic fragments of mutant presenilin 1 and accelerated amyloid deposition are co-regulated in transgenic mice." Neurobiol Aging **23**(2): 171-177.

Borchelt, D. R., T. Ratovitski, J. van Lare, M. K. Lee, V. Gonzales, N. A. Jenkins, N. G. Copeland, D. L. Price and S. S. Sisodia (1997). "Accelerated amyloid deposition in the brains of transgenic mice coexpressing mutant presenilin 1 and amyloid precursor proteins." Neuron **19**(4): 939-945.

Buee, L., T. Bussiere, V. Buee-Scherrer, A. Delacourte and P. R. Hof (2000). "Tau protein isoforms, phosphorylation and role in neurodegenerative disorders." Brain Res Brain Res Rev **33**(1): 95-130.

Burger, A. M. and A. K. Seth (2004). "The ubiquitin-mediated protein degradation pathway in cancer: therapeutic implications." Eur J Cancer **40**(15): 2217-2229.

Campion, D., J. M. Flaman, A. Brice, D. Hannequin, B. Dubois, C. Martin, V. Moreau, F. Charbonnier, O. Didierjean, S. Tardieu and et al. (1995). "Mutations of the presenilin I gene in families with early-onset Alzheimer's disease." Hum Mol Genet **4**(12): 2373-2377.

Castellani, R. J., A. Nunomura, H. G. Lee, G. Perry and M. A. Smith (2008). "Phosphorylated tau: toxic, protective, or none of the above." J Alzheimers Dis **14**(4): 377-383.

Chitra, S., G. Nalini and G. Rajasekhar (2012). "The ubiquitin proteasome system and efficacy of proteasome inhibitors in diseases." Int J Rheum Dis **15**(3): 249-260.

Chondrogianni, N. and E. S. Gonos (2012). "Structure and function of the ubiquitin-proteasome system: modulation of components." Prog Mol Biol Transl Sci **109**: 41-74.

Chung, C. W., Y. H. Song, I. K. Kim, W. J. Yoon, B. R. Ryu, D. G. Jo, H. N. Woo, Y. K. Kwon, H. H. Kim, B. J. Gwag, I. H. Mook-Jung and Y. K. Jung (2001). "Proapoptotic effects of tau cleavage product generated by caspase-3." Neurobiol Dis **8**(1): 162-172.

Cripps, D., S. N. Thomas, Y. Jeng, F. Yang, P. Davies and A. J. Yang (2006). "Alzheimer disease-specific conformation of hyperphosphorylated paired helical filament-Tau is polyubiquitinated through Lys-48, Lys-11, and Lys-6 ubiquitin conjugation." J Biol Chem **281**(16): 10825-10838.

Czaja, M. J., W. X. Ding, T. M. Donohue, S. L. Friedman, J. S. Kim, M. Komatsu, J. J. Lemasters, A. Lemoine, J. D. Lin, J. H. Ou, D. H. Perlmutter, G. Randall, R. B. Ray, A. Tsung and X. M. Yin (2013). "Functions of autophagy in normal and diseased liver." Autophagy **9**(8).

Dang, L. C., F. D. Melandri and R. L. Stein (1998). "Kinetic and mechanistic studies on the hydrolysis of ubiquitin C-terminal 7-amido-4-methylcoumarin by deubiquitinating enzymes." Biochemistry **37**(7): 1868-1879.

David, D. C., R. Layfield, L. Serpell, Y. Narain, M. Goedert and M. G. Spillantini (2002). "Proteasomal degradation of tau protein." J Neurochem **83**(1): 176-185.

Dayal, S., A. Sparks, J. Jacob, N. Allende-Vega, D. P. Lane and M. K. Saville (2009). "Suppression of the deubiquitinating enzyme USP5 causes the accumulation of unanchored polyubiquitin and the activation of p53." J Biol Chem **284**(8): 5030-5041.

de Vrij, F. M., D. F. Fischer, F. W. van Leeuwen and E. M. Hol (2004). "Protein quality control in Alzheimer's disease by the ubiquitin proteasome system." Prog Neurobiol **74**(5): 249-270.

Deshaies, R. J. and C. A. Joazeiro (2009). "RING domain E3 ubiquitin ligases." Annu Rev Biochem **78**: 399-434.

Dickey, C. A., A. Kamal, K. Lundgren, N. Klosak, R. M. Bailey, J. Dunmore, P. Ash, S. Shoraka, J. Zlatkovic, C. B. Eckman, C. Patterson, D. W. Dickson, N. S. Nahman, Jr., M. Hutton, F. Burrows and L. Petrucelli (2007). "The high-affinity HSP90-CHIP complex recognizes and selectively degrades phosphorylated tau client proteins." J Clin Invest **117**(3): 648-658.

Ding, H., T. A. Matthews and G. V. Johnson (2006). "Site-specific phosphorylation and caspase cleavage differentially impact tau-microtubule interactions and tau aggregation." J Biol Chem **281**(28): 19107-19114.

Ding, W. X., H. M. Ni, W. Gao, T. Yoshimori, D. B. Stolz, D. Ron and X. M. Yin (2007). "Linking of autophagy to ubiquitin-proteasome system is important for the regulation of endoplasmic reticulum stress and cell viability." Am J Pathol **171**(2): 513-524.

Dixit, R., J. L. Ross, Y. E. Goldman and E. L. Holzbaur (2008). "Differential regulation of dynein and kinesin motor proteins by tau." Science **319**(5866): 1086-1089.

Duan, A. R. and H. V. Goodson (2012). "Taxol-stabilized microtubules promote the formation of filaments from unmodified full-length Tau in vitro." Mol Biol Cell **23**(24): 4796-4806.

Eckroat, T. J., A. S. Mayhoub and S. Garneau-Tsodikova (2013). "Amyloid-beta probes: Review of structure-activity and brain-kinetics relationships." Beilstein J Org Chem **9**: 1012-1044.

Edelmann, M. J., A. Iphofer, M. Akutsu, M. Altun, K. di Gleria, H. B. Kramer, E. Fiebiger, S. Dhe-Paganon and B. M. Kessler (2009). "Structural basis and specificity of human otubain 1-mediated deubiquitination." Biochem J **418**(2): 379-390.

Ewers, M., G. B. Frisoni, S. J. Teipel, L. T. Grinberg, E. Amaro, Jr., H. Heinsen, P. M. Thompson and H. Hampel (2011). "Staging Alzheimer's disease progression with multimodality neuroimaging." Prog Neurobiol **95**(4): 535-546.

Fan, X., Q. Huang, X. Ye, Y. Lin, Y. Chen, X. Lin and J. Qu (2014). "Drosophila USP5 Controls the Activation of Apoptosis and the Jun N-Terminal Kinase Pathway during Eye Development." PLoS One **9**(3): e92250.

Fauquant, C., V. Redeker, I. Landrieu, J. M. Wieruszeski, D. Verdegem, O. Laprevote, G. Lippens, B. Gigant and M. Knossow (2011). "Systematic identification of tubulin-interacting fragments of the microtubule-associated protein Tau leads to a highly efficient promoter of microtubule assembly." J Biol Chem **286**(38): 33358-33368.

Fischer, D., M. D. Mukrasch, J. Biernat, S. Bibow, M. Blackledge, C. Griesinger, E. Mandelkow and M. Zweckstetter (2009). "Conformational changes specific for pseudophosphorylation at serine 262 selectively impair binding of tau to microtubules." Biochemistry **48**(42): 10047-10055.

Friedhoff, P., A. Schneider, E. M. Mandelkow and E. Mandelkow (1998). "Rapid assembly of Alzheimer-like paired helical filaments from microtubule-associated protein tau monitored by fluorescence in solution." Biochemistry **37**(28): 10223-10230.

Gelino, S. and M. Hansen (2012). "Autophagy - An Emerging Anti-Aging Mechanism." J Clin Exp Pathol **Suppl 4**.

Grabbe, C., K. Husnjak and I. Dikic (2011). "The spatial and temporal organization of ubiquitin networks." Nat Rev Mol Cell Biol **12**(5): 295-307.

Gracia-Sancho, J., S. Guixe-Muntet, D. Hide and J. Bosch (2014). "Modulation of autophagy for the treatment of liver diseases." Expert Opin Investig Drugs.

Grune, T., D. Botzen, M. Engels, P. Voss, B. Kaiser, T. Jung, S. Grimm, G. Ermak and K. J. Davies (2010). "Tau protein degradation is catalyzed by the ATP/ubiquitin-independent 20S proteasome under normal cell conditions." Arch Biochem Biophys **500**(2): 181-188.

Guo, J. L. and V. M. Lee (2011). "Seeding of normal Tau by pathological Tau conformers drives pathogenesis of Alzheimer-like tangles." J Biol Chem **286**(17): 15317-15331.

Holowaty, M. N., Y. Sheng, T. Nguyen, C. Arrowsmith and L. Frappier (2003). "Protein interaction domains of the ubiquitin-specific protease, USP7/HAUSP." J Biol Chem **278**(48): 47753-47761.

Honjo, K., S. E. Black and N. P. Verhoeff (2012). "Alzheimer's disease, cerebrovascular disease, and the beta-amyloid cascade." Can J Neurol Sci **39**(6): 712-728.

Huang, Z., Q. Wu, O. A. Guryanova, L. Cheng, W. Shou, J. N. Rich and S. Bao (2011). "Deubiquitylase HAUSP stabilizes REST and promotes maintenance of neural progenitor cells." Nat Cell Biol **13**(2): 142-152.

Huang, Z., W. Zhou and S. Bao (2011). "Role of deubiquitylase HAUSP in stem cell maintenance." Cell Cycle **10**(8): 1182-1183.

Jarome, T. J. and F. J. Helmstetter (2013). "The ubiquitin-proteasome system as a critical regulator of synaptic plasticity and long-term memory formation." Neurobiol Learn Mem.

Jeganathan, S., M. von Bergen, E. M. Mandelkow and E. Mandelkow (2008). "The natively unfolded character of tau and its aggregation to Alzheimer-like paired helical filaments." Biochemistry **47**(40): 10526-10539.

Johnson, G. V. and J. A. Hartigan (1999). "Tau protein in normal and Alzheimer's disease brain: an update." J Alzheimers Dis **1**(4-5): 329-351.

Jucker, M. and L. C. Walker (2011). "Pathogenic protein seeding in Alzheimer disease and other neurodegenerative disorders." Ann Neurol **70**(4): 532-540.

Kandimalla, R. J., R. Anand, R. Veeramanikandan, W. Y. Wani, S. Prabhakar, V. K. Grover, N. Bharadwaj, K. Jain and K. D. Gill (2014). "CSF Ubiquitin as a Specific Biomarker in Alzheimer's Disease." Curr Alzheimer Res.

Kon, N., Y. Kobayashi, M. Li, C. L. Brooks, T. Ludwig and W. Gu (2010). "Inactivation of HAUSP in vivo modulates p53 function." Oncogene **29**(9): 1270-1279.

Kudo, T., K. Iqbal, R. Ravid, D. F. Swaab and I. Grundke-Iqbal (1994). "Alzheimer disease: correlation of cerebro-spinal fluid and brain ubiquitin levels." Brain Res **639**(1): 1-7.

Lambert, J. C. and P. Amouyel (2011). "Genetics of Alzheimer's disease: new evidences for an old hypothesis?" Curr Opin Genet Dev **21**(3): 295-301.

Lee, M. J., J. H. Lee and D. C. Rubinsztein (2013). "Tau degradation: the ubiquitin-proteasome system versus the autophagy-lysosome system." Prog Neurobiol **105**: 49-59.

Lim, F., F. Hernandez, J. J. Lucas, P. Gomez-Ramos, M. A. Moran and J. Avila (2001). "FTDP-17 mutations in tau transgenic mice provoke lysosomal abnormalities and Tau filaments in forebrain." Mol Cell Neurosci **18**(6): 702-714.

Lin, W. L., J. Lewis, S. H. Yen, M. Hutton and D. W. Dickson (2003). "Ultrastructural neuronal pathology in transgenic mice expressing mutant (P301L) human tau." J Neurocytol **32**(9): 1091-1105.

Liu, F., I. Grundke-Iqbal, K. Iqbal and C. X. Gong (2005). "Contributions of protein phosphatases PP1, PP2A, PP2B and PP5 to the regulation of tau phosphorylation." Eur J Neurosci **22**(8): 1942-1950.

Liu, Y. H., W. Wei, J. Yin, G. P. Liu, Q. Wang, F. Y. Cao and J. Z. Wang (2009). "Proteasome inhibition increases tau accumulation independent of phosphorylation." Neurobiol Aging **30**(12): 1949-1961.

Loomis, P. A., T. H. Howard, R. P. Castleberry and L. I. Binder (1990). "Identification of nuclear tau isoforms in human neuroblastoma cells." Proc Natl Acad Sci U S A **87**(21): 8422-8426.

Mandelkow, E. M. and E. Mandelkow (1998). "Tau in Alzheimer's disease." Trends Cell Biol **8**(11): 425-427.

Martin, L., X. Latypova and F. Terro (2011). "Post-translational modifications of tau protein: implications for Alzheimer's disease." Neurochem Int **58**(4): 458-471.

Melvin, A. T., G. S. Woss, J. H. Park, M. L. Waters and N. L. Allbritton (2013). "Measuring Activity in the Ubiquitin-Proteasome System: From Large Scale Discoveries to Single Cells Analysis." Cell Biochem Biophys.

Mietelska-Porowska, A., U. Wasik, M. Goras, A. Filipek and G. Niewiadomska (2014). "Tau protein modifications and interactions: their role in function and dysfunction." Int J Mol Sci **15**(3): 4671-4713.

Mizushima, F., K. Minoura, K. Tomoo, M. Sumida, T. Taniguchi and T. Ishida (2007). "Marked difference between self-aggregations of first and fourth repeat peptides on tau microtubule-binding domain in acidic solution." J Biochem **142**(1): 49-54.

Mizushima, N. and T. Yoshimori (2007). "How to interpret LC3 immunoblotting." Autophagy **3**(6): 542-545.

Mizushima, N., T. Yoshimori and B. Levine (2010). "Methods in mammalian autophagy research." Cell **140**(3): 313-326.

Mondragon-Rodriguez, S., G. Perry, X. Zhu and J. Boehm (2012). "Amyloid Beta and tau proteins as therapeutic targets for Alzheimer's disease treatment: rethinking the current strategy." Int J Alzheimers Dis **2012**: 630182.

Morgan, K. (2011). "The three new pathways leading to Alzheimer's disease." Neuropathol Appl Neurobiol **37**(4): 353-357.

Morishima-Kawashima, M., M. Hasegawa, K. Takio, M. Suzuki, K. Titani and Y. Ihara (1993). "Ubiquitin is conjugated with amino-terminally processed tau in paired helical filaments." Neuron **10**(6): 1151-1160.

Nicholson, B. and K. G. Suresh Kumar (2011). "The multifaceted roles of USP7: new therapeutic opportunities." Cell Biochem Biophys **60**(1-2): 61-68.

Nixon, R. A. and D. S. Yang (2011). "Autophagy failure in Alzheimer's disease--locating the primary defect." Neurobiol Dis **43**(1): 38-45.

Park, C. and A. M. Cuervo (2013). "Selective Autophagy: Talking with the UPS." Cell Biochem Biophys.

Park, W. H. and S. H. Kim (2012). "MG132, a proteasome inhibitor, induces human pulmonary fibroblast cell death via increasing ROS levels and GSH depletion." Oncol Rep **27**(4): 1284-1291.

Petersen, R. C. (2004). "Mild cognitive impairment as a diagnostic entity." J Intern Med **256**(3): 183-194.

Pike, C. J., D. Burdick, A. J. Walencewicz, C. G. Glabe and C. W. Cotman (1993). "Neurodegeneration induced by beta-amyloid peptides in vitro: the role of peptide assembly state." J Neurosci **13**(4): 1676-1687.

Poppek, D., S. Keck, G. Ermak, T. Jung, A. Stolzing, O. Ullrich, K. J. Davies and T. Grune (2006). "Phosphorylation inhibits turnover of the tau protein by the proteasome: influence of RCAN1 and oxidative stress." Biochem J **400**(3): 511-520.

Ramesh Babu, J., M. Lamar Seibenhener, J. Peng, A. L. Strom, R. Kemppainen, N. Cox, H. Zhu, M. C. Wooten, M. T. Diaz-Meco, J. Moscat and M. W. Wooten (2008). "Genetic inactivation of p62 leads to accumulation of hyperphosphorylated tau and neurodegeneration." J Neurochem **106**(1): 107-120.

Randall, C., L. Mosconi, M. Leon and L. Glodzik (2013). "Cerebrospinal fluid biomarkers of Alzheimers disease in cognitively healthy elderly." Front Biosci **18**: 1150-1173.

Reitz, C., C. Brayne and R. Mayeux (2011). "Epidemiology of Alzheimer disease." Nat Rev Neurol **7**(3): 137-152.

Reverdy, C., S. Conrath, R. Lopez, C. Planquette, C. Atmanene, V. Collura, J. Harpon, V. Battaglia, V. Vivat, W. Sippl and F. Colland (2012). "Discovery of specific inhibitors of human USP7/HAUSP deubiquitinating enzyme." Chem Biol **19**(4): 467-477.

Reyes-Turcu, F. E., J. R. Horton, J. E. Mullally, A. Heroux, X. Cheng and K. D. Wilkinson (2006). "The ubiquitin binding domain ZnF UBP recognizes the C-terminal diglycine motif of unanchored ubiquitin." Cell **124**(6): 1197-1208.

Reyes-Turcu, F. E., K. H. Ventii and K. D. Wilkinson (2009). "Regulation and cellular roles of ubiquitin-specific deubiquitinating enzymes." Annu Rev Biochem **78**: 363-397.

Roberson, E. D., K. Scearce-Levie, J. J. Palop, F. Yan, I. H. Cheng, T. Wu, H. Gerstein, G. Q. Yu and L. Mucke (2007). "Reducing endogenous tau ameliorates amyloid beta-induced deficits in an Alzheimer's disease mouse model." Science **316**(5825): 750-754.

Sato, Y., A. Yamagata, S. Goto-Ito, K. Kubota, R. Miyamoto, S. Nakada and S. Fukai (2012). "Molecular basis of Lys-63-linked polyubiquitination inhibition by the interaction between human deubiquitinating enzyme OTUB1 and ubiquitin-conjugating enzyme UBC13." J Biol Chem **287**(31): 25860-25868.

Schrader, E. K., K. G. Harstad and A. Matouschek (2009). "Targeting proteins for degradation." Nat Chem Biol **5**(11): 815-822.

Schwertman, P., W. Vermeulen and J. A. Marteijn (2013). "UVSSA and USP7, a new couple in transcription-coupled DNA repair." Chromosoma **122**(4): 275-284.

Schwickart, M., X. Huang, J. R. Lill, J. Liu, R. Ferrando, D. M. French, H. Maecker, K. O'Rourke, F. Bazan, J. Eastham-Anderson, P. Yue, D. Dornan, D. C. Huang and V. M. Dixit (2010). "Deubiquitinase USP9X stabilizes MCL1 and promotes tumour cell survival." Nature **463**(7277): 103-107.

Seiberlich, V., O. Goldbaum, V. Zhukareva and C. Richter-Landsberg (2012). "The small molecule inhibitor PR-619 of deubiquitinating enzymes affects the microtubule network and causes protein aggregate formation in neural cells: implications for neurodegenerative diseases." Biochim Biophys Acta **1823**(11): 2057-2068.

Selkoe, D. J. (2001). "Alzheimer's disease: genes, proteins, and therapy." Physiol Rev **81**(2): 741-766.

Sengupta, A., J. Kabat, M. Novak, Q. Wu, I. Grundke-Iqbal and K. Iqbal (1998). "Phosphorylation of tau at both Thr 231 and Ser 262 is required for maximal inhibition of its binding to microtubules." Arch Biochem Biophys **357**(2): 299-309.

Sergeant, N., A. Bretteville, M. Hamdane, M. L. Caillet-Boudin, P. Grognet, S. Bombois, D. Blum, A. Delacourte, F. Pasquier, E. Vanmechelen, S. Schraen-Maschke and L. Buee (2008). "Biochemistry of Tau in Alzheimer's disease and related neurological disorders." Expert Rev Proteomics **5**(2): 207-224.

Sharma, V. M., J. M. Litersky, K. Bhaskar and G. Lee (2007). "Tau impacts on growth-factor-stimulated actin remodeling." J Cell Sci **120**(Pt 5): 748-757.

Singh, S., A. S. Kushwah, R. Singh, M. Farswan and R. Kaur (2012). "Current therapeutic strategy in Alzheimer's disease." Eur Rev Med Pharmacol Sci **16**(12): 1651-1664.

Sjogren, M., H. Vanderstichele, H. Agren, O. Zachrisson, M. Edsbagge, C. Wikkelso, I. Skoog, A. Wallin, L. O. Wahlund, J. Marcusson, K. Nagga, N. Andreasen, P. Davidsson, E. Vanmechelen and K. Blennow (2001). "Tau and Abeta42 in cerebrospinal fluid from healthy adults 21-93 years of age: establishment of reference values." Clin Chem **47**(10): 1776-1781.

Slooter, A. J. and C. M. van Duijn (1997). "Genetic epidemiology of Alzheimer disease." Epidemiol Rev **19**(1): 107-119.

Sparks, D. L., S. W. Scheff, H. Liu, T. M. Landers, C. M. Coyne and J. C. Hunsaker, 3rd (1995). "Increased incidence of neurofibrillary tangles (NFT) in non-demented individuals with hypertension." J Neurol Sci **131**(2): 162-169.

Stanisic, V., A. Malovannaya, J. Qin, D. M. Lonard and B. W. O'Malley (2009). "OTU Domain-containing ubiquitin aldehyde-binding protein 1 (OTUB1) deubiquitinates estrogen receptor (ER) alpha and affects ERalpha transcriptional activity." J Biol Chem **284**(24): 16135-16145.

Stegeman, S., L. A. Jolly, S. Premarathne, J. Gecz, L. J. Richards, A. Mackay-Sim and S. A. Wood (2013). "Loss of Usp9x disrupts cortical architecture, hippocampal development and TGFbeta-mediated axonogenesis." PLoS One **8**(7): e68287.

Sun, Q. and T. C. Gamblin (2009). "Pseudohyperphosphorylation causing AD-like changes in tau has significant effects on its polymerization." Biochemistry **48**(25): 6002-6011.

Tan, Z., X. Sun, F. S. Hou, H. W. Oh, L. G. Hilgenberg, E. M. Hol, F. W. van Leeuwen, M. A. Smith, D. K. O'Dowd and S. S. Schreiber (2007). "Mutant ubiquitin found in Alzheimer's disease causes neuritic beading of mitochondria in association with neuronal degeneration." Cell Death Differ **14**(10): 1721-1732.

Vlachostergios, P. J., I. A. Voutsadakis and C. N. Papandreou (2013). "The role of ubiquitin-proteasome system in glioma survival and growth." Growth Factors **31**(3): 106-113.

von Bergen, M., S. Barghorn, J. Biernat, E. M. Mandelkow and E. Mandelkow (2005). "Tau aggregation is driven by a transition from random coil to beta sheet structure." Biochim Biophys Acta **1739**(2-3): 158-166.

Vossel, K. A., K. Zhang, J. Brodbeck, A. C. Daub, P. Sharma, S. Finkbeiner, B. Cui and L. Mucke (2010). "Tau reduction prevents Abeta-induced defects in axonal transport." Science **330**(6001): 198.

Wang, T., L. Yin, E. M. Cooper, M. Y. Lai, S. Dickey, C. M. Pickart, D. Fushman, K. D. Wilkinson, R. E. Cohen and C. Wolberger (2009). "Evidence for bidentate substrate binding as the basis for the K48 linkage specificity of otubain 1." J Mol Biol **386**(4): 1011-1023.

Wang, Y. and E. Mandelkow (2012). "Degradation of tau protein by autophagy and proteasomal pathways." Biochem Soc Trans **40**(4): 644-652.

Wiener, R., A. T. DiBello, P. M. Lombardi, C. M. Guzzo, X. Zhang, M. J. Matunis and C. Wolberger (2013). "E2 ubiquitin-conjugating enzymes regulate the deubiquitinating activity of OTUB1." Nat Struct Mol Biol **20**(9): 1033-1039.

Wille, H., G. Drewes, J. Biernat, E. M. Mandelkow and E. Mandelkow (1992). "Alzheimer-like paired helical filaments and antiparallel dimers formed from microtubule-associated protein tau in vitro." J Cell Biol **118**(3): 573-584.

Wing, S. S. (2003). "Deubiquitinating enzymes--the importance of driving in reverse along the ubiquitin-proteasome pathway." Int J Biochem Cell Biol **35**(5): 590-605.

Witte, H., D. Neukirchen and F. Bradke (2008). "Microtubule stabilization specifies initial neuronal polarization." J Cell Biol **180**(3): 619-632.

Xie, Y., M. Avello, M. Schirle, E. McWhinnie, Y. Feng, E. Bric-Furlong, C. Wilson, R. Nathans, J. Zhang, M. W. Kirschner, S. M. Huang and F. Cong (2013). "Deubiquitinase FAM/USP9X interacts with the E3 ubiquitin ligase SMURF1 protein and protects it from ligase activity-dependent self-degradation." J Biol Chem **288**(5): 2976-2985.

Yoshioka, Y., Y. Q. Ye, K. Okada, K. Taniguchi, A. Yoshida, K. Sugaya, J. Onose, H. Koshino, S. Takahashi, A. Yajima, S. Yajima and N. Abe (2013). "Ubiquitin-specific peptidase 5, a target molecule of vialinin A, is a key molecule of TNF-alpha production in RBL-2H3 cells." PLoS One **8**(12): e80931.

You, B. R. and W. H. Park (2011). "Proteasome inhibition by MG132 induces growth inhibition and death of human pulmonary fibroblast cells in a caspase-independent manner." Oncol Rep **25**(6): 1705-1712.

Supplemental data

```
TauP301L-5xKR-HaloTag       PDLRKVRSKIGSTENLKHQPGGGKVQIINKKLDLSNVQSKCGSKDNIKHV 300
TauP301L-3xKR-HaLoTag       PDLRKVKSKIGSTENLKHQPGGGKVQIINKKLDLSNVQSKCGSKDNIKHV 300
TauP301L-HaloTag            PDLKKVKSKIGSTENLKHQPGGGKVQIINKKLDLSNVQSKCGSKDNIKHV 300
                            **:**:*************************************** 

TauP301L-5xKR-HaloTag       LGGGSVQIVYRPVDLSRVTSKCGSLGNIHHKPGGGQVEVKSEKLDFKDRV 350
TauP301L-3xKR-HaLoTag       LGGGSVQIVYRPVDLSKVTSKCGSLGNIHHKPGGGQVEVKSEKLDFKDRV 350
TauP301L-HaloTag            LGGGSVQIVYKPVDLSKVTSKCGSLGNIHHKPGGGQVEVKSEKLDFKDRV 350
                            **********:*******:********************************** 

TauP301L-5xKR-HaloTag       QSRIGSLDNITHVPGGGNKKIETHKLTFRENAKAKTDHGAEIVYKSPVVS 400
TauP301L-3xKR-HaLoTag       QSRIGSLDNITHVPGGGNKKIETHKLTFRENAKAKTDHGAEIVYKSPVVS 400
TauP301L-HaloTag            QSKIGSLDNITHVPGGGNKKIETHKLTFRENAKAKTDHGAEIVYKSPVVS 400
                            **:************************************************* 
```

Figure 38 – Schematic representation of plasmids with three, five or no mutations. Mutations: the TauP301L and TauP301L-HaloTag were used as vectors and here are the point mutations when compared with the original vector.

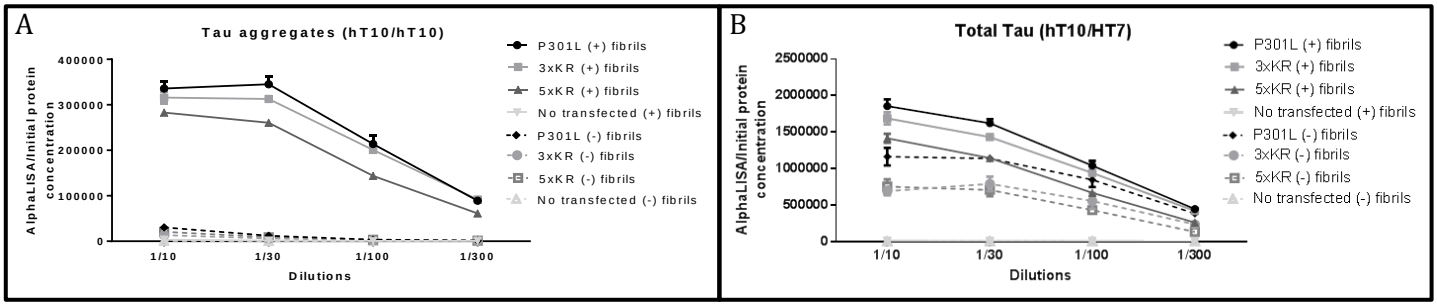

Figure 39 - AlphaLISA's results from cells non transfected or transfected with the plasmid without or with 3 or 5 mutation. (A) Tau aggregates quantification using hT10/hT10 antibodies combination and different dilutions. The result's normalization was done with the initial protein concentration of each sample. (B) Total Tau quantification using hT10/HT7 antibodies combination and different dilutions. The result's normalization was done with the initial protein concentration of each sample. Each data point is the mean ±S.E.M of 6 biological and 3 mechanic repetitions.

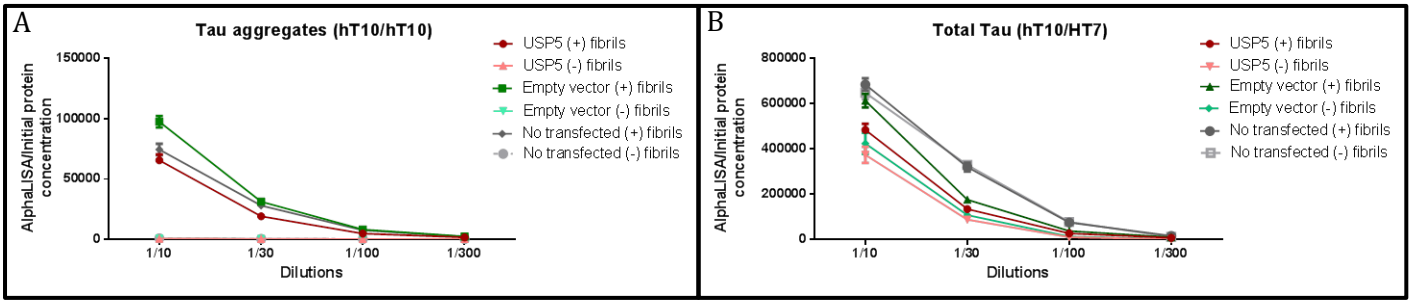

Figure 40 - AphaLISA's results from USP5 overexpression cells with 0.25µg. (A) Tau aggregates quantification using hT10/hT10 antibodies combination and different dilutions. The result's normalization was done with the initial protein concentration of each sample. (B) Total Tau quantification using hT10/HT7 antibodies combination and different dilutions. The result's normalization was done with the initial protein concentration of each sample. Each data point is the mean ±S.E.M of 6 biological and 3 mechanic repetitions.

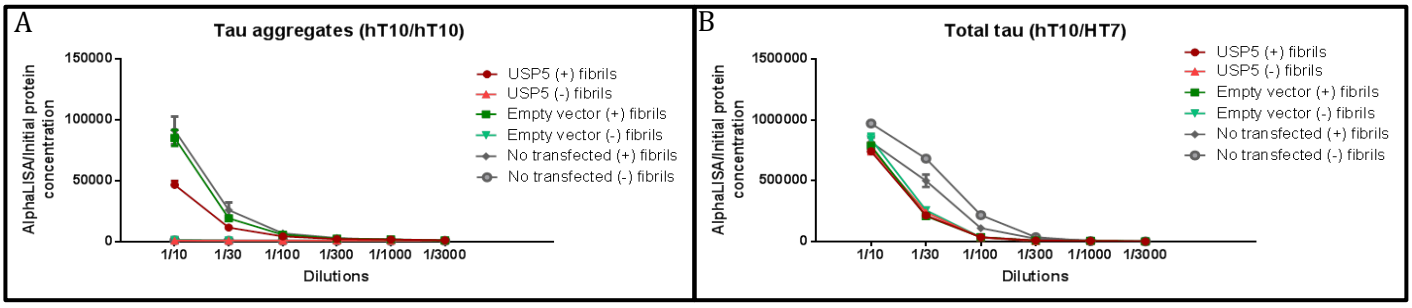

Figure 43 - AphaLISA's results from USP5 overexpression cells with 0.5µg. (A) Tau aggregates quantification using hT10/hT10 antibodies combination and different dilutions. The result's normalization was done with the initial protein concentration of each sample. (B) Total Tau quantification using hT10/HT7 antibodies combination and different dilutions. The result's normalization was done with the initial protein concentration of each sample. Each data point is the mean ±S.E.M of 6 biological and 3 mechanic repetitions.

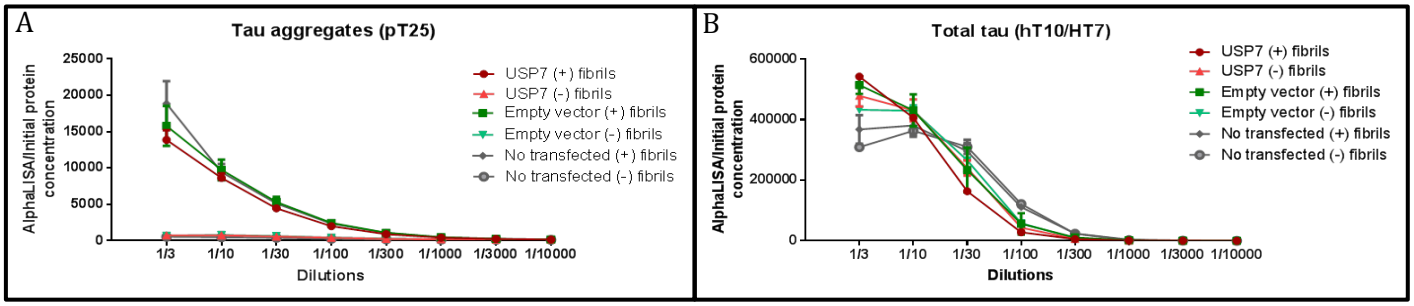

Figure 42 - AphaLISA's results from USP7 overexpression cells with 0.5µg. (A) Tau aggregates quantification using hT10/hT10 antibodies combination and different dilutions. The result's normalization was done with the initial protein concentration of each sample. (B) Total Tau quantification using hT10/HT7 antibodies combination and different dilutions. The result's normalization was done with the initial protein concentration of each sample. Each data point is the mean ±S.E.M of 6 biological and 3 mechanic repetitions.

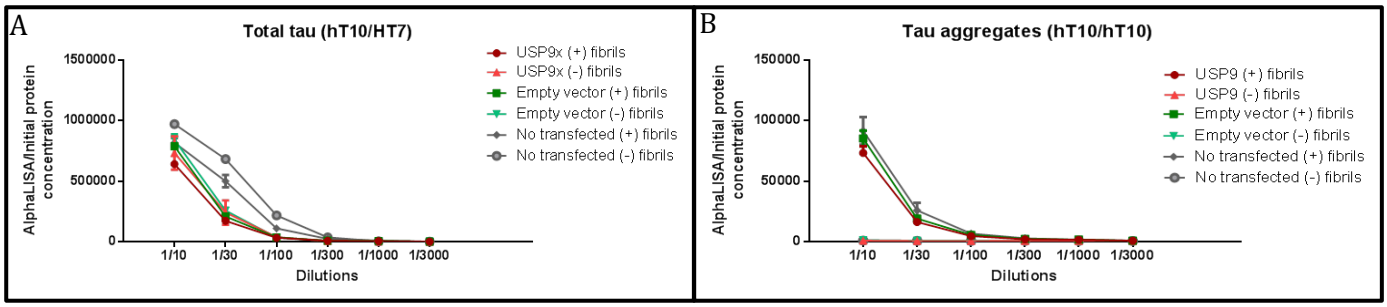

Figure 41 - AphaLISA's results from USP9 overexpression cells with 0.5µg. (A) Tau aggregates quantification using hT10/hT10 antibodies combination and different dilutions. The result's normalization was done with the initial protein concentration of each sample. (B) Total Tau quantification using hT10/HT7 antibodies combination and different dilutions. The result's normalization was done with the initial protein concentration of each sample. Each data point is the mean ±S.E.M of 6 biological and 3 mechanic repetitions.

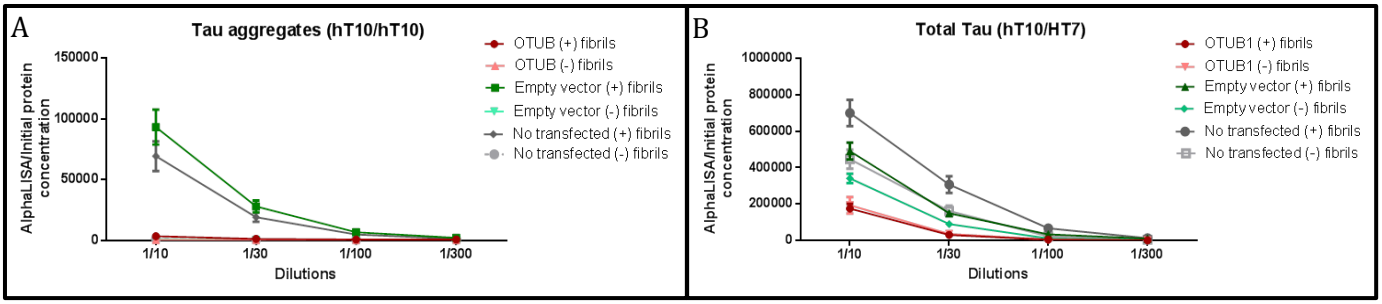

Figure 44 - AphaLISA's results from OTUB1 overexpression cells with 0.25µg. (A) Tau aggregates quantification using hT10/hT10 antibodies combination and different dilutions. The result's normalization was done with the initial protein concentration of each sample. (B) Total Tau quantification using hT10/HT7 antibodies combination and different dilutions. The result's normalization was done with the initial protein concentration of each sample. Each data point is the mean ±S.E.M of 6 biological and 3 mechanic repetitions.

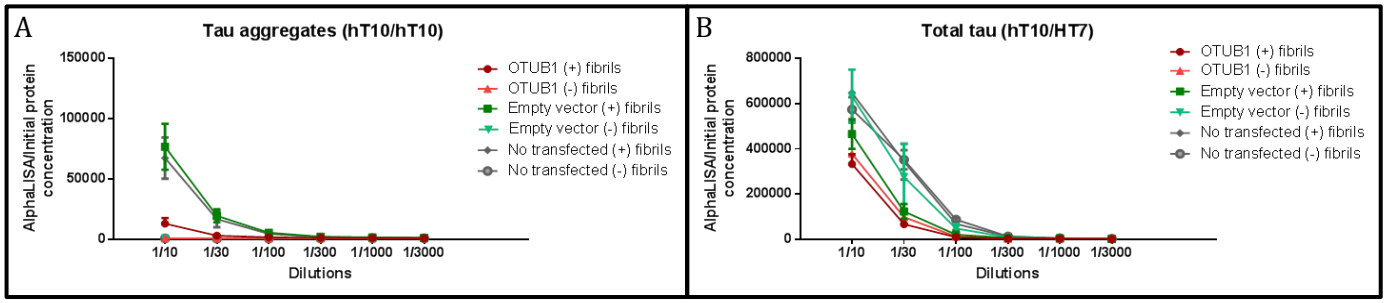

Figure 45 - AphaLISA's results from OTUB1 overexpression cells with 0.5µg. (A) Tau aggregates quantification using hT10/hT10 antibodies combination and different dilutions. The result's normalization was done with the initial protein concentration of each sample. (B) Total Tau quantification using hT10/HT7 antibodies combination and different dilutions. The result's normalization was done with the initial protein concentration of each sample. Each data point is the mean ±S.E.M of 6 biological and 3 mechanic repetitions.

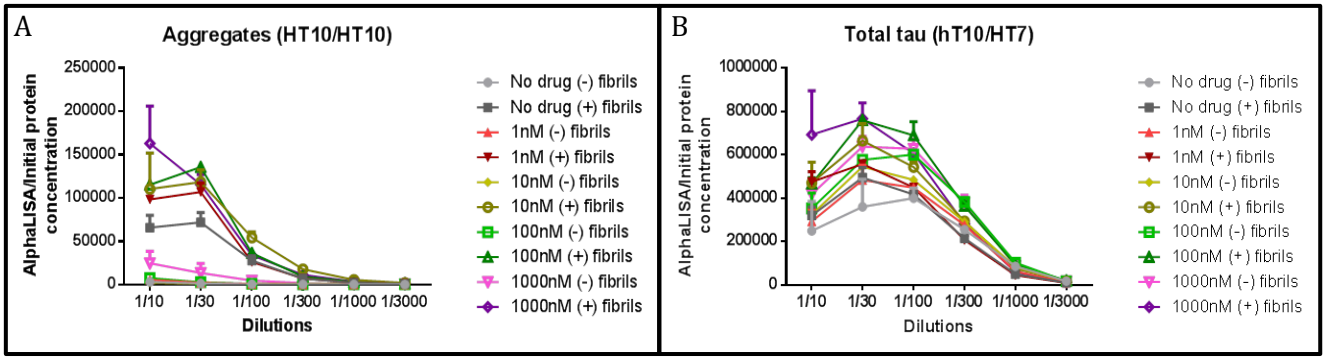

Figure 46 - AphaLISA's results from autophagy enhance through Rapamycin. (A) Tau aggregates quantification using hT10/hT10 antibodies combination and different dilutions. The result's normalization was done with the initial protein concentration of each sample. (B) Total Tau quantification using hT10/HT7 antibodies combination and different dilutions. The result's normalization was done with the initial protein concentration of each sample. Each data point is the mean ±S.E.M of 2 biological and 3 mechanic repetitions.

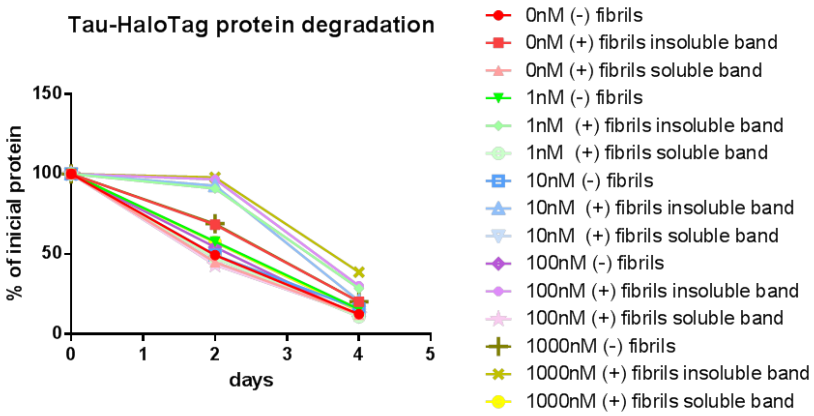

Figure 47 - TauP301L-HaloTag protein degradation after the exposition to a 0, 1, 10, 100 or 1000nM of Rapamycin for 2 and 4 days. Quantitative analysis of Tau-HaloTag protein degradation of soluble band (without K18), insoluble band and soluble band (with K18) where the initial amount of protein was considered as 100%. Each data point is the mean ±S.E.M of 2 biological repetitions.